Institute of Animal breeding and Genetics

Professor for Animal Genetics and Pathogenetics

Justus Liebig University Gießen

Genomic and transcriptomic analyses for markers, genes and regions associated with liver copper concentration in sheep

INAUGURAL-DISSERTATION

Submitted for the degree of Doctor of Agricultural Science (Dr. agr.) to the Faculty of Agricultural Sciences, Nutritional Sciences and Environmental Management

Submitted by

Olusegun O. Adeniyi (M.Sc.)

from Abeokuta, Nigeria

Gießen, 2024

With the permission of the Faculty of Agricultural Sciences,

Nutritional Sciences and Environmental Management of the

Justus Liebig University Giessen

Examination board:

1st reviewer(s): Prof. Dr. Gesine Lühken

2nd reviewer: Prof. Dr. Klaus Eder

Examiner: Prof. Dr. Rod Snowdon

Examiner: Prof. Dr. Marc Schetelig

Chairperson: Prof. Dr. Joachim Aurbacher

Date of disputation: 24. 02.2025

I TABLE OF CONTENTS

II TABLES

III FIGURES

IV ABBREVIATIONS

Cu	copper
DM	dry matter
Fe	Iron
F_{ST}	Fixation index
GO	gene ontology
GWAS	genome-wide association study
hapFLK	haplotype-based FLK
KEGG	Kyoto encyclopaedia of genes and genomes
Mo	Molybdenum
S	sulfur
SNP	single nucleotide polymorphism
ww	wet weight
XP-EHH	cross-population extended haplotype homozygosity

1. GENERAL INTRODUCTION

Copper (Cu) is an essential microelement for animals and holds significant importance in many biological processes. It is a vital component of some cuproenzymes involved in anti-oxidation of free radicals, energy metabolism and iron metabolism (De Bie et al., 2005; Suttle, 2010). Thus, intracellular Cu concentrations are tightly regulated to ensure the proper functioning of biological processes, and the prevention of cytotoxicity. In both humans and animals, Cu is generally absorbed in the gastrointestinal tract, transported to the liver for storage and distribution and excreted in the bile (Gaetke et al., 2014; Hordyjewska et al., 2014; Chen et al., 2022).

However, deficient and high diagnostic liver Cu levels have been associated with several diseases such as Cu deficiency and intoxication which impact livestock performance that result in economic losses to farmers (De Sousa et al., 2012; Kumaratilake, 2014; Kendall et al., 2015). Determination of Cu concentration can be performed with blood plasma as well as in the liver samples (Suttle and Jones, 2007). However, information on liver Cu concentration is by far more reliable for diagnosis of Cu intoxication and deficiency (Borobia et al., 2022). Existing documented evidence indicates that liver Cu levels are subject to the effects of dietary Cu levels, age, breed and Cu antagonists such as molybdenum (Mo) and iron (Fe) (Suttle and Field, 1983; van der Berg et al., 1983; Suttle et al., 2002; De Sousa et al., 2012; Fry et al., 2013; Ranches et al., 2021; Spears et al., 2022).

However, liver copper levels have been reported to vary within breeds reared under similar conditions (Woolliams et al., 1986; Suttle et al., 2002; Johnston et al., 2014). Suttle et al. (2002) observed that the coefficients of variation for liver copper concentration within Suffolk and Texel sheep fed similar diet were 40% and 34%, respectively. Likewise, Johnston et al. (2014) reported a wide range of liver Cu values for Jersey cows. In the report by Johnston et al. (2014), the death of six cattle from Cu intoxication was recorded from a herd of 250 cows. In the study by Woolliams et al. (1986), a higher mortality and incidence of swayback was recorded in Scottish Blackface lambs genetically selected for low Cu status when compared to lambs selected for high Cu status. This indicates that within-breed variation in liver Cu concentration may expose some animals within the herd to deficient or toxic Cu levels resulting in Cu-related diseases or death in severe cases, and it necessitates the need to understand the genetic background modulating liver Cu

levels with the aim to reduce the incidence of Cu deficiency and intoxication in sheep. Aside from within-breed variation in liver Cu accumulation, between-breed differences have been reported for cattle (Mullis et al., 2003) and sheep (van der Berg et al., 1983). Evidence of within or between breed variation in liver Cu concentrations indicates that this trait is influenced by genetic variation.

Over the years, studies on genes and genetic markers influencing liver Cu concentration have revolved around the determination of genetic mutations that result in Cu-related disorders such as the Wilson and Menke diseases in humans (Huster and Lutsenko, 2007; Hordyjewska et al., 2014), and Cu toxicosis in Bedlington terriers (De Bie et al., 2005). However, these studies did not investigate genetic variations that are associated with differences in liver Cu accumulation in sheep.

1.1. Copper supply and metabolism

Mineral elements including Cu are considered an important part of dietary nutrition due to their involvement in structural, physiological, catalytic and regulatory functions in animals. The inclusion of Cu as well as other minerals in the diet despite the incidence of mineral poisoning underscores the importance of trace elements in nutrition.

1.1.1. Copper supply

Since animals do not produce Cu, requirements are usually met by the supply of Cu through dietary foodstuffs. Sources of Cu for animals include roughages and concentrates. Estimates of Cu absorbability is known to differ between feedstuffs. Suttle (2010) found that cereals (9.1%) have a higher absorbability than silage (4.9%) in sheep. Furthermore, bioavailability of supplemental sources of Cu including Cu sulphate, Cu acetate or Cu carbonate is reported to vary for cattle and sheep (Byrne and Murphy, 2022). Likewise, Cu content varies among foodstuffs (EFSA Panel on Additives and Products or Substances used in Animal Feed, 2016). Due to the general susceptibility of sheep to oversupply with Cu, farmers usually try to ensure that the Cu concentration of concentrated feed does not exceed recommended limits ranging from 4–8 mg/kg dry matter (DM) (NRC, 2007a). The European Union national scientific bodies consider varying ranges of 6–25.2 for bovine, 5–15 for caprine and 5–14.3 for ovine mg Cu/kg DM

as copper requirements/allowances in diet (EFSA Panel on Additives and Products or Substances used in Animal Feed, 2016).

1.1.2. Copper metabolism

The metabolism of Cu is a chemical process involving diverse biological cells, tissues and organs that aid the absorption, distribution and excretion of Cu following intake of dietary sources.

Copper absorption

Absorption of dietary Cu predominantly takes place in the duodenum and jejunum regions of the small intestine (Wu et al., 2016). Cu absorption into the intestinal mucosa cells is facilitated by copper transport protein 1 (CTR1) located on the apical surface of the enterocytes (Chen et al., 2022). Divalent metal transporter 1 (DMT1) is another transporter reported to mediate the cellular uptake of divalent metals including Cu (Arredondo et al., 2003). However, DMT1 mediates Cu uptake only when other meatal cations such as iron (Fe) are deficient or absent in the small intestine (Jiang et al., 2013). After Cu uptake into intestinal cells, Cu is conveyed across the basolateral membrane into the hepatic-portal circulation with the aid of Cu-transporting ATPase 7A (ATP7A) (Lutsenko et al., 2007).

Copper redistribution

Following absorption, Cu is mainly transported to the liver via the hepatic portal system for storage in hepatocytes and redistribution to other organs of the body (Tao and Gitlin, 2003; Linder, 2020). In portal circulation, Cu binds to albumin and trancuprein for delivery to the liver and kidney (Linder, 2016). In hepatocytes, Cu is found in different forms including free Cu, bound to Cu chaperons such as antioxidant 1 (ATOX1), and incorporated into enzymes or Cu-dependent proteins such as ceruloplasmin which are secreted into plasma. Prior to this, Cu is transferred into hepatic cells by CTR1 (Chen et al., 2020). Blood plasma is reported to contain Cu binding components such as albumin, transcuprein and ceruloplasmin which aids the distribution of Cu to extrahepatic organs (Linder, 2016). Though albumin is the most abundant of the three, the largest fraction of Cu in the plasma is found in ceruloplasmin (Linder et al., 1998; Linder, 2016).

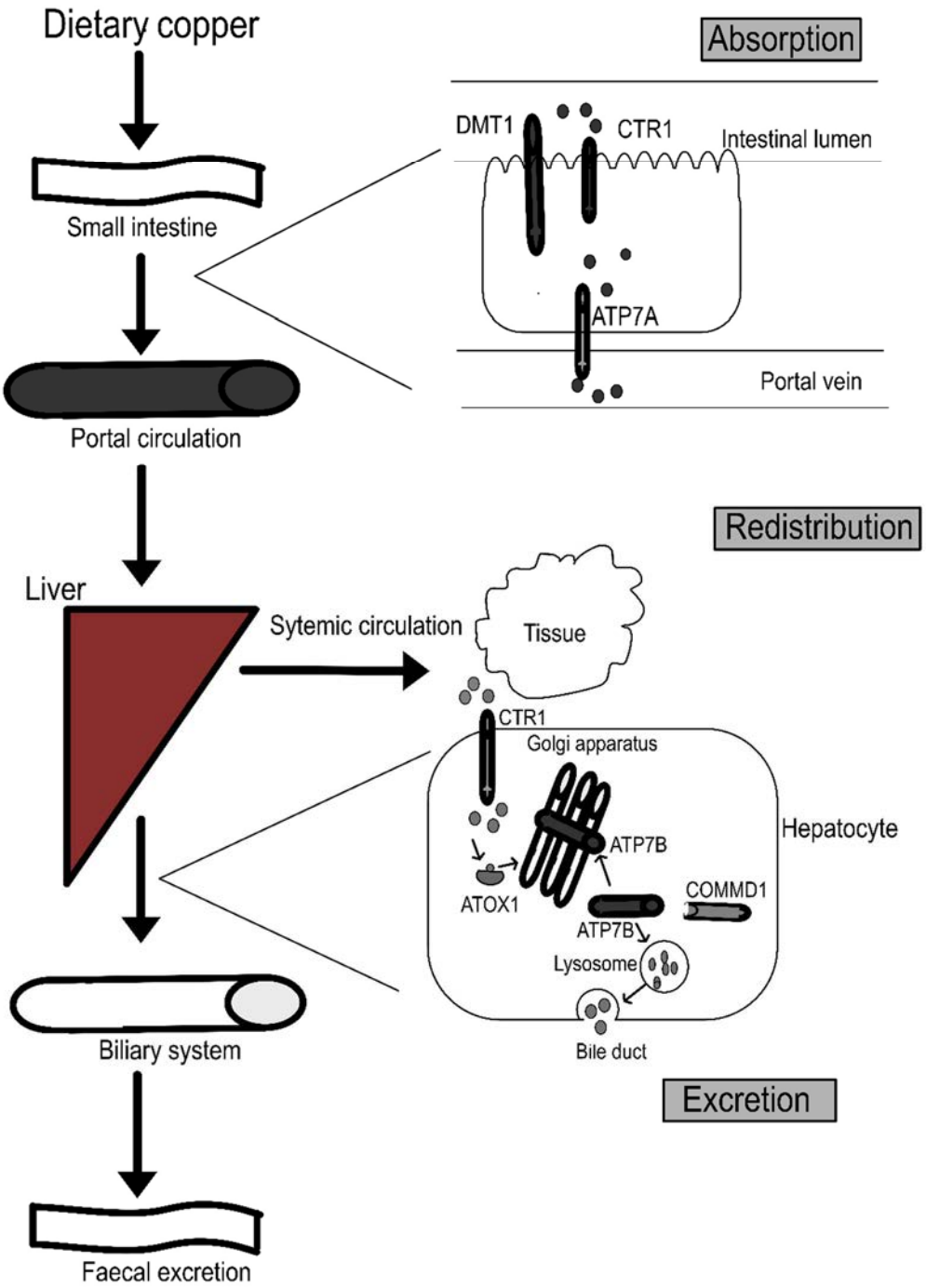

Figure 1. Process of copper absorption. redistribution and excretion adapted from Wu et al. (2016). Copper transport protein 1 (CTR1), Divalent metal transporter 1 (DMT1), Cu-transporting ATPase 7A (ATP7A), Cu-transporting ATPase 7B (ATP7B), antioxidant 1 (ATOX1) and copper metabolism MURR1 domain–containing 1 (COMMD1).

Copper excretion

Excess Cu is toxic to both humans and animals with biliary excretion the main form of elimination (Barceloux and Barceloux, 1999). The liver is important for maintenance of Cu homeostasis because it is the main organ for Cu excretion in mammals (Roberts and Sarkar, 2008). Moreover, Cu-transporting ATPase 7B (ATP7B) reported to play a role in biliary Cu excretion is predominantly expressed in the liver (Wijmenga and Klomp, 2004; Polishchuk et al., 2014). Mutation in the ATP7B protein has been associated with the commonly known Wilson disease (WD) which results in Cu retention by the liver that leads to Cu overload in humans (Huster and Lutsenko, 2007; Prohaska, 2008). Biliary Cu is mainly deposited into the gastrointestinal tract for fecal excretion. In addition to biliary excretion, Cu can be excreted through sweat and urine (Chen et al., 2022).

1.2. Regulation and determination of liver copper concentration

Cu can be found in tissues (e.g. liver, kidney) and bodily fluids (e.g. saliva and bile) within the body (Linder, 2020). However, liver serves as the main storage organ for Cu and other minerals in the body of animals. In addition, liver aids supply and excretion of Cu in the body to maintain Cu balance required for normal physiological processes during adequate, deficient and excess dietary Cu supply (Roberts and Sarkar, 2008). Moreover, liver Cu levels have been repeatedly observed to be low and high in incidences of Cu deficiency and intoxication making this organ the most suitable sample for the determination of Cu deficiency and toxicosis.

1.2.1. Homeostasis of liver copper concentration

Hepatocyte uptake of copper occurs at the plasma membrane with the aid of CTR1 protein. The CTR1 protein has been associated with acquiring Cu in hepatocytes as reported by Kim et al. (2009). In this study by Kim et al. (2009), compensatory mechanisms that aided Cu uptake in the liver was also observed after deletion of the *CTR1* gene suggesting that other modes for liver Cu uptake exist. After Cu uptake, chaperone for superoxide dismutase 1 (CCS), cyclooxygenase 17 (COX17) and antioxidant 1(ATOX1) assist in the incorporation of Cu into the cytosol, mitochondria and ATP7B, respectively (Clarkson et al., 2020). The ATP7B is localized to the Golgi body where

it is involved in the incorporation of hepatocyte Cu into caeruloplasmin and in other cases Cu excretion (Tao and Gitlin, 2003; Clarkson et al., 2020). Other proteins involved in liver Cu homeostasis include metallothioneins (MTs) and copper metabolism MURR1 domain–containing 1 (COMMD1).

1.2.2. Determination of liver copper concentration

Freshly collected liver samples are usually frozen and stored until analysis for copper content with determination of liver Cu content performed using wet or dry samples (Suttle et al., 2002; Sivertsen and Løvberg, 2014). The wet or dry samples are usually chemically digested with industrial grade chemicals such as HNO_3, HCL and H_2O_2 with the resulting digests analyzed with an atomic absorption spectrophotometer (Suttle et al., 2002) or inductively coupled plasma spectrometer (Galyean et al., 1996). Measurements are often recorded as dry matter (DM) or wet weight (ww) in parts per million (ppm), mg/ kg or µg/g (Puls, 1994).

1.2.3. Diagnostic ranges for liver copper concentration

Generally, ruminants are more susceptible to copper intoxication or deficiency when compared to other animals. Among ruminants, sheep is regarded as the most susceptible with diagnostic ranges of deficient adequate and toxic liver Cu levels (mg/kg ww) of 0.5 – 4.0, 25 – 100 and 250 – 1000, respectively (Puls, 1994) (Table 1).

Table 1. Diagnostic liver copper levels for sheep and cattle adapted from reviews by Papachristodoulou et al. (2015) for sheep and Kincaid (2000)for cattle, respectively.

Diagnostic levels	**Sheep (mg Cu /kg ww)**	**Cattle (µg Cu /g DM)**
Deficient	0.5 – 4.0	<33
Marginal	5 – 20	33 – 125
Adequate	25 – 100	125 – 600
High	100 – 500	600 – 1250
Toxic	250 – 1000	>1250

In a review by Kincaid (2000) , the author reported hepatic Cu ranges of < 33 µg/g DM for deficient, 125 – 600 µg/g DM for adequate and > 1250 µg/g DM for toxic in cattle. Furthermore, diagnostic ranges of deficient (0.4 – 10 mg/kg ww), adequate (25 – 150 mg/kg ww) and toxic (230 – 2000 mg/kg ww) levels of liver Cu have been documented for goats by Puls (1994).

1.3. Factors affecting liver copper concentration in sheep

Some factors such as Cu intake, age, breed and Cu antagonist are reported to affect the amount of Cu observed in sheep liver.

1.3.1. Dietary copper levels

The higher the Cu content of the diet, the higher the amount of Cu intake which leads to an increase in quantity of Cu available in the small intestine for absorption. Consequently, this results in increased liver Cu levels. This was demonstrated in a study by van der Berg et al. (1983) for sheep. In this study, different sheep breeds were fed diets containing high and low Cu content with higher liver Cu concentration found in sheep fed higher dietary Cu levels. For sheep fed low Cu diet, the authors reported average liver Cu values of 775, 482 and 225 mg/kg DM for Texel, Flemish milk and Finnsh Landrace, respectively. On the other hand, sheep fed high Cu diet had mean liver Cu values of 1652, 959, 486 mg/kg DM for Texel, Flemish milk and Finnsh Landrace, respectively. Similar results have been reported in cattle by Fry et al. (2013).

1.3.2. Copper antagonists

Competition occurs among mineral elements including Cu, Mo and Fe for absorption within the small intestine. In a report by De Sousa et al. (2012) on sheep showing symptoms of Cu deficiency, the authors reported that the high liver Fe observed in the sheep indicates a possible antagonism of Cu during absorption. Additionally, a Cu/Mo antagonism has been documented in ruminants. It was first observed in cattle and sheep when signs of Cu deficiency resulted from feeding animals pasture grown on soils with high Mo content (Ferguson et al., 1938, 1943). This finding has been further supported by other studies including Clarke and Laurie (1980) and Suttle and Field (1983). These reports revealed that thiomolybdates formed because of high Mo and sulfur (S) in the

ruminant's rumen creates complexes with Cu, thereby impairing absorption which may result in low liver Cu levels. Consequently, this may lead to Cu deficiency. This indicates that some trace elements reduce available Cu that may impact liver Cu levels.

1.3.3. Age

In sheep, liver Cu levels have been observed to increase with age. Woolliams et al. (1982) reported higher liver Cu concentration (mg/kg DM) for sheep at 13 weeks compared to 6 weeks for various breeds including Scottish Blackface (567.1 vs 384), Texel (1491.5 vs 676.1, Finnish Landrace (766.7 vs 418.3) and Suffolk (1116.1 vs 635.4). Similarly, an increase in hepatic Cu concentration over time was observed for both Texel and Suffolk in another study by Suttle et al. (2002). These studies show that age has an impact on Cu concentration in the liver. In addition, the effect of age on liver Cu levels has been documented in an experiment by Ranches et al. (2021) on Angus and Simmental cows. This study revealed increasing liver Cu concentration during Cu supplementation phase from 90.5 mg/kg DM at 90 days to 136 mg/kg DM at 150 days. During the Cu restriction phase, Ranches et al. (2021) reported an initial increase in liver Cu levels from day 0 and 30, and followed by a decrease from day 30 and 60. These findings suggest that the increase in liver Cu levels with age or time may be contingent on consistent Cu supplementation.

1.3.4. Breed

Breed differences have been considered to influence liver Cu concentration in sheep. Reports comparing hepatic Cu levels of sheep breeds fed similar diets have revealed variation in liver copper concentration. Studies dating back to the late 60's by Wiener and Field (1969) revealed differences in liver Cu concentration for three breeds exposed to similar feeding and environmental conditions. In this study, liver Cu levels were lowest in the Scottish Blackface and highest in the Welsh Mountain breed. Likewise, van der Berg et al. (1983) reported significant breed differences in liver Cu concentration for sheep fed similar diet for the same period. In like manner, breed differences in liver Cu concentration has been documented for cattle (Fry et al., 2013; Ranches et al., 2021). Aside from between-breed differences, within-breed variations in liver Cu concentration has also been observed in some studies (Judson et al., 1994; Suttle et al., 2002).

Within-breed variation in liver copper concentration

The quantity of Cu in the liver of sheep varies within breed. In a study by Suttle et al. (2002) on sheep fed similar diets, the authors reported that the liver Cu concentration values varied by 34% and 40% for Suffolk and Texel, respectively. In another study, within breed variation for liver Cu values ranging from 30 to 100 µmol/ kg DM were reported for Scottish Blackface in a study by Woolliams et al. (1986). Moreover, Sivertsen and Løvberg (2014) documented ranges of 89 – 221 µg/g ww and 87 – 186 µg/g ww for hepatic Cu values of 1 year old ewes of the Norwegian Dala breed sampled from a flock during two consecutive years. Comparable results have been observed in New Zealand dairy cattle (Jersey breed) with varying levels of liver Cu concentration (ranging from 1900 to 3500 µmol/kg ww) observed in the herd (Johnston et al., 2014). Variations in liver Cu concentrations reported in these studies suggest that within-breed variations in liver Cu accretion exist.

Between-breed variation in liver copper concentration

Variation in hepatic Cu levels have been reported between breeds fed similar dietary Cu concentration. Woolliams et al. (1982) showed that liver copper levels (mg Cu /kg DM) were lowest in Scottish Blackface (567.1) followed by intermediate levels for Finnish Landrace (766.7) and East Friesian (754.2), high in Suffolk (1116.1), and highest in Texel (1491.5). Comparable reports by other authors confirm differences between breeds in hepatic Cu accumulation for sheep (van der Berg et al., 1983; Suttle et al., 2002). In the study by van der Berg et al. (1983) on sheep fed high and low Cu diets, the authors found the highest and lowest liver Cu concentration in Texel (1675 and 775 mg / kg DM) and Finnish Landrace (486 and 225 mg / kg DM) sheep, respectively. In studies with cattle, lower liver Cu levels were reported for Simmental when compared to Angus cattle breed (Fry et al., 2013). On the other hand, Ranches et al. (2021) revealed lower liver Cu values for Angus when compared to Braham breed. All these reports indicate that breed difference in liver Cu accretion is influenced by genetic factors.

1.4. Copper-related problems and treatment in sheep farming

Sheep are prone to Cu overload or intoxication. On the other hand, Cu deficiency is also a familiar problem in sheep husbandry. The susceptibility of sheep to Cu deficiency and

intoxication is well documented as reviewed by Gooneratne et al. (1989) and Borobia et al. (2022), respectively.

1.4.1. Copper intoxication

Cu toxicosis occurs when excess Cu accumulates in the liver and is released causing haemolytic crises. Two kinds of Cu poisoning can occur namely acute and chronic with the chronic form more commonly present than the acute form (McCaughey, 2007). Acute Cu poisoning occurs because of high exposure to Cu sources such as oral administration of Cu supplements or ingestion of food within a short period as reviewed by Borobia et al. (2022). In contrast, chronic Cu poisoning ensues from exposure to toxic or non- toxic levels of Cu over extended periods like weeks or months leading to Cu accretion in the liver (Bostwick, 1982; Bremner, 1998). Copper poisoning is well documented and common in more susceptible animal species including sheep (Hidiroglou et al., 1984; Humann-Ziehank et al., 2001; Kumaratilake, 2014). Symptoms of copper poisoning include jaundice, haemoglobinuria and death (McCaughey, 2007).

1.4.2. Copper deficiency

Another problem encountered by sheep farmers is Cu deficiency. Cu Deficiency occurs from low intake of Cu as well as reduced absorption due to feed type or high content of Cu antagonist such as Mo and Fe (Suttle and Jones, 2007). Suttle and Jones (2007) reported that Cu absorption yield from fresh grass was twice less than that of grass conserved as hay. In addition, increased Mo intake has been reported to induce Cu deficiency in sheep (Suttle, 2010) and in cattle as reviewed by López-Alonso and Miranda (2020). Symptoms of Cu deficiency include swayback (ataxia), anaemia, abnormal wool and hair, depigmentation and bone disorders (Suttle, 2010).

1.4.3. Treatment of copper intoxication and deficiency

Various methods have been suggested and implemented for treatment of Cu intoxication. Treatment with orally ingested ammonium molybdate and sodium sulphate have also been recommended for the treatment of sheep with a risk of Cu poisoning showing haemolytic signs (McCaughey, 2007). McCaughey (2007) also suggested other treatments for Cu poisoning such as subcutaneous injection of ammonium

tetrathiomolybdate at 3.4 mg/kg on 3 alternate days has been used with varying success. According to a review by Sargison (2008) this method had poor rate of success amongst animals with advanced clinical signs, but was effective in sheep at risk of haemolytic crises. However, it must be noted that the use of ammonium tetrathiomolybdate is prohibited for use in food-producing animals (Sargison, 2008). In a review of Cu toxicosis treatment in cattle by Johnston et al. (2014), a daily drenching program with ammonium molybdate and sodium sulphate was used to mitigate the effect of Cu toxicosis and reduce liver Cu concentration in dairy cattle with toxic levels of Cu. This report indicated that an average of 37% reduction in liver Cu content was achieved using this method.

Similarly, Cu deficiency can be fatal with considerable damage to the central nervous system resulting in swayback (Sieuchand, 2016). To prevent swayback in newborn lambs, oral solutions containing 1g Cu have been given to ewes at 8 and 4 weeks prior to lambing for many years (Suttle and Jones, 2007). In a review by Gooneratne et al. (1989), effective prevention of swayback has been reported after oral dosing of expecting ewes with 220 mg Cu at both 8 and 4 weeks before lambing. Feed supplementation with Cu has also been suggested and used to reduce the incidence of sheep flocks prone to Cu deficiency. Although the use of subcutaneous or intramuscular injection of has been documented by Gooneratne et al. (1989), the implementation of this method can impact carcass value negatively (Suttle and Jones, 2007).

1.5. Economic impact of Cu toxicosis and deficiency in sheep farming

Cu intoxication or deficiency often results in the loss of farm animals such as sheep. In other cases, they could lead to high cost of production caused by treatment of affected animals (Varga and Puschner, 2012). Cases of Cu poisoning have been reported in Norway (Sivertsen and Løvberg, 2014), and in Greece, France, Italy and Spain as reviewed by Guitart et al. (2010). According to the report from Spain, 24 and 31 sheep died due to grazing on contaminated pasture and feeding with sunflower grown on Cu-fertilized soil, respectively. Recently a case of Cu deficiency initiated by high molybdenum intake was reported in White Horned Heath sheep in Northern Germany by Helmer et al. (2021). In this report, mortality of sheep was observed despite treatment. The poor health status,

cost of treatment and death in severe cases of Cu toxicosis or deficiency in sheep result in heavy economic losses to the farmers. Therefore, preventive approaches should be adopted.

1.6. Candidate genes associated with variation in liver Cu concentration

Some candidate genes have been associated with increased liver Cu concentration. Some of these genes are involved in inherited Cu-related diseases while others are identified in expression analysis for association with differences in hepatocyte or liver Cu concentration.

1.6.1. Genes involved in inherited Cu-related diseases

Some candidate genes have been associated with increased liver Cu concentration in humans and dogs. Mutation in the *ATP7B* gene, which is highly expressed in the liver, is associated with Wilson disease in humans (Cox and Moore, 2002). Wilson disease is an autosomal recessive disorder that causes individuals to lose their ability to excrete Cu from the liver leading to Cu intoxication (Lutsenko, 2014). Likewise, another Cu-ATPase gene known as *ATP7A* gene has been associated with Menkes disease in humans (Horn and Wittung-Stafshede, 2021). Menkes disease is a X-linked disorder that causes inability in humans (mainly males) to transport dietary Cu from the intestine resulting in Cu deficiency (Cox and Moore, 2002). In dogs, van de Sluis et al. (2002) identified *COMMD1* (Copper Metabolism Domain Containing 1) as the gene responsible for Cu toxicosis in Bedlington terrier. These findings suggest that genes along the Cu metabolism pathway may be responsible for variations in liver Cu concentration in sheep.

1.6.2. Genes identified in expression analysis

Analysis to unravel the association of hepatic Cu content on gene expression has been performed in various studies (Song and Freedman, 2005; Fry et al., 2013; Ranches et al., 2021). Song and Freedman (2005) reported an upregulation in gene expression for genes such as Cytochrome P450, Family 1, Subfamily A, Polypeptide 1 (*CYP1A1*), metallothionein 2A (*MT2A*), ATP Binding Cassette Subfamily C Member 3 (*ABCC3*) and ATP Binding Cassette Subfamily A Member 5 (*ABCA5*) after exposure of HepG2 cells to

Cu. Analysis of between-breed differences in Cu-related gene expression revealed significantly lower duodenal *CTR1* expression in Simmentals when compared with Angus (Fry et al., 2013). Another study by Ranches et al. (2021) observed significant difference in metallothionein 1A (*MT1A*) expression when comparing Angus and Braham cattle. Recently, a transcriptomic and metabolomic study on Wu Ranke sheep initially fed with Cu deficient multi-nutrient salts, and later fed with Cu supplement multi-nutrient salt was published (Jin et al., 2024). In this study, Jin et al. (2024) observed that genes including Forkhead Box O3 (*FOXO3*) and Tryptase Beta 2 (*TPSB2*) were upregulated during Cu deficient feeding period whereas genes such as Actinin Alpha 2 (*ACTN2*) and Growth Hormone Releasing Hormone Receptor (*GHRHR*) were upregulated during the period of Cu supplement feeding.

1.7. Other methods for identification of genome regions, genes and markers associated with liver copper concentration

Information on within- and between-breed differences in liver Cu accumulation suggests that this trait is possibly influenced by genetic factors. To the best of our knowledge prior to the commencement of this work, other methods including genome-wide association study (GWAS) and selection signatures analysis were yet to be employed in the determination of regions, markers and genes within the genome that may influence liver Cu levels in sheep.

1.7.1. Genome-wide association studies

Genome-wide association study (GWAS) using single nucleotide polymorphism (SNP) markers is a way to detect genetic markers, genes and genomic regions associated with a liver Cu content. Following the development of genome-wide SNP chips for different animal species, this method has been employed for the determination of SNPs associated with various traits in animals such as sheep and cattle by Purdie et al. (2011). The GWAS has been utilized in the analyses of both qualitative (Kijas et al., 2016) and quantitative (Ghasemi et al., 2019; Sutera et al., 2021a) traits. Prior to the commencement of this thesis, there was no published study analyzing genome-wide

markers for association with liver Cu concentration in sheep. Since this trait is measurable, we consider it a quantitative trait that can be assessed using GWAS.

1.7.2. Genome-wide selection signatures analysis

Similarly, whole genome scan for selection signatures can be employed to determine regions under selection for various traits in animals. In a study by Kijas et al. (2012), genome-wide scan for SNP differentiation between polled and horned sheep using genome-wide scan of Fixation index (F_{ST}) revealed a selection region that harbours the relaxin Family Peptide Receptor 2 (*RXFP2*) gene associated with horned status in sheep by Johnston et al. (2011). Other studies have employed various selection signatures analysis methods including scans of the Fixation index (F_{ST}) (Flori et al., 2009), cross-population extended haplotype homozygosity (XP-EHH) (Sabeti et al., 2007)and haplotype-based FLK (hapFLK) (Fariello et al., 2013) to determine regions under selection and genes associated with varying traits such as adaptation to high altitude (Wei et al., 2016),local adaptation (Simoni Gouveia et al., 2017) and milk production (Campos et al., 2017; Asadollahpour Nanaei et al., 2020). Therefore, analysis of selection signatures may help unravel the genetic architecture underlining variation in Cu accretion.

1.8. Aims and structure of the thesis

1.8.1. Aim of the thesis

Sheep are known to be susceptible to Cu toxicosis as well as deficiency that have negative economic impact on sheep farmers as earlier described. Moreover, wide variation in liver Cu concentration has been reported among individuals within a breed showing high and low liver Cu concentrations with the possibility of Cu intoxication or deficiency. In like manner, between-breed differences in liver Cu accretion have been observed in sheep indicating breed variability. These findings suggest that hepatic Cu variations (within or between sheep breeds) are possibly modulated by differences in the sheep genome. Therefore, the aims of the study were to:

I. estimate that within-breed variation in liver Cu concentration occur in sheep of a target breed (Merinoland) kept together and on the same diet,

II. identify markers and genes associated with within-breed variation in liver Cu concentration for the target breed,
III. estimate heritability (h^2) for liver Cu concentration in the target breed,
IV. identify genes and genetic regions associated with between-breed differences in liver Cu accretion for sheep,
V. support the marker association analysis by identifying differentially expressed genes associated with within-breed variation in liver Cu concentration in another Merino-type breed.

1.8.2. Structure of the thesis

The thesis is divided into 3 parts

Study 1

The goal of this study was to estimate that differences in hepatic Cu content occur within a target breed, identify markers and genes associated with within-breed differences in liver Cu concentration, and estimate heritability for within-breed liver Cu variation. For this purpose, 89 and 45 male lambs of the Merinoland breed from two private farms in Bavaria were sampled. Details of the statistical analysis, used models, results and discussion will be presented in chapter 2.

Adeniyi, O.O.; Medugorac, I.; Grochowska, E.; Düring, R.-A.; Lühken, G. Single-Locus and Multi-Locus Genome-Wide Association Studies Identify Genes Associated with Liver Cu Concentration in Merinoland Sheep. *Genes* **2023**, *14*, 1053. https://doi.org/10.3390/genes14051053

Study 2

In the second part of this thesis, we assessed the ovine genome for regions, genes and markers under selection for between-breed variation in liver Cu accretion for sheep. For this reason, 3 breeds with generally high Cu accretion and 3 breeds with generally low Cu accumulation were selected based on available published information on hepatic Cu accumulation status. Following this, genomic data of breed-groups with high and low Cu accretion was analyzed in a comparative study to identify genes and genetic regions

under selection for liver Cu accretion. The data, analyses and results are discussed in the study documented in chapter 3.

Adeniyi, O. O.; Lenstra, J. A.; Mastrangelo, S.; Lühken, G. (2024): Genome-wide comparative analyses for selection signatures indicate candidate genes for between-breed variability in copper accretion in sheep. In animal 18 (10), p. 101329. DOI: 10.1016/j.animal.2024.101329.

Study 3

In the third part of the thesis, we supported our first study by evaluating the sheep genome for differentially expressed genes associated with within-breed variation in liver Cu concentration using another Merino-type breed. For the whole genome transcriptome study, 12 liver samples from Polish-Merino sheep with low and high liver Cu concentration were selected from a group of sheep exposed to similar dietary Cu and environmental conditions. The methods, results as well as discussion are given in chapter 4.

2. Single-locus and multi-locus genome-wide association studies identify genes associated with liver Cu concentration in Merinoland sheep

Olusegun O. Adeniyi [1], Ivica Medugorac [2], Ewa Grochowska [3], Rolf-Alexander Düring [4] and Gesine Lühken [1]

[1]Institute of Animal Breeding and Genetics, Justus Liebig University, Giessen 35390, Germany.

[2]Population Genomics Group, Department of Veterinary Sciences, LMU Munich, Lena-Christ-Str. 48, 82152 Martinsried, Germany.

[3]Department of Animal Biotechnology and Genetics, UTP University of Science and Technology, Mazowiecka 28 St, 85-084 Bydgoszcz, Poland.

[4]Institute of Soil Science and Soil Conservation, Interdisciplinary Research Centre for Biosystems, Land Use and Nutrition (IFZ), Justus Liebig University, Heinrich-Buff-Ring 26-32, D-35392 Giessen, Germany.

Published in:
Genes 2023, 14(5), 1053; https://doi.org/10.3390/genes14051053

Submitted: 30 March 2023
Accepted: 4 May 2023

ABSTRACT

Economic losses due to copper intoxication or deficiency is a problem encountered by sheep farmers. The aim of this study was to investigate the ovine genome for genomic regions and candidate genes responsible for variability in liver copper concentration. Liver samples were collected from slaughtered lambs of the Merinoland breed from two farms, and used for measurement of copper con-centration and genome-wide association study (GWAS). A total of 45,511 SNPs and 130 samples were finally used for analysis, in which single-locus and several multi-locus GWAS (SL-GWAS; ML-GWAS) methods were employed. Gene enrichment analysis was performed for identified candidate genes to detect gene ontology (GO) terms significantly associated with hepatic copper levels. The SL-GWAS and a minimum of two ML-GWAS identified two and thirteen significant SNPs, respectively. Within genomic regions surrounding identified SNPs, we observed nine promising candidate genes such as DYNC1I2, VPS35, SLC38A9 and CHMP1A. GO terms such as lysosomal membrane, mitochondrial inner membrane and sodium:proton antiporter activity were significantly enriched. Genes involved in these identified GO terms mediate multivesicular body (MVB) fusion with lysosome for degradation and control membrane permeability. This reveals the polygenic status of this trait and candidate genes for further studies on breeding for copper tolerance in sheep.

Keywords: Liver copper concentration; SL-GWAS; ML-GWAS; candidate genes; Merinoland sheep

INTRODUCTION

Sheep farming is continuously challenged with the risks of copper intoxication and deficiency. Copper is an essential trace element for many species. It serves as a cofactor for the proper functioning of some copper-containing enzymes, so called ”cuproenzymes” such as copper-zinc superoxide dismutase, cytochrome c oxidase and hephaestin which function in anti-oxidation of free radicals, energy metabolism and iron metabolism, respectively (De Bie et al., 2005; Suttle, 2010). However, sheep are known to be impaired in their ability to excrete excess copper from the liver, which leads to copper intoxication (Haywood et al., 2005). On the other hand, copper deficiency is also a known problem in sheep husbandry (Suttle and Jones, 2007).

Hepatic copper levels in sheep have been classified into diagnostic levels of deficient, marginal, adequate, high, and toxic (Puls, 1994; Underwood and Suttle, 1999). Deficient and high diagnostic levels of hepatic copper have been associated with poor performance and health status of sheep (De Sousa et al., 2012; Kumaratilake, 2014)Liver copper levels have been reported to vary between as well as within sheep breeds (van der Berg et al., 1983; Suttle et al., 2002). A report on Suffolk and Texel sheep fed a similar diet showed that the coefficient of variation for liver copper concentration within each breed was 40% and 34%, respectively (Suttle et al., 2002). Furthermore, results of selection for low and high copper status in Scottish Blackface lambs have been reported by Woolliams et al. (1986). According to these authors plasma copper concentration was higher in high copper lines than in low copper lines. In another report by Knowles et al. (1998), variation in copper status was observed for two flocks of the Romney breed suggesting the availability of lines with distinct copper metabolism. These findings suggest that copper status within sheep breeds may be influenced by genetic factors.

Association of genes such as copper transporter 1 (*CTR1*), chaperone for superoxide dismutase 1 (*CCS*), antioxidant-1 (*ATOX1*), metallothionein (MT), copper-transporting ATPase 1 (*ATP7A*) *and* copper-transporting ATPase 2 (*ATP7B*) with copper metabolism are well documented for humans (Tao and Gitlin, 2003; Lutsenko et al., 2007; Barry et al., 2010; Lutsenko, 2010; Kaler, 2013). CTR1, CCS and ATOX1 are proteins involved in copper transport from circulation, distribution to superoxide dismutase (SOD1), and transport to the secretory pathway and nucleus, respectively (Lutsenko, 2010). In addition, ATP7A/B supports the transfer of copper to the secretory pathways and mediates copper excretion by sequestration in vesicles/vacuoles, while MT functions as copper scavenger in hepatocytes (Tao and Gitlin, 2003; Barry et al., 2010; Lutsenko, 2010). Variations in liver copper levels have been reported for humans with mutations in the *ATP7A* and/or *ATP7B* genes that result in Menkes and Wilson disease, respectively (Fuentealba and Aburto, 2003; Horn and Wittung-Stafshede, 2021). Likewise, mutation in the copper metabolism MURR1 domain–containing 1 (*COMMD1*) gene has been implicated in copper toxicity in dogs (De Bie et al., 2005). However, information on candidate genes and genetic markers associated with within-breed variation in liver copper concentration of sheep is unknown.

The Illumina Ovine 50K SNP chip is a powerful tool to analyze the sheep genome with respect to an association with diverse traits as confirmed in various single-locus genome-wide association studies (SL-GWAS) (Kijas et al., 2009; Kijas et al., 2012; Lakhssassi et al., 2021; Yilmaz et al., 2022) and multi-locus GWAS (ML-GWAS) (Ding et al., 2019; Zhao et al., 2022) in animals. SL-GWAS aim to identify associations of single nucleotide polymorphisms (SNPs) with varying phenotypes of individuals by assessing the differences in allelic frequencies of their genetic variants (Marees et al., 2018; Uffelmann et al., 2021). This is currently implemented in various mixed linear model methods such as MLMA (Yang et al., 2014), EMMAX (Kang et al., 2010) and GEMMA (Zhou and Stephens, 2012). These methods are usually subjected to Bonferroni correction due to multiple testing, which may result in the exclusion of some important loci with small effects. In this context, ML-GWAS is a better alternative because it does not require the conservative Bonferroni correction, therefore leading to the identification of more trait-associated markers especially for polygenic traits (Li et al., 2018; Zhao et al., 2022). Moreover, an earlier report indicated that a multi-locus GWAS approach is better suited for the analysis of complex traits (Segura et al., 2012). As a solution, several ML-GWAS models have been developed, such as multi-locus random-SNP-effect mixed linear model (mrMLM) (Wang et al., 2016), the fast multi-locus random-SNP-effect mixed linear model (FASTmrMLM) (Tamba and Zhang, 2018), the fast multi-locus random-SNP-effect efficient mixed model association (FASTmrEMMA) (Wen et al., 2017), polygenic-background-control-based least angle regression plus empirical Bayes (pLARmEB) (Zhang et al., 2017), polygenic-background-control-based Kruskal–Wallis test plus empirical Bayes (pKWmEB) (Ren et al., 2018), and Iterative sure independence screening expectation maximization Bayesian least absolute shrinkage and selection operator (ISIS EM–BLASSO) (Tamba et al., 2017). These methods are implemented in two phases. The first phase involves the selection of potentially associated markers after analyses using various algorithms. For the second phase, all the effects in a model harboring the selected markers are estimated by empirical Bayes, after which further identification by a likelihood ratio test for true quantitative trait nucleotides (QTNs) of all the non-zero effects is performed.

To the best of our knowledge, a genome-wide analysis regarding liver copper concentration in sheep has not been conducted until now. Therefore, the aim of this study was to identify candidate genes associated with variability in hepatic copper

concentration in sheep using both SL-GWAS and ML-GWAS methods. This analysis was done using liver samples from slaughter lambs of the Merinoland sheep breed, a breed of high economic importance in Germany.

Materials and Methods

Sample and data collection

The animals were kept under standard farming regulations on two private sheep farms in Bavaria. For this study, only male lambs were sampled after slaughter for human consumption. Documented information on date of birth and date of slaughter were obtained from the farmers. Regarding farm 1, eighty-nine (89) lambs from the flock with ages between 4 – 5.5 months were sampled after slaughter in batches over a period of 46 days. They were kept indoors with unlimited access to their dams and fed ad libitum with grass silage and compound feed consisting of lucerne pellets (5.53 %), concentrate pellets (58.84 %), barley (22.93 %) and beet pulp (12.70 %). Concentrate feeding of lambs started 14 days after birth. All dams had unhindered access to grass silage with occasional input of the above-mentioned compound feed. A total of 45 lambs were sampled from the flock located at farm 2. These lambs were kept in pasture and under uniform feeding conditions until slaughter. In addition, fresh water was made available ad libitum for all animals by the farmers. The nutrient composition of the feed, and the mineral content of the grass silage, components of compound feed, and pasture grass were determined by a nutrient analysis laboratory (Intertek Food Services GmbH, Linden Germany) (Table S1a and S1b). Liver samples from all lambs were collected directly after slaughter by cutting approximately 20 g of sheep liver from the tip of the *lobus caudatus*, packed separately in plastic tubes, labelled and stored at -20 °C prior to determination of liver copper concentration and DNA extraction.

Determination of liver copper concentration

Liver samples were freeze-dried, pulverized and stored in airtight tubes. Duplicate samples of approximately 0.5 g were digested in 5 ml deionized H_2O, 5 ml HNO_3 and 3 ml H_2O_2 with a StarT-1500 microwave oven (MLS GmbH Cooperation, Leutkirch, Germany). Conditions for the microwave digestion system are shown in Table S2. Digested samples were filtered into a 50 ml flask and filled up to a volume of 50 ml with deionized water. The

copper concentration was determined with an inductively coupled plasma-optical emission spectrometer (ICP-OES; Agilent 720ES, Darmstadt, Germany) at a wavelength of 327.4 nm. Used operating parameters for the ICP-OES were published elsewhere (Öztan and Düring, 2012). For quality assurance reagent blanks were measured and a detection limit corresponding to 0.039 mg/kg was calculated (limit of detection = mean blank + 3 standard deviations of the mean blank value). Also, certified reference materials (Bovine Liver ERM-BB185, European Commission, Joint Research Centre, Geel, Belgium) were used for testing the precision of measurement. Mean recovery percentage was 91.4 % ± 2.6.

Genotyping and quality control

DNA was extracted from liver samples using the Macherey-Nagel NucleoSpin Tissue Kit (Düren, Germany) according to manufacturer's instructions. All 134 liver samples were genotyped with the Illumina Ovine 50k SNP BeadChip. Quality control (QC) was performed to exclude loci with minor allele frequency (< 5%), SNPs with a low call rate (< 95%), samples with more than 5% of missing genotypes, and SNPs for which Hardy–Weinberg equilibrium test *P* values were lower than 1.0×10^{-6}. After QC, a total of 45,511 SNPs and 130 samples were left for analysis.

Single-locus and multi-locus genome-wide association analyses

SL-GWAS and ML-GWAS were performed for all samples and data obtained after QC. All 130 samples were used to estimate genome-wide association of markers with liver copper concentration. To perform a single-locus GWAS, genetic relatedness was estimated using "pcrelate" and "pcrelateToMatrix" functions in the GENESIS R package (Gogarten et al., 2019). Next, a linear mixed model analyses for quantitative phenotypes was implemented using the same software. Genetic relationship matrix was included in the analysis as a random effect to account for cryptic relatedness. The model includes: $\mathrm{y} = \mathrm{X}\beta + Z_1\mathrm{a} + Z_2\mathrm{c} + e$ where y is the vector of observed liver copper concentration (mg/kg dry matter, DM) at slaughter, ß is a vector of fixed effects including the intercept term, farm, age at slaughter, a is the vector of the additive effect (fixed) of the candidate SNP to be tested for association, c is the vector of polygenic effect (random) of all markers (as captured by the genetic relationship matrix calculated using all SNPs), and e is a vector of residuals. X, Z_1 and Z_2 are the incidence matrices relating observations to β, a

and c, respectively. Due to the conservative nature of Bonferroni threshold (Johnson et al., 2010) and possibility that associated SNP effects can be missed (Nelson et al., 2017), a false discovery rate (FDR) *P*-value threshold was used (Benjamini, Y. and Hochberg, Y., 1995). FDR was set at 0.01, with the *P*-value level of significance defined as $P = N/M \times 0.01$, where N is the number of SNP markers with *P*-values below the FDR threshold and M represents the total number of SNPs (Wang et al., 2017). Manhattan plot of $-\log_{10}$(*P*-value) was constructed with the package "ggplot" in R (R Core Team, 2023). SNPs above the given *P*-value threshold were considered significant and selected for further analysis. The proportion of total variability explained by SNPs (V_G) and error variance (V_E) were computed using "varCompCI" function in GENESIS R package (Gogarten et al., 2019). Estimation of heritability was done from the variance components with the formula: $h^2 = V_G / (V_G + V_E)$ according to Yang et al. (2017).

Regarding ML-GWAS analysis, the mrMLM v4.0.2 (Zhang et al., 2020) software implemented in R was used to determine SNPs associated with liver copper concentration in Merinoland sheep. Five ML-GWAS methods including mrMLM, FASTmrMLM, FASTmrEMMA, pLARmEB, and ISIS EM–BLASSO were performed according to methods described by Wang et al. (2016), Tamba and Zhang (2018), Wen et al. (2017), Zhang et al. (2017), and Tamba et al. (2017), respectively. In the first stage and for the selection of potential SNPs, all SNPs were treated as random effects in the five methods. In the second stage, all selected SNPs in the first stage of each method were placed into one multi-locus model and the markers with effects above the logarithm of odds (LOD) threshold value regarded as possible candidate SNPs associated with liver copper concentration. For all methods except pLARmEB, the critical *P*-values for selection of SNP in the first stage were set at default. These values were employed in order to maximize power for SNP detection as suggested by the respective authors (Wang et al., 2016; Tamba et al., 2017; Wen et al., 2017; Tamba and Zhang, 2018). The default values were 0.01 for mrMLM, 0.01 for FASTmrMLM, 0.005 for FASTmrEMMA, and 0.01 for ISIS EM–BLASSO. With regards to pLARmEB analysis, a value of 50 was set as the number of potentially associated markers selected by least angle regression (LARS) according to Zhang et al. (2017). The critical LOD score was set to 3 in the second stage according to previous reports using ML-GWAS methods (Ding et al., 2019; Zhao et al., 2022). Covariates of farm and age at slaughter were included in the analysis, which was

corrected for cryptic relatedness using K (genomic relatedness) matrix calculated using the R package mrMLM v4.0.2. To increase the accuracy of this result, SNPs identified by at least two ML-GWAS methods were selected for further analysis.

Gene annotation and enrichment

Genes located within 0.5 megabase (Mb) regions upstream and 0.5 Mb downstream of putative SNPs after SL-GWAS and ML-GWAS were identified according to the UCSC genome browser (Karolchik et al., 2011) with the selection of the Oar_v4.0 assembly in the National Center for Biotechnology Information (NCBI). Functional enrichment analysis was performed on all genes identified by both GWAS methods using the Database for Annotation, Visualization and Integrated Discovery (DAVID) software (https://david.ncifcrf.gov; accessed 23.02.2023) (Dennis et al., 2003; Huang et al., 2009b, 2009a). The human gene annotation was selected for analysis due to a higher number of recognized genes in comparison to sheep gene annotations.

The gene ontology (GO) annotation category including biological process (BP), cellular component (CC) and molecular function (MF) terms, with the parameter set to a minimum of two genes, was investigated in this study. Using the Fishers exact test, GO TERMS of enriched genes with a *P*-value threshold of ≤ 0.05 were considered significant (Rivals et al., 2007). A subset of genes with functional relationship to cellular transport and excretion using available gene annotations from GeneCards (http://www.genecards.org (accessed on: 23 February 2023)) and Uniprot (http://www.uniprot.org (accessed on: 23.02.2023)) databases were considered as functional candidate genes. Additionally, a second subset of all genes was considered as positional candidate genes when harboring a significant SNP or located near such an SNP.

Results

Liver copper levels and estimated heritability

Descriptive statistics of hepatic copper concentration and age of slaughtered lambs whose samples were included in the SL-GWAS and ML-GWAS analyses are shown in Table 1. A heritability of 0.67 ± 0.29 was estimated for this trait.

Table 1. Descriptive statistics and estimated heritability of liver copper concentration for Merinoland sheep lambs used in SL-GWAs and ML-GWAS analyses.

Farm	N[1]	Mean (SE) Cu (mg/kg DM)	Min	Max	Mean (SE) age at slaughter (days)	Min	Max	h^2(SE)[2]
1	89	159.54 ± 5.22	67.67	273.42	150.76 ± 1.30	119	165	0.67(0.29)
2	41	79.05 ± 6.80	20.57	188.28	136.78 ± 3.04	89	172	

[1]N refers to number of samples; [2]h^2 refers to Heritability of liver copper concentration.

Identification of genomic regions and candidate genes

Relating to the SL-GWAS analysis of markers association with liver copper concentration in this study, two significant SNPs (OAR2_145591151.1 and s62875.1) located on chromosome 2 and below the given threshold (P-value = 8.77 × 10-5; $-\log_{10}(P\text{-value})$ = 4.06; λ =0.98) were observed (Table 2; Figure 1). Likewise, 35 significant SNPs above the LOD score cutoff value of 3 were observed after performance of ML-GWAS methods (Table S3). Among these, 13 significant SNPs distributed on chromosomes 1, 2, 3, 4, 6, 7, 14, 16 and 23 (Table 3; Figure 2a-e) were detected by a minimum of two ML-GWAS methods. The two SNPs observed using the SL-GWAS were also identified by ML-GWAS. Of these, only one SNP (OAR2_145591151.1) was observed by more than one ML-GWAS method. Concerning candidate genes identified with SL-GWAS, 4 positional candidate genes (Table 2) within putative SNP regions were detected. Furthermore, two of these candidate genes were identified as both positional and functional. As regards ML-GWAS and within possible SNP regions associated with liver copper concentration, we observed 21 potential candidate genes (Table 3). Among them were 9 functional candidate genes, with 4 genes identified as both positional and functional candidate genes.

Table 2. Significant SNPs and genes associated with liver Cu concentration for Merinoland sheep using SL-GWAS.

CHR	SNP[1]	Position	*P*-value	Genes[2] (1Mb)
2	OAR2_145591151.1	136897136	5.11 × 10-5	***SLC25A12***, ***DYNC1I2***
2	s62875.1	150905130	6.59 × 10-5	*ACVR1C, ACVR1*

[1]SNP positions are based on Oar_v4.0 assembly in NCBI. [2]Candidate genes: underlined = positional candidate genes; bold = functional candidate genes within of SNP within a 1 Mb region; italics only = nearest gene located up- and downstream of SNP within a 1 Mb region.

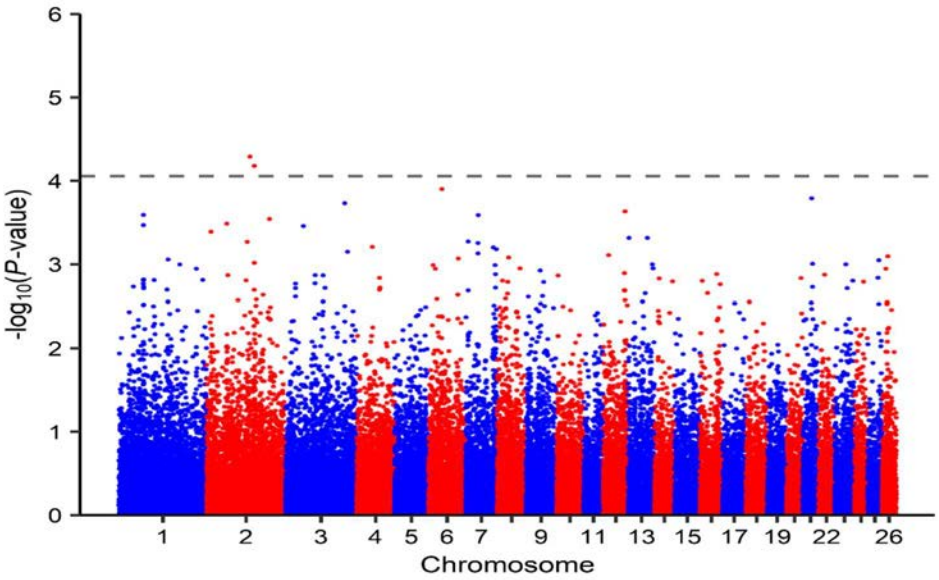

Figure 1. Manhattan plot of single-locus genome wide association study (SL-GWAS) of liver Cu concentration for Merinoland sheep. The dashed line represents the FDR threshold ($-\log_{10}(P\text{-value}) = 4.06$).

Table 3. Significant SNPs and genes associated with liver Cu concentration for Merinoland sheep using ML-GWAS.

CHR	SNP	Position (BP)[1]	Genes (1Mb)[2]	ML-GWAS Methods[3]
1	s66850.1	77025732	*GPR88*, ***ATP5MF***	2, 3, 4, 5
1	OAR1_285395930.1	263664109	*COL6A1*, *COL6A2*	2, 4, 5
2	s05644.1	14172465	*FRRS1L*	1, 2, 4
2	OAR2_145591151.1*	136897136	***SLC25A12***, ***DYNC1I2***	3, 4
3	OAR3_132833292.1	124516955	*KITLG*	1, 2, 4
4	OAR4_77358490.1	73042599	*ZNF804B*	2, 3, 5
6	s42668.1	21789865	*CENPE*, ***SLC9B2, SLC9B2***	2, 4
6	OAR6_47263223.1	42315913	*GBA3*	2, 3, 4, 5
7	s25674.1	87187746	*NRXN3*	2, 3, 4
7	OAR7_101357352.1	93147667	-	1, 3, 5
14	OAR14_14650208.1	14404415	***SPG7, CHMP1A,*** *SHCBP1*, ***VPS35***	3, 5
16	OAR16_25377664_X.1	23278766	*IL6ST*, ***SLC38A9***	2, 4
23	OAR23_37101686.1	35080540	*GREB1L*	2, 4

[1]SNP positions are based on Oar_v4.0 assembly in NCBI. [2]Candidate genes: underlined = positional candidate genes; bold = functional candidate genes of SNP within a 1 Mb region. [3]ML-GWAS Methods: 1 = mrMLM , 2 = FASTmrMLM, 3 = FASTmrEMMA, 4 = pLARmEB, 5 = ISIS EM-BLASSO; *SNP identified by both SL-GWAS and ML-GWAS.

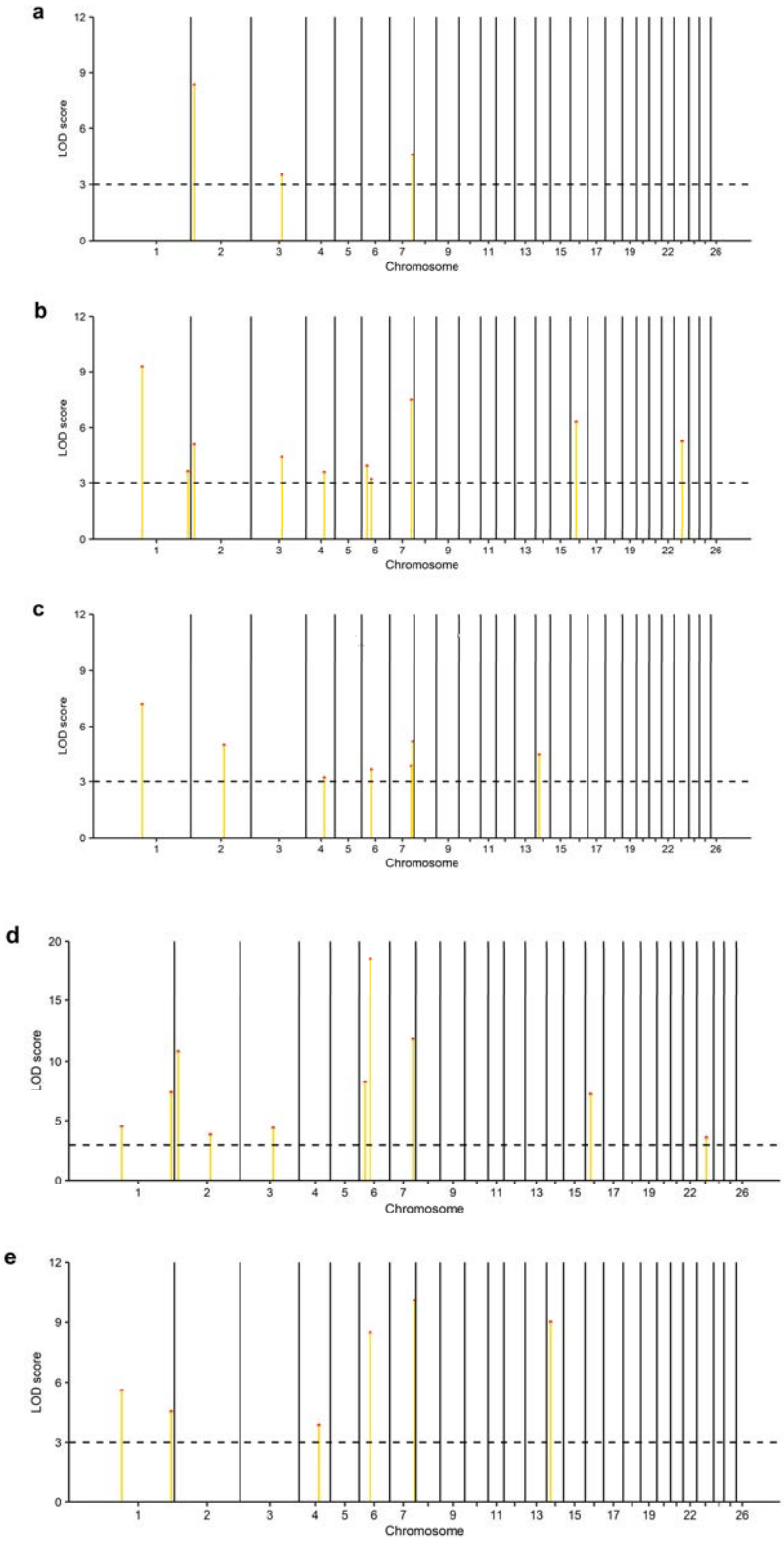

Figure 2. Manhattan plots of the five multi-locus genome wide association studies (ML-GWAS) (a) mrMLM, (b) FASTmrMLM, (c) FASTmrEMMA and (d) pLARmEB, (e) ISIS EM-BLASSO for liver Cu concentration in Merinoland sheep. Dashed lines represent the thresholds for significance (LOD > 3).

Finally, our results revealed a total of 16 GO terms, for example integral component of membrane, lysosomal membrane, hydrogen ion transmembrane transport, mitochondrial inner membrane and sodium:proton antiporter activity were significantly enriched ($P \leq 0.05$; Table 4).

Table 4. Enriched GO terms determined by DAVID from genes identified in regions (1 Mb) of SNPs for liver copper variation in Merinoland sheep using SL-GWAS and ML-GWAS.

Category	Term	Genes	*P*-value[1]
GOTERM_MF_DIRECT	GO:0016361~activin receptor activity, type I	*ACVR1, ACVR1C*	0.006
GOTERM_CC_DIRECT	GO:0005765~lysosomal membrane	*COL6A1, CHMP1A, VPS35, SLC38A9*	0.007
GOTERM_CC_DIRECT	GO:0048179~activin receptor complex	*ACVR1, ACVR1C*	0.008
GOTERM_BP_DIRECT	GO:1902600~hydrogen ion transmembrane transport	*SLC9B1, ATP5MF, SLC9B2*	0.010
GOTERM_CC_DIRECT	GO:0005743~mitochondrial inner membrane	*SPG7, SLC25A12, ATP5MF, SLC9B2*	0.014
GOTERM_CC_DIRECT	GO:0016021~integral component of membrane	*ACVR1, KITLG, FRRS1L, GREB1L, NRXN3, SLC38A9, SPG7, IL6ST, SLC25A12, SLC9B1, ATP5MF, SLC9B2*	0.014
GOTERM_MF_DIRECT	GO:0015385~sodium:proton antiporter activity	*SLC9B1, SLC9B2*	0.015
GOTERM_CC_DIRECT	GO:0030496~midbody	*CENPE, CHMP1A, SHCBP1*	0.016
GOTERM_CC_DIRECT	GO:0005828~kinetochore microtubule	*CENPE, CHMP1A*	0.021
GOTERM_BP_DIRECT	GO:0032924~activin receptor signaling pathway	*ACVR1, ACVR1C*	0.023
GOTERM_CC_DIRECT	GO:0043235~receptor complex	*ACVR1, ACVR1C, IL6ST*	0.023
GOTERM_CC_DIRECT	GO:0097228~sperm principal piece	*SLC9B1, SLC9B2*	0.035
GOTERM_MF_DIRECT	GO:0019838~growth factor binding	*ACVR1C, IL6ST*	0.040
GOTERM_MF_DIRECT	GO:0030020~extracellular matrix structural constituent conferring tensile strength	*COL6A2, COL6A1*	0.045
GOTERM_BP_DIRECT	GO:0007080~mitotic metaphase plate congression	*CENPE, CHMP1A*	0.047
GOTERM_BP_DIRECT	GO:0001755~neural crest cell migration	*ACVR1, KITLG*	0.049

[1]*P* = p-value significant at 0.05; Please note that GOTERM_MF, GOTERM_CC and GOTERM_BP refers to molecular function, cellular component and biological process, respectively.

Discussion

Copper homoeostasis is less efficient in sheep compared to other farm animals like cattle and goats (Haywood et al., 2005). This impairment can more easily lead to copper intoxication or deficiency and is reported to vary within and between breeds (van der Berg

et al., 1983; Suttle et al., 2002; Suttle, 2010). The study of copper related genes is well documented (Tao and Gitlin, 2003; Lutsenko et al., 2007; Barry et al., 2010; Lutsenko, 2010). However, there is scarcity of information on the gene or genes responsible for control of hepatic copper levels for sheep. This study aimed at identifying possible SNP markers and. candidate genes associated with liver copper variation in Merinoland sheep. Measured hepatic copper concentrations were within marginal and normal levels expected for sheep (Puls, 1994). The estimated, high heritability (h^2 ± SE= 0.67 ± 0.29) confirmed that this trait is largely influenced by genetic factors. This value is in the same range as estimated in Merino sheep by Judson et al. (1994) (h^2 ± SE = 0.60 ± 0.32; n =208). However, the high SE for h^2 observed in our study indicates that heritability value may be inflated due to cryptic relatedness since SNP-based heritability is reported to increase with higher number of related samples (Yang et al., 2017). Therefore, further work with a larger sample size of unrelated animals is needed to validate this finding.

Among the candidate genes identified in this study, three genes including *dynein cytoplasmic 1 intermediate chain 2* (*DYNC1I2*), *retromer complex component* (*VPS35*) and *solute carrier family 38 member 9* (*SLC38A9*) located on chromosomes 2, 14 and 16, have been reported to indirectly influence cellular transport and excretion (Rebsamen et al., 2015; Liu, 2017; Wang et al., 2018). The *DYNC1I2* gene expresses a subunit of the cytoplasmic dynein motor protein which is important for microtubule-based transport towards minus end (Pfister, 2015). Cytoplasmic dynein transports cargoes such as cytoskeleton filaments, endosome and lysosome, and has been reported to bind dynactin, an important protein complex associated with dynein activity through its p150Glued subunit (Morgan et al., 2011; McKenney et al., 2014). Likewise, dynactin is reported to interact with the copper P-type ATPase (ATP7B) via its subunit p62 (Lim et al., 2006). Interestingly, lysosomal copper exocytosis has been directly associated with dynactin in a report by Polishchuk et al. (2014). Findings in this report suggest that the targeting of ATP7B to the canalicular surface in hepatocyte cells, which precedes lysosomal exocytosis, requires copper-dependent interaction with p62 dynactin subunit. This suggests that changes in the activity of cytoplasmic dynein motor protein may determine hepatic copper levels by impacting lysosomal exocytosis. Besides VPS29 and VPS26, VPS35 is one of three core proteins of the retromer complex, involved in cargo sorting and endosomal trafficking including the homeostasis of transmembrane proteins

located at the plasma membrane and within endosomes/ lysosomes (Chen et al., 2019). The retromer complex is reported to bind sorting nexin 3 (SNX3) resulting in the cargo recognition and binding of divalent metal transporter 1 (also known as solute carrier family 11 member 2) (Lucas et al., 2016; Chen et al., 2019). The DMT1 has been implicated in copper ion transport in the intestine with a reduced expression resulting in lower copper absorption (Arredondo et al., 2003). In addition, the VPS35 associates with FAM21 (a subunit of the WASH complex) and aids the recruitment of the WASH complex to endosomes (Da Jia et al., 2012; Harbour et al., 2012; Helfer et al., 2013). Findings suggest that copper metabolism MURR1 domain–containing 1 (COMMD1) protein, which functions as a copper chaperone and binds to the copper-transporting P-type ATPases ATP7A/ATP7B (Materia et al., 2012; Phillips-Krawczak et al., 2015), interacts with the WASH complex and modulates copper-dependent trafficking of ATP7A (Phillips-Krawczak et al., 2015). For perspective, the ATP7A is an important copper transporter that regulates the absorption of copper in the intestinal tract (Cox and Moore, 2002). Yeast cells are considered an ideal model for the genetic analysis of mammalian genomes (Zhou et al., 2019; Akram et al., 2020). Interestingly, a report by Sowada et al. (2016) showed increased copper sensitivity of yeast cells lacking VPS35. Therefore, the interaction of VPS35 with the DMT1 and WASH complex may have an influence on liver copper concentration in Merinoland sheep. The *SLC38A9* gene encodes a lysosomal amino acid transporter protein reported in mechanistic target of rapamycin complex 1 (mTORC1) signaling (Rebsamen et al., 2015; Wyant et al., 2017; Lei et al., 2021). The mTORC1 controls transcription factor EB (TFEB) which regulates the expression of genes involved in lysosomal degradation and biogenesis such as vacoular H^+ -ATPase (V-ATPase) and metallothionein 1 (MT1) (Peña-Llopis and Brugarolas, 2011; Nnah et al., 2019). The MT1 protein has been identified as a chaperon involved in copper homoeostasis (Calvo et al., 2017). This indicates that the involvement of SLC38A9 in mTORC1 signaling and TFEB expression may impact liver copper levels in Merinoland sheep. Notably, TFEB expression has been associated with lysosomal copper exocytosis (Polishchuk et al., 2014). In this report, increased TFEB expression in hepatocyte cells resulted in increased lysosomal copper exocytosis suggesting a possible influence of TFEB expression on liver copper exocytosis.

Regarding GO analysis, our findings revealed that lysosomal membrane and midbody were enriched GO terms in this study. Genes observed in these GO terms including *VPS35, SLC38A9* and *charged multivesicular body protein 1 A* (*CHMP1A*) are reportedly involved in cellular transport and excretion (Woodman, 2016; Wyant et al., 2017; Chen et al., 2019). Generally, endosomal sorting complex required for transport (ESCRT) is important for the sorting and delivery of ubiquitinated cargo such as membrane transporters to the lysosome for degradation (Henne et al., 2011). The CHMP1A is the member of the ESCRT-III family required for formation of multivesicular bodies (MVBs), which fuse with lysosomes for the degradation of its content (Tanikawa et al., 2012; Woodman, 2016). Additionally, the ESCRT III is involved in abscission of budding vesicles which mature into MVBs (Henne et al., 2011). These findings suggest a possible influence of ESCRT on the degradation of copper transporters and consequently liver copper concentration. Furthermore, some genes including *matrix AAA peptidase subunit, paraplegin (SPG7)* and *ATP synthase membrane subunit f (ATP5MF)* were observed as functional genes involved in mitochondrial inner membrane, which is a significant GO term observed in this study. The *SPG7* and *ATP5MF* genes are implicated in the opening of the mitochondrial permeability transition pore (PTP) (Bonora et al., 2013; Shanmughapriya et al., 2015; Bonora et al., 2022). The opening of the PTP results in loss of ATP production, mitochondrial swelling and cell death due to cytosolic calcium overload and oxidative stress (Shanmughapriya et al., 2015). Interestingly, another gene (*solute carrier family 25 member 12* (*SLC25A12*)) identified in this GO term is also required for the calcium-dependent maintenance of ATP homoestasis in the mitochondria (Llorente-Folch et al., 2013; Rueda et al., 2016). The mitochondria are important cellular organelles implicated in copper homeostasis (Horn and Barrientos, 2008). Earlier reports suggest that copper toxicity in cells results in swelling and rupture of the mitochondria, as well as induction of oxidation stress (Haywood et al., 2005; Hosseini et al., 2014). According to Bernardi et al. (2006), mitochondrial swelling is associated with changes in the inner mitochondrial membrane permeability and consequent expansion of the inner membrane matrix. In the report by Haywood et al. (2005), mitochondria swelling in hepatocytes from the North Ronaldsay sheep breed, which is considered highly susceptible to copper intoxication, were observed at a lower liver copper concentration when compared to a less susceptible sheep breed

(Cambridge sheep). These observations suggest possible association of hepatic copper levels with gene functions regulating mitochondrial membrane permeability. Finally, the GO terms hydrogen ion transmembrane transport and sodium:proton antiporter activity were also strongly enriched with involved genes such as *solute carrier family 9 member B1* (*SLC9B1*) and *solute carrier family 9 member B2* (*SLC9B2*). These genes encode Na+/H+ exchangers (NHEs) important in cytoplasmic and organelle pH (Anderegg et al., 2022). The *SLC9B1* gene is predominantly expressed in the testis while *SLC9B2* is highly expressed in the liver and brain. In earlier studies on yeast NHE (Nhx1p), it was observed that Nhx1p localized to the trans-Golgi network compartments, late endosomes, and recycling endosomes, is critical for protein sorting and endocytic pathway (Bowers et al., 2000; Kojima et al., 2012). In another report, Nhx1 was found to aid MVB fusion with lysosomes (Karim and Brett, 2018). These findings suggest that NHEs may influence endosomal sorting and trafficking of important copper transporters and consequently copper concentration in hepatocytes.

Conclusions

The results revealed a number of identified SNPs potentially contributing to variability in hepatic copper levels in Merinoland sheep. The identified regions surrounding these SNPs harbor some promising functional candidate genes such as *DYNC1I2*, *VPS35*, *SLC38A9* and *CHMP1A* associated with endosomal cargo sorting and trafficking, as well as lysosomal transport. Additionally, genes such as *SPG7, ATP5MF* and *SLC25A12* were identified as functional genes involved in mitochondrial membrane permeability which has been associated with copper toxicity. Likewise, the genes *SLC9B1* and *SLC9B2* which are involved in luminal and intraluminal pH and MVB fusion to lysosome, were observed as potential candidate genes influencing hepatic copper levels in Merinoland sheep. In total, 9 promising candidate genes were observed in this study. These genes need to be further investigated to ascertain their involvement in liver copper variation in Merinoland sheep in particular, and other sheep breeds in general. This study provides evidence for a polygenic trait with high heritability, and delivers promising clues for further studies to identify potential causal variants that may be associated with variation in copper tolerance in sheep and used for practical breeding.

Funding

This research was funded by the H. Wilhelm Schaumann Stiftung and by the Deutsche Forschungsgemeinschaft (DFG, grant no. 62202147).

Acknowledgments

The authors would like to thank the sheep farmers for providing animal data and samples after slaughter, and Carina Crispens and Stephanie Steitz for technical assistance.

References

Akram, Z., Ahmed, I., Mack, H., Kaur, R., Silva, R.C., Castilho, B.A., Friant, S., Sattlegger, E., Munn, A.L., 2020. Yeast as a Model to Understand Actin-Mediated Cellular Functions in Mammals-Illustrated with Four Actin Cytoskeleton Proteins. Cells 9.

Anderegg, M.A., Gyimesi, G., Ho, T.M., Hediger, M.A., Fuster, D.G., 2022. The Less Well-Known Little Brothers: The SLC9B/NHA Sodium Proton Exchanger Subfamily-Structure, Function, Regulation and Potential Drug-Target Approaches. Frontiers in physiology 13, 898508.

Arredondo, M., Muñoz, P., Mura, C.V., Nùñez, M.T., 2003. DMT1, a physiologically relevant apical Cu1+ transporter of intestinal cells. American journal of physiology. Cell physiology 284, C1525-30.

Barry, A.N., Shinde, U., Lutsenko, S., 2010. Structural organization of human Cu-transporting ATPases: learning from building blocks. Journal of biological inorganic chemistry : JBIC : a publication of the Society of Biological Inorganic Chemistry 15, 47–59.

Benjamini, Y. and Hochberg, Y., 1995. Controlling the False Discovery Rate: A Practical and Powerful Approach to Multiple Testing. Journal of the Royal Statistical Society. Series B (Methodological) 57, 289–300.

Bernardi, P., Krauskopf, A., Basso, E., Petronilli, V., Blalchy-Dyson, E., Di Lisa, F., Forte, M.A., 2006. The mitochondrial permeability transition from in vitro artifact to disease target. The FEBS Journal 273, 2077–2099.

Bonora, M., Bononi, A., Marchi, E. de, Giorgi, C., Lebiedzinska, M., Marchi, S., Patergnani, S., Rimessi, A., Suski, J.M., Wojtala, A., Wieckowski, M.R., Kroemer, G., Galluzzi, L., Pinton, P., 2013. Role of the c subunit of the FO ATP synthase in mitochondrial permeability transition. Cell cycle (Georgetown, Tex.) 12, 674–683.

Bonora, M., Giorgi, C., Pinton, P., 2022. Molecular mechanisms and consequences of mitochondrial permeability transition. Nature reviews. Molecular cell biology 23, 266–285.

Bowers, K., Levi, B.P., Patel, F.I., Stevens, T.H., 2000. The sodium/proton exchanger Nhx1p is required for endosomal protein trafficking in the yeast Saccharomyces cerevisiae. Molecular biology of the cell 11, 4277–4294.

Calvo, J., Jung, H., Meloni, G., 2017. Copper metallothioneins. IUBMB life 69, 236–245.

Chen, K.-E., Healy, M.D., Collins, B.M., 2019. Towards a molecular understanding of endosomal trafficking by Retromer and Retriever. Traffic 20, 465–478.

Cox, D.W., Moore, S.D.P., 2002. Copper Transporting P-Type ATPases and Human Disease. J. Bioenergy. 34, 333–338.

Da Jia, Gomez, T.S., Billadeau, D.D., Rosen, M.K., 2012. Multiple repeat elements within the FAM21 tail link the WASH actin regulatory complex to the retromer. Molecular biology of the cell 23, 2352–2361.

De Bie, P., van de Sluis, B., Klomp, L., Wijmenga, C., 2005. The many faces of the copper metabolism protein MURR1/COMMD1. The Journal of heredity 96, 803–811.

De Sousa, I.K.F., Hamad Minervino, A.H., Sousa, R.D.S., Chaves, D.F., Soares, H.S., Barros, I.d.O., De Araújo, C.A.S.C., Júnior, R.A.B., Ortolani, E.L., 2012. Copper deficiency in sheep with high liver iron accumulation. Veterinary medicine international 2012, 207950.

Dennis, G., Sherman, B.T., Hosack, D.A., Yang, J., Gao, W., Lane, H.C., Lempicki, R.A., 2003. DAVID: Database for Annotation, Visualization, and Integrated Discovery. Genome Biol. 4, R60.

Ding, R., Yang, M., Quan, J., Li, S., Zhuang, Z., Zhou, S., Zheng, E., Hong, L., Li, Z., Cai, G., Huang, W., Wu, Z., Yang, J., 2019. Single-Locus and Multi-Locus Genome-Wide Association Studies for Intramuscular Fat in Duroc Pigs. Frontiers in genetics 10, 619.

Fuentealba, C., Aburto, E.M., 2003. Review: Animal models of copper-associated liver disease. Comparative Hepatology 2, 5–16.

Gogarten, S.M., Sofer, T., Chen, H., Yu, C., Brody, J.A., Thornton, T.A., Rice, K.M., Conomos, M.P., 2019. Genetic association testing using the GENESIS R/Bioconductor package. Bioinformatics (Oxford, England) 35, 5346–5348.

Harbour, M.E., Breusegem, S.Y., Seaman, M.N.J., 2012. Recruitment of the endosomal WASH complex is mediated by the extended 'tail' of Fam21 binding to the retromer protein Vps35. The Biochemical journal 442, 209–220.

Haywood, S., Simpson, D.M., Ross, G., Beynon, R.J., 2005. The greater susceptibility of North Ronaldsay sheep compared with Cambridge sheep to copper-induced oxidative stress, mitochondrial damage and hepatic stellate cell activation. Journal of comparative pathology 133, 114–127.

Helfer, E., Harbour, M.E., Henriot, V., Lakisic, G., Sousa-Blin, C., Volceanov, L., Seaman, M.N.J., Gautreau, A., 2013. Endosomal recruitment of the WASH complex: active sequences and mutations impairing interaction with the retromer. Biology of the cell 105, 191–207.

Henne, W.M., Buchkovich, N.J., Emr, S.D., 2011. The ESCRT pathway. Developmental cell 21, 77–91.

Horn, D., Barrientos, A., 2008. Mitochondrial copper metabolism and delivery to cytochrome c oxidase. IUBMB life 60, 421–429.

Horn, N., Wittung-Stafshede, P., 2021. ATP7A-Regulated Enzyme Metalation and Trafficking in the Menkes Disease Puzzle. Biomedicines 9.

Hosseini, M.-J., Shaki, F., Ghazi-Khansari, M., Pourahmad, J., 2014. Toxicity of copper on isolated liver mitochondria: impairment at complexes I, II, and IV leads to increased ROS production. Cell biochemistry and biophysics 70, 367–381.

Huang, W.D., Sherman, B.T., Lempicki, R.A., 2009a. Bioinformatics enrichment tools: paths toward the comprehensive functional analysis of large gene lists. Nucleic acids research 37, 1–13.

Huang, W.D., Sherman, B.T., Lempicki, R.A., 2009b. Systematic and integrative analysis of large gene lists using DAVID bioinformatics resources. Nature protocols 4, 44–57.

Johnson, R.C., Nelson, G.W., Troyer, J.L., Lautenberger, J.A., Kessing, B.D., Winkler, C.A., O'Brien, S.J., 2010. Accounting for multiple comparisons in a genome-wide association study (GWAS). BMC genomics 11, 724.

Judson, G.J., Walkley, J. R. W., James Peter J., Kleemann David O., Ponzoni R. W., 1994. Genetic variation in trace element status of Merino sheep. Proc. Aust. Soc. Anim. Prod. 20, 438.

Kaler, S.G., 2013. Inborn errors of copper metabolism. Handbook of clinical neurology 113, 1745–1754.

Kang, H.M., Sul, J.H., Service, S.K., Zaitlen, N.A., Kong, S., Freimer, N.B., Sabatti, C., Eskin, E., 2010. Variance component model to account for sample structure in genome-wide association studies. Nature genetics 42, 348–354.

Karim, M.A., Brett, C.L., 2018. The Na+(K+)/H+ exchanger Nhx1 controls multivesicular body–vacuolar lysosome fusion. Molecular biology of the cell 29, 317–325.

Karolchik, D., Hinrichs, A.S., Kent, W.J., 2011. The UCSC Genome Browser. Curr. Protoc. Hum. Genet. Chapter 18, Unit18.6.

Kijas, J.W., Lenstra, J.A., Hayes, B., Boitard, S., Porto Neto, L.R., San Cristobal, M., Servin, B., McCulloch, R., Whan, V., Gietzen, K., Paiva, S., Barendse, W., Ciani, E.,

Raadsma, H., McEwan, J., Dalrymple, B., 2012. Genome-wide analysis of the world's sheep breeds reveals high levels of historic mixture and strong recent selection. PLoS biology 10, e1001258.

Kijas, J.W., Townley, D., Dalrymple, B.P., Heaton, M.P., Maddox, J.F., McGrath, A., Wilson, P., Ingersoll, R.G., McCulloch, R., McWilliam, S., Tang, D., McEwan, J., Cockett, N., Oddy, V.H., Nicholas, F.W., Raadsma, H., 2009. A genome wide survey of SNP variation reveals the genetic structure of sheep breeds. PloS one 4, e4668.

Knowles, S.O., ROUNCE, J.R., GRACE, N.D., Lee, J.H., 1998. Variation in copper metabolism between two flocks of Romney sheep in response to increasing dietary copper.

Kojima, A., Toshima, J.Y., Kanno, C., Kawata, C., Toshima, J., 2012. Localization and functional requirement of yeast Na+/H+ exchanger, Nhx1p, in the endocytic and protein recycling pathway. Biochimica et biophysica acta 1823, 534–543.

Kumaratilake, J.S., 2014. Chronic Copper Poisoning in Sheep: Liver Injury. JTEA.

Lakhssassi, K., Lahoz, B., Sarto, P., Iguácel, L.P., Folch, J., Alabart, J.L., Serrano, M., Calvo, J.H., 2021. Genome-Wide Association Study Demonstrates the Role Played by the CD226 Gene in Rasa Aragonesa Sheep Reproductive Seasonality. Animals : an open access journal from MDPI 11.

Lei, H.-T., Mu, X., Hattne, J., Gonen, T., 2021. A conformational change in the N terminus of SLC38A9 signals mTORC1 activation. Structure (London, England : 1993) 29, 426-432.e8.

Li, C., Fu, Y., Sun, R., Wang, Y., Wang, Q., 2018. Single-Locus and Multi-Locus Genome-Wide Association Studies in the Genetic Dissection of Fiber Quality Traits in Upland Cotton (Gossypium hirsutum L.). Frontiers in plant science 9, 1083.

Lim, C.M., Cater, M.A., Mercer, J.F.B., La Fontaine, S., 2006. Copper-dependent interaction of dynactin subunit p62 with the N terminus of ATP7B but not ATP7A. J. Biol. Chem. 281, 14006–14014.

Liu, J.-J., 2017. Regulation of dynein-dynactin-driven vesicular transport. Traffic (Copenhagen, Denmark) 18, 336–347.

Llorente-Folch, I., Rueda, C.B., Amigo, I., Del Arco, A., Saheki, T., Pardo, B., Satrústegui, J., 2013. Calcium-regulation of mitochondrial respiration maintains ATP homeostasis and requires ARALAR/AGC1-malate aspartate shuttle in intact cortical neurons. The Journal of neuroscience : the official journal of the Society for Neuroscience 33, 13957-71, 13971a.

Lucas, M., Gershlick, D.C., Vidaurrazaga, A., Rojas, A.L., Bonifacino, J.S., Hierro, A., 2016. Structural Mechanism for Cargo Recognition by the Retromer Complex. Cell 167, 1623-1635.e14.

Lutsenko, S., 2010. Human copper homeostasis: a network of interconnected pathways. Current opinion in chemical biology 14, 211–217.

Lutsenko, S., Barnes, N.L., Bartee, M.Y., Dmitriev, O.Y., 2007. Function and regulation of human copper-transporting ATPases. Physiological reviews 87, 1011–1046.

Marees, A.T., Kluiver, H. de, Stringer, S., Vorspan, F., Curis, E., Marie-Claire, C., Derks, E.M., 2018. A tutorial on conducting genome-wide association studies: Quality control and statistical analysis. International journal of methods in psychiatric research 27, e1608.

Materia, S., Cater, M.A., Klomp, L.W.J., Mercer, J.F.B., La Fontaine, S., 2012. Clusterin and COMMD1 independently regulate degradation of the mammalian copper ATPases ATP7A and ATP7B. J. Biol. Chem. 287, 2485–2499.

McKenney, R.J., Huynh, W., Tanenbaum, M.E., Bhabha, G., Vale, R.D., 2014. Activation of cytoplasmic dynein motility by dynactin-cargo adapter complexes. Science (New York, N.Y.) 345, 337–341.

Morgan, J.L., Song, Y., Barbar, E., 2011. Structural dynamics and multiregion interactions in dynein-dynactin recognition. J. Biol. Chem. 286, 39349–39359.

Nelson, C.P., Goel, A., Butterworth, A.S., Kanoni, S., Webb, T.R., Marouli, E., Zeng, L., Ntalla, I., Lai, F.Y., Hopewell, J.C., Giannakopoulou, O., Jiang, T., Hamby, S.E., Di Angelantonio, E., Assimes, T.L., Bottinger, E.P., Chambers, J.C., Clarke, R., Palmer, C.N.A., Cubbon, R.M., Ellinor, P., Ermel, R., Evangelou, E., Franks, P.W., Grace, C., Gu, D., Hingorani, A.D., Howson, J.M.M., Ingelsson, E., Kastrati, A., Kessler, T., Kyriakou, T., Lehtimäki, T., Lu, X., Lu, Y., März, W., McPherson, R., Metspalu, A., Pujades-Rodriguez, M., Ruusalepp, A., Schadt, E.E., Schmidt, A.F., Sweeting, M.J., Zalloua, P.A., AlGhalayini, K., Keavney, B.D., Kooner, J.S., Loos, R.J.F., Patel, R.S., Rutter, M.K., Tomaszewski, M., Tzoulaki, I., Zeggini, E., Erdmann, J., Dedoussis, G., Björkegren, J.L.M., Schunkert, H., Farrall, M., Danesh, J., Samani, N.J., Watkins, H., Deloukas, P., 2017. Association analyses based on false discovery rate implicate new loci for coronary artery disease. Nature genetics 49, 1385–1391.

Nnah, I.C., Wang, B., Saqcena, C., Weber, G.F., Bonder, E.M., Bagley, D., Cegli, R. de, Napolitano, G., Medina, D.L., Ballabio, A., Dobrowolski, R., 2019. TFEB-driven endocytosis coordinates MTORC1 signaling and autophagy. Autophagy 15, 151–164.

Öztan, S., Düring, R.-A., 2012. Microwave assisted EDTA extraction-determination of pseudo total contents of distinct trace elements in solid environmental matrices. Talanta 99, 594–602.

Peña-Llopis, S., Brugarolas, J., 2011. TFEB, a novel mTORC1 effector implicated in lysosome biogenesis, endocytosis and autophagy. Cell cycle (Georgetown, Tex.) 10, 3987–3988.

Pfister, K.K., 2015. Distinct functional roles of cytoplasmic dynein defined by the intermediate chain isoforms. Experimental cell research 334, 54–60.

Phillips-Krawczak, C.A., Singla, A., Starokadomskyy, P., Deng, Z., Osborne, D.G., Li, H., Dick, C.J., Gomez, T.S., Koenecke, M., Zhang, J.-S., Dai, H., Sifuentes-Dominguez, L.F., Geng, L.N., Kaufmann, S.H., Hein, M.Y., Wallis, M., McGaughran, J., Gecz, J., van Sluis, B. de, Billadeau, D.D., Burstein, E., 2015. COMMD1 is linked to the WASH complex and regulates endosomal trafficking of the copper transporter ATP7A. Molecular biology of the cell 26, 91–103.

Polishchuk, E.V., Concilli, M., Iacobacci, S., Chesi, G., Pastore, N., Piccolo, P., Paladino, S., Baldantoni, D., van IJzendoorn, S.C.D., Chan, J., Chang, C.J., Amoresano, A., Pane, F., Pucci, P., Tarallo, A., Parenti, G., Brunetti-Pierri, N., Settembre, C., Ballabio, A., Polishchuk, R.S., 2014. Wilson disease protein ATP7B utilizes lysosomal exocytosis to maintain copper homeostasis. Developmental cell 29, 686–700.

Puls, R., 1994. Mineral Levels in Animal Health: Diagnostic Data. Sherpa International.

R Core Team, 2023. R: A Language and Environment for Statistical Computing, Vienna, Austria. https://www.R-project.org/. Accessed 20 January 2023.

Rebsamen, M., Pochini, L., Stasyk, T., Araújo, M.E.G. de, Galluccio, M., Kandasamy, R.K., Snijder, B., Fauster, A., Rudashevskaya, E.L., Bruckner, M., Scorzoni, S., Filipek, P.A., Huber, K.V.M., Bigenzahn, J.W., Heinz, L.X., Kraft, C., Bennett, K.L., Indiveri, C., Huber, L.A., Superti-Furga, G., 2015. SLC38A9 is a component of the lysosomal amino acid sensing machinery that controls mTORC1. Nature 519, 477–481.

Ren, W.-L., Wen, Y.-J., Dunwell, J.M., Zhang, Y.-M., 2018. pKWmEB: integration of Kruskal-Wallis test with empirical Bayes under polygenic background control for multi-locus genome-wide association study. Heredity 120, 208–218.

Rivals, I., Personnaz, L., Taing, L., Potier, M.-C., 2007. Enrichment or depletion of a GO category within a class of genes: which test? Bioinformatics (Oxford, England) 23, 401–407.

Rueda, C.B., Llorente-Folch, I., Gonzalez-Sanchez, P., Contreras, L., Juaristi, I., Martinez-Valero, P., Pardo, B., Del Arco, A., Satrustegui, J., 2016. Glutamate excitotoxicity and Ca2+-regulation of respiration: Role of the Ca2 + activated mitochondrial transporters (CaMCs). Biochimica et Biophysica Acta (BBA) - Bioenergetics 1857, e17-e18.

Segura, V., Vilhjálmsson, B.J., Platt, A., Korte, A., Seren, Ü., Long, Q., Nordborg, M., 2012. An efficient multi-locus mixed-model approach for genome-wide association studies in structured populations. Nature genetics 44, 825–830.

Shanmughapriya, S., Rajan, S., Hoffman, N.E., Higgins, A.M., Tomar, D., Nemani, N., Hines, K.J., Smith, D.J., Eguchi, A., Vallem, S., Shaikh, F., Cheung, M., Leonard, N.J., Stolakis, R.S., Wolfers, M.P., Ibetti, J., Chuprun, J.K., Jog, N.R., Houser, S.R., Koch, W.J., Elrod, J.W., Madesh, M., 2015. SPG7 Is an Essential and Conserved Component of the Mitochondrial Permeability Transition Pore. Molecular cell 60, 47–62.

Sowada, N., Stiller, B., Kubisch, C., 2016. Increased copper toxicity in Saccharomyces cerevisiae lacking VPS35, a component of the retromer and monogenic Parkinson disease gene in humans. Biochemical and biophysical research communications 476, 528–533.

Suttle, N.F., 2010. Mineral nutrition of livestock, 4th ed. CABI, Wallingford, Cambridge, Mass., 255-305.

Suttle, N.F., Jones, D.G., 2007. Miconutrient imbalance. In: Aitken I. D. (Ed.), Diseases of sheep, 4th ed. Blackwell, Oxford, pp. 377–394.

Suttle, N.F., Lewis, R.M., Small, J.N.W., 2002. Effects of breed and family on rate of copper accretion in the liver of purebred Charollais, Suffolk and Texel lambs. Anim. Sci. 75, 295–302.

Tamba, C.L., Ni, Y.-L., Zhang, Y.-M., 2017. Iterative sure independence screening EM-Bayesian LASSO algorithm for multi-locus genome-wide association studies. PLoS computational biology 13, e1005357.

Tamba, C.L., Zhang, Y.-M., 2018. A fast mrMLM algorithm for multi-locus genome-wide association studies. bioRxiv.

Tanikawa, S., Mori, F., Tanji, K., Kakita, A., Takahashi, H., Wakabayashi, K., 2012. Endosomal sorting related protein CHMP2B is localized in Lewy bodies and glial cytoplasmic inclusions in α-synucleinopathy. Neuroscience letters 527, 16–21.

Tao, T.Y., Gitlin, J.D., 2003. Hepatic copper metabolism: insights from genetic disease. Hepatology (Baltimore, Md.) 37, 1241–1247.

Uffelmann, E., Huang, Q.Q., Munung, N.S., Vries, J. de, Okada, Y., Martin, A.R., Martin, H.C., Lappalainen, T., Posthuma, D., 2021. Genome-wide association studies. Nat Rev Methods Primers 1.

Underwood, E.J., Suttle, N.F., 1999. The mineral nutrition of livestock, 3rd ed. CABI, Wallingford, Cambridge, Mass., 283-342.

van der Berg, R., Levels, F.H., van der Schee, W., 1983. Breed differences in sheep with respect to the accumulation of copper in the liver. Veterinary Quarterly 5, 26–31.

Wang, J., Fedoseienko, A., Chen, B., Burstein, E., Da Jia, Billadeau, D.D., 2018. Endosomal receptor trafficking: Retromer and beyond. Traffic (Copenhagen, Denmark) 19, 578–590.

Wang, S.-B., Feng, J.-Y., Ren, W.-L., Huang, B., Zhou, L., Wen, Y.-J., Zhang, J., Dunwell, J.M., Xu, S., Zhang, Y.-M., 2016. Improving power and accuracy of genome-wide association studies via a multi-locus mixed linear model methodology. Sci Rep. 6, 19444.

Wang, Y., Ding, X., Tan, Z., Ning, C., Xing, K., Yang, T., Pan, Y., Sun, D., Wang, C., 2017. Genome-Wide Association Study of Piglet Uniformity and Farrowing Interval. Frontiers in genetics 8, 194.

Wen, Y.-J., Zhang, H., Ni, Y.-L., Huang, B., Zhang, J., Feng, J.-Y., Wang, S.-B., Dunwell, J.M., Zhang, Y.-M., Wu, R., 2017. Methodological implementation of mixed linear models in multi-locus genome-wide association studies. Briefings in bioinformatics 18, 906.

Woodman, P., 2016. ESCRT-III on endosomes: new functions, new activation pathway. The Biochemical journal 473, e5-8.

Woolliams, J.A., Woolliams, C., Suttle, N.F., Jones, D.G., Wiener, G., 1986. Studies on lambs from lines genetically selected for low and high copper status 2. Incidence of hypocuprosis on improved hill pasture. Anim. Sci. 43, 303–317.

Wyant, G.A., Abu-Remaileh, M., Wolfson, R.L., Chen, W.W., Freinkman, E., Danai, L.V., Vander Heiden, M.G., Sabatini, D.M., 2017. mTORC1 Activator SLC38A9 Is Required to Efflux Essential Amino Acids from Lysosomes and Use Protein as a Nutrient. Cell 171, 642-654.e12.

Yang, J., Zaitlen, N.A., Goddard, M.E., Visscher, P.M., Price, A.L., 2014. Advantages and pitfalls in the application of mixed-model association methods. Nature genetics 46, 100–106.

Yang, J., Zeng, J., Goddard, M.E., Wray, N.R., Visscher, P.M., 2017. Concepts, estimation and interpretation of SNP-based heritability. Nature genetics 49, 1304–1310.

Yilmaz, O., Kizilaslan, M., Arzik, Y., Behrem, S., Ata, N., Karaca, O., Elmaci, C., Cemal, I., 2022. Genome-wide association studies of preweaning growth and in vivo carcass composition traits in Esme sheep. Journal of animal breeding and genetics = Zeitschrift fur Tierzuchtung und Zuchtungsbiologie 139, 26–39.

Zhang, J., Feng, J.-Y., Ni, Y.-L., Wen, Y.-J., Niu, Y., Tamba, C.L., Yue, C., Song, Q., Zhang, Y.-M., 2017. pLARmEB: integration of least angle regression with empirical Bayes for multilocus genome-wide association studies. Heredity 118, 517–524.

Zhang, Y.-W., Tamba, C.L., Wen, Y.-J., Li, P., Ren, W.-L., Ni, Y.-L., Gao, J., Zhang, Y.-M., 2020. mrMLM v4.0.2: An R Platform for Multi-locus Genome-wide Association Studies. Genomics, proteomics & bioinformatics 18, 481–487.

Zhao, Y., Pu, Y., Liang, B., Bai, T., Liu, Y., Jiang, L., Ma, Y., 2022. A study using single-locus and multi-locus genome-wide association study to identify genes associated with teat number in Hu sheep. Animal Genetics 53, 203–211.

Zhou, F.-L., Li, S.C., Zhu, Y., Guo, W.-J., Shao, L.-J., Nelson, J., Simpkins, S., Yang, D.-H., Liu, Q., Yashiroda, Y., Xu, J.-B., Fan, Y.-Y., Yue, J.-M., Yoshida, M., Xia, T., Myers, C.L., Boone, C., Wang, M.-W., 2019. Integrating yeast chemical genomics and mammalian cell pathway analysis. Acta pharmacologica Sinica 40, 1245–1255.

Zhou, X., Stephens, M., 2012. Genome-wide efficient mixed-model analysis for association studies. Nature genetics 44, 821–824.

APPENDIX

Table S1a. Nutrient composition of compound feed fed to Merinoland sheep on farm 1.

Parameter *	Amount (%)
Moisture	10.10
Crude protein	15.00
Fat	2.60
Crude fiber	11.50
Ash	6.80
Neutral detergent fiber	25.00

*Analysis performed by Intertek Food Services GmbH

Table S1b. Mineral content of grass, compound feed and pasture grass fed to Merinoland sheep on farm 1 and 2.

Mineral* (mg/kg DM)	Grass[1]	Compound feed[1]	Pasture grass[2]
Cu	11.80	7.10	9.60
Zn	52.00	75.30	32.50
Fe	746.00	338.00	103.00
Mo	1.21	0.57	3.78
Mn	181.00	72.20	16.20

*Analysis performed by Intertek Food Services GmbH; [1]Farm 1; [2]Farm 2

Table S2. Operating conditions for microwave assisted extraction of freeze-dried liver samples.

Step	Power (W)	Limit Temp. (°C)	Holding time (min)
1	250	80	1
2	850	150	5
3	850	150	12
Ventilation/cooling			30

Table S3. Significant SNPs associated with liver Cu concentration in Merinoland sheep detected by ML-GWAS analysis methods (LOD score > 3).

Method	SNP	Chromosome	Position	QTN effect	LOD score	r2 (%)
mrMLM	OAR1_82047913.1	1	76716240	16.36	3.87	6.77
mrMLM	s62875.1	2	150905130	19.77	5.11	10.98
mrMLM	s05644.1	2	14172465	-23.61	8.35	17.15
mrMLM	OAR3_132833292.1	3	124516955	-17.57	3.50	8.76
mrMLM	OAR7_101357352.1	7	93147667	-17.41	4.59	8.01
mrMLM	s53902.1	8	26160457	-17.69	4.70	7.91
mrMLM	s63605.1	8	9646944	14.84	4.10	5.56
mrMLM	s42079.1	9	55632383	-19.78	6.75	9.38
FASTmrMLM	s66850.1	1	77025732	-18.31	9.27	9.47
FASTmrMLM	OAR1_285395930.1	1	263664109	6.66	3.61	1.23
FASTmrMLM	s05644.1	2	14172465	-14.57	5.09	7.55
FASTmrMLM	OAR2_209399752.1	2	197824613	12.65	5.29	4.89
FASTmrMLM	OAR3_132833292.1	3	124516955	-12.72	4.42	5.31
FASTmrMLM	OAR4_77358490.1	4	73042599	-9.68	3.56	2.69
FASTmrMLM	s42668.1	6	21789865	10.63	3.90	3.19
FASTmrMLM	OAR6_47263223.1	6	42315913	-10.90	3.19	3.86
FASTmrMLM	s25674.1	7	87187746	-14.66	7.51	6.98
FASTmrMLM	OAR13_65858135.1	13	60516573	10.27	4.23	3.23
FASTmrMLM	OAR16_25377664_X.1	16	23278766	22.81	6.30	12.28
FASTmrMLM	OAR23_37101686.1	23	35080540	12.29	5.25	5.35
FASTmrMLM	s55689.1	24	40674922	-17.36	6.95	9.08
FASTmrEMMA	s66850.1	1	77025732	-38.44	7.15	7.80
FASTmrEMMA	OAR2_145591151.1	2	136897136	-31.48	4.99	5.33
FASTmrEMMA	OAR4_77358490.1	4	73042599	-22.20	3.19	2.92
FASTmrEMMA	OAR6_47263223.1	6	42315913	-32.49	3.67	4.68
FASTmrEMMA	s25674.1	7	87187746	-23.26	3.86	3.05
FASTmrEMMA	OAR7_101357352.1	7	93147667	-30.86	5.17	5.75
FASTmrEMMA	OAR14_14650208.1	14	14404415	-28.17	4.46	4.38

r2 (%) proportion of total phenotypic variation explained by Quantitative trait nucleotides (QTNs)

Table S3. (continued)

Method	SNP	Chromosome	Position	QTN effect	LOD score	r2 (%)
pLARmEB	s66850.1	1	77025732	-9.81	4.46	2.06
pLARmEB	OAR1_285395930.1	1	263664109	10.90	7.33	2.49
pLARmEB	s05644.1	2	14172465	-16.86	10.79	7.65
pLARmEB	OAR2_145591151.1	2	136897136	-8.81	3.80	2.02
pLARmEB	OAR3_126004681.1	3	117982174	-11.05	6.19	3.31
pLARmEB	OAR3_132833292.1	3	124516955	-9.01	4.35	2.02
pLARmEB	s19082.1	3	162336610	-14.23	10.25	4.62
pLARmEB	s42668.1	6	21789865	12.69	8.28	3.44
pLARmEB	OAR6_47263223.1	6	42315913	-23.94	18.45	14.08
pLARmEB	OAR6_68186441.1	6	61990819	-10.80	6.16	2.54
pLARmEB	s25674.1	7	87187746	-15.35	11.76	5.79
pLARmEB	OAR13_58466890.1	13	53657897	-15.07	3.64	2.37
pLARmEB	s23482.1	13	78241135	-11.34	6.39	3.42
pLARmEB	s02342.1	16	7056519	10.00	3.94	2.24
pLARmEB	OAR16_25377664_X.1	16	23278766	18.98	7.19	6.43
pLARmEB	s63540.1	22	12110759	-13.96	8.71	5.27
pLARmEB	OAR23_37101686.1	23	35080540	6.94	3.56	1.29
ISIS EM-BLASSO	s45507.1	1	60949585	8.26	4.16	2.14
ISIS EM-BLASSO	s66850.1	1	77025732	-13.96	5.59	5.26
ISIS EM-BLASSO	OAR1_261769723.1	1	242156016	9.32	3.49	2.82
ISIS EM-BLASSO	OAR1_285395930.1	1	263664109	9.94	4.53	2.62
ISIS EM-BLASSO	s32732.1	2	127994859	14.79	6.45	5.45
ISIS EM-BLASSO	OAR4_77358490.1	4	73042599	-10.14	3.88	2.82
ISIS EM-BLASSO	OAR6_47263223.1	6	42315913	-19.35	8.52	11.62
ISIS EM-BLASSO	OAR7_101357352.1	7	93147667	-17.70	10.09	9.15
ISIS EM-BLASSO	s14128.1	12	69110592	16.02	6.37	8.45
ISIS EM-BLASSO	OAR14_14650208.1	14	14404415	-16.99	9.01	8.76
ISIS EM-BLASSO	OAR18_59466542.1	18	55568095	-10.79	5.09	3.57
ISIS EM-BLASSO	OAR25_33621277.1	25	32127214	-14.13	4.83	6.57
ISIS EM-BLASSO	OAR25_43838949.1	25	41318475	-19.55	8.31	9.73

r2 (%) proportion of total phenotypic variation explained by Quantitative trait nucleotides (QTNs)

3. Genome-wide comparative analyses for selection signatures indicate candidate genes for between-breed variability in copper accretion in sheep

O. O. Adeniyi [a], J. A. Lenstra [b], S. Mastrangelo [c], G. Lühken [a]

[a] Institute of Animal Breeding and Genetics, Justus Liebig University of Giessen, Ludwigstrasse 21,35390 Giessen, Germany

[b] Faculty of Veterinary Medicine, Utrecht University, Yalelaan 104, 3584CM Utrecht, The Netherlands

[c] Department of Agricultural, Food and Forest Sciences, University of Palermo, Viale delle Scienze, 90128 Palermo (PA), Italy

Published in:
animal 18 (10), p. 101329. DOI: 10.1016/j.animal.2024.101329

Received: 29 May 2024
Accepted: 10 September 2024

Abstract

The problem of copper (**Cu**) intoxication and deficiency continues to impact economic gains and animal welfare in sheep husbandry. This study investigated the ovine genome for regions and potential genes under selection for Cu accretion between sheep breeds. For this, we compared ovine single nucleotide polymorphism (**SNP**) data of three Cu-susceptible breeds with three Cu-tolerant breeds. After merging SNP data of breeds and removal of related individuals, a total of 229 sheep and 45 640 autosomal SNPs were left. Then, we selected 14 individuals per breed into two datasets (datasets 1 and 2) for analysis of selection signatures using the Fixation index, cross-population extended haplotype homozygosity and haplotype-based FLK methods. Selection regions shared by both datasets detected by at least two methods revealed regions on OAR 4, 8 and 11 containing 54 candidate genes under selection for Cu accretion. Enrichment analysis revealed that 19 gene ontologies and 1 enriched Kyoto encyclopaedia of genes and genomes pathway terms were associated with the candidate genes under selection. Genes such as *TP53*, *TNFSF13*, *TNFSF12*, *ALOX15*, *ALOX12*, *EIF5A* and *PREP* are associated with the regulation of Cu homeostasis, programmed cell death or inflammatory response. We also found an enrichment of arachidonate 15-lipoxygenase activity, arachidonate 12-lipoxygenase activity and ferroptosis that influence cellular inflammation and cell death. These results shed light on ovine genomic regions under selection for Cu accretion and provide information on candidate genes for further studies on breed differences in ovine Cu accretion.

Keywords: Ovine, Copper accumulation, Selection signals, Genomic regions, Single nucleotide polymorphism

Implications

Copper intoxication and deficiency in sheep may be fatal and result in severe economic losses to sheep farmers. Sheep breeds vary widely in their accumulation of copper with the attendant need for varying levels of copper supplementation to prevent intoxication and deficiency. In this study, we investigated the genetic basis for differences in copper

accretion between copper-tolerant and copper-susceptible sheep breeds by assessing signatures of selection. We observed candidate regions and genes that may help to understand the genetic basis for variability in copper accretion and reduce the incidence of copper-related diseases in sheep husbandry.

Introduction

Copper (**Cu**) is a trace mineral element that is essential for the function of several enzymes (Suttle, 2010). However, it results in toxicity and sudden death when consumed in excess. Among ruminants, sheep are known to be impaired in their ability to excrete excess Cu from the liver, thereby leading to increased susceptibility to Cu intoxication (Haywood et al., 2005). Cu poisoning in sheep ensues from exposure to toxic or non- toxic levels of Cu through food ingestion that lead to Cu accretion in the liver, as reviewed by Borobia et al. (2022). On the other hand, some sheep breeds are reportedly prone to Cu deficiency when compared with others (Wiener, 1979). Several studies show that body Cu levels depend not only on dietary Cu (van der Berg et al., 1983), but also on the age (Woolliams et al., 1982), on the breed (van der Berg et al., 1983) and on the presence of Cu antagonists such as molybdenum (Mo) (Suttle and Field, 1983). Existing documented information on breed differences in liver Cu accumulation date back to the 1960's. An initial study by Wiener and Field (1969) revealed significantly lower fitted liver Cu values for Scottish Blackface (14.3) compared to Welsh Mountain sheep (49.7) fed on the same pasture. Variations in liver (antilog of least squares means of $\log_{10}$ liver Cu concentration) and blood (µg/100ml) Cu concentrations reported by G. Wiener et al. (1976) were low for Scottish Blackface (Liver Cu = 24.7, blood Cu = 92.3), intermediate for Cheviot (Liver Cu = 31.5, blood Cu = 99.2) and high for Welsh Mountain (Liver Cu =65.8, blood Cu = 111.3), under similar environmental conditions, age and dietary Cu content. Likewise, Woolliams et al. (1982) found liver copper levels (mg Cu /kg DM) highest in Texel (1491.5), followed by Suffolk (1116.1), intermediate levels for East Friesian (754.2) and Finnish Landrace (766.7) and again low levels for Scottish Blackface (567.1) sheep fed similar Cu concentration in the diet. Similar findings by other authors confirm differences between breeds in hepatic Cu accretion for sheep when exposed to the same dietary Cu level (van

der Berg et al., 1983; Suttle et al., 2002). All these studies suggest that Cu accretion is influenced by genetic factors.

Haywood et al. (2005) identified that hepatocytes of the Cu-susceptible North Ronaldsay sheep have a higher sensitivity to oxidative injury than the Cu-tolerant Cambridge sheep. Additionally, the report revealed that antioxidant protein-1 was increased 4 to 5 fold in the hepatic cytosol of the North Ronaldsay (but not Cambridge) sheep implying increased sensitivity of the mitochondria to Cu-induced oxidative stress. Simpson et al. (2006) also pointed to the involvement of mitochondria in the sensitivity of this sheep breed to Cu-induced oxidative stress. This report identified a high expression of Cu-responsive proteins such as cathepsin D, ferritin light chain, peroxiredoxin 3 and plasma retinol-binding protein in North Ronaldsay sheep whereas high levels of epoxide hydrolase and methionine adenosine transferase were observed in Cambridge sheep. These findings indicate that some biological processes modulated by genes influence Cu susceptibility or tolerance among sheep breeds.

Furthermore, several studies identified the involvement of genes such as copper transporter 1 (*CTR1*), chaperone for superoxide dismutase 1 (*CCS*), antioxidant 1 (*ATOX1*), synthesis of cytochrome c oxidase 1 (*SCO1*), synthesis of cytochrome c oxidase 2 (*SCO2*), metallothionein (*MT*), copper-transporting ATPase 1 (*ATP7A*) and copper-transporting ATPase 2 (*ATP7B*) in cellular Cu transport, circulation and distribution (Tao and Gitlin, 2003; Leary et al., 2004; Lutsenko et al., 2007; Barry et al., 2010; Lutsenko, 2010; Kaler, 2013). A comparison of the Cu-tolerant Simmental with the less Cu-tolerant Angus cows showed only for *CTR1 a* significant difference in liver expression, but not for other Cu-metabolism genes such as *ATOX1, ATP7A* and *ATP7B* (Fry et al., 2013).

The genome-wide single nucleotide polymorphism (**SNP**) genotyping allowed the development of various methods in order to identify selection signals within the genome. Selection signatures are genomic regions that were the main targets of selective breeding and may correspond to the differences in breed/populations (Saravanan et al., 2020). For this study, we employed genomic scans of the Fixation index ($\mathbf{F_{ST}}$) (Flori et al., 2009), cross-population extended haplotype homozygosity (**XP-EHH**) (Sabeti et al., 2007) and haplotype-based FLK (**hapFLK**) (Fariello et al., 2013) methods that allow the localisation

of candidate selection sweeps within the genome. Unlike other methods such as Tajima's D and composite likelihood ratio which detect intra-population selections signals, the methods selected for this study aid the detection of inter-population selection signatures (Saravanan et al., 2020). Both XP-EHH and hapFLK statistics are based on homozygosity and differentiation of haplotypes, respectively. In combination with the genomic F_{ST} scan, this allows the detection of selection signals that overlap across methods.

Despite available information on the Cu accretion status of some sheep breeds, there has been no genome-wide approach trying to unravel the genetic architecture influencing between-breed variability in the Cu accretion of sheep. We recently published a study that identified candidate genes associated with liver Cu concentration within the Merino Land sheep (Adeniyi et al., 2023). However, genes and genetic regions associated with breed-dependent variations in Cu accretion of sheep have not yet been investigated. In this study, genome-wide information from the SNP genotypes and three different approaches (F_{ST}, XP-EHH and hapFLK) were used in comparative analyses to identify selection signals associated with Cu accretion in sheep. For this purpose, we grouped sheep breeds according to susceptibility or tolerance to Cu using available published information on breed differences in liver Cu accumulation. The aim of this study was to reveal genes and genomic regions that influence between-breed variation in Cu accretion and aid in the selection for reduced incidence of Cu toxicity or deficiency in sheep.

Material and methods

Animal and genomic data collection

Illumina Ovine 50K SNP BeadChip genotyping data was retrieved from published sources for the sheep breeds including Scottish Texel (n= 80), Finnsheep (n= 96), Irish Suffolk (n= 55), Scottish Blackface (n= 56) (Kijas et al., 2012) and Welsh Mountain Hill flock (n= 24) (Beynon et al., 2015). Additionally, new SNP data for Scottish Blackface (n= 43) and German Grey Hearth (n= 14) are included in the dataset (Supplementary Table S1). These datasets were merged using PLINK v1.90 (Chang et al., 2015) and checked for relatedness which was estimated using –related option in KING v2.2.4 (Manichaikul et al., 2010). Prior to this, chromosomes and positions of SNPs were referred to the Oar_v4.0

Ovis aries genome assembly using the commands --update-map and --update-chr in PLINK v1.90. We excluded one of each pair of sheep within a breed with an Identity-by-descent > 0.30. A total of 229 sheep and 45 640 autosomal SNPs were left for further analysis (Supplementary Table S1).

Breed grouping for selection signature analysis

Prior to the performance of F_{ST}, XP-EHH and hapFLK analysis, the sheep breeds in our data were grouped according to Cu accretion, namely Cu-susceptible and Cu-tolerant based on the published reports (Wiener and Field, 1969; Herbert et al., 1978; Woolliams et al., 1982; van der Berg et al., 1983; Meyer and Coenen, 1994; Borobia et al., 2022). The breeds Scottish Texel and Irish Suffolk were considered as Cu-susceptible , whereas Finnsheep and Scottish Blackface were regarded as Cu-tolerant breeds (Woolliams et al., 1982; van der Berg et al., 1983) (Table 1). In addition, we classified the Welsh Mountain Hill flock and German Grey Hearth as Cu-susceptible and Cu-tolerant, respectively. This is based on published information comparing the Welsh Mountain Hill flock with Scottish Blackface (Wiener and Field, 1969; G. Wiener et al., 1976; Herbert et al., 1978), and German Grey Hearth with Texel (Meyer and Coenen, 1994) (Table 1). To avoid samples size bias due to the lower number of samples for the German Grey Hearth (n = 14), Welsh Mountain Hill flock (n = 14) and Scottish Texel (n = 20) breeds, after merging and removal of related samples, a subset of our data consisting of all Welsh Mountain Hill flock and German Grey Hearth samples, as well as 14 selected sheep from each of the other four breeds (Finnsheep, Irish Suffolk, Scottish Blackface and Scottish Texel) were included for analysis of selection signatures (dataset 1). We repeated the analyses with a different subset of Finnsheep, Irish Suffolk, and Scottish Blackface samples (dataset 2). For Scottish Texel samples in dataset 2, we included 8 samples from the first data subset to the 6 Scottish Texel samples remaining after initial selection for dataset 1. Both datasets contain 84 individuals.

Quality control of datasets

The data subsets (Supplementary Table S2) were filtered for quality control by the removal of loci with minor allele frequency (<1%), SNPs with a low call rate (<95%) and animals with more than 5% of missing genotypes using PLINK v1.90. A total of 45 080 and

45 076 autosomal SNPs remained in the datasets for genomic-based determination of selection signals after quality control for dataset 1 and 2, respectively (Supplementary Table S2). In addition, no sample was excluded from both datasets after quality control.

Table 1. Overview of published information on differences in liver copper (Cu) accretion (mg Cu/Kg DM) for Cu-tolerant and Cu-susceptible sheep breeds in this study.

Sources	Cu content of diet (mg Cu/kg DM)	Breeds[1]						Days of feeding
		Cu-tolerant			Cu-susceptible			
		Finnsheep	Blackface	German Hearth	Texel	Suffolk	Welsh Mountain	
Woolliams et al. (1982)	12	408.8	291.6	-	695.6	615.2	-	91
Woolliams et al. (1982)	20	766.7	567.9	-	1 491.5	1 116.1	-	91
van der Berg et al. (1983)	10	225	-	-	775	-	-	103
van der Berg et al. (1983)	34	486	-	-	1 652	-	-	103
Herbert et al. (1978)	30	-	240	-	-	-	316	105
Wiener and Field (1969)[2]	-	-	14.3	-	-	-	49.7	-
G. Wiener et al. (1976)[3]	-	-	24.7	-	-	-	65.8	168
Meyer and Coenen (1994)[4]	-	-	-	< 50	> 500	-	-	-

[1] This column contains liver Cu values for all breeds measured in mg Cu/Kg DM except stated otherwise.

[2] This row contains fitted liver copper values. Fed the same pasture.

[3] This row contains the antilog of least square means of log10 liver Cu concentration. Fed the same pasture.

[4] Over 60% of German Hearth sample were < 50 mg Cu/Kg DM whereas over 47% of Texel sheep were > 500 mg Cu/Kg DM. Fed the same pasture.

Population structure analysis

After quality control and linkage disequilibrium pruning using PLINK v1.90 (--indep-pairwise), datasets 1 and 2 including 42 107 and 42 150 autosomal SNPs (Supplementary Table S2), respectively, were analysed by principal component analysis (**PCA**) with the

dudi.pca function of the package "ade4" (Dray and Dufour, 2007) in R Statistical Software v4.2.3 (R Core Team, 2024) and plotted by using the R v4.2.3 "GGPLOT2" package (Wickham, 2016). Pairwise distances between samples were calculated with the *dist.gene* function of the "ape" R v4.2.3 package (Paradis et al., 2004) and visualised in a neighbour-joining tree constructed with the Splitstree4 software v4.15.1 (Huson and Bryant, 2006).

Selection signature analysis

F_{ST} analysis comparing the Cu-susceptible (Scottish Texel, Irish Suffolk and Welsh Mountain Hill flock) group with the Cu-tolerant (Finnsheep, Scottish Blackface and German Grey Hearth) group was performed on quality control data subsets (datasets 1 and 2, Supplementary Table S2) using the --fst function in PLINK v1.90. The resulting F_{ST} values were Z-transformed to normalise its distribution using the formula: ZFST = (x – μ) / σ, where x refers to the F_{ST} value for each SNP, μ is the mean of all F_{ST} values and σ is the standard deviation of all F_{ST} values as described by Eydivandi et al. (2021), and averaged for SNPs in non-overlapping windows of 500 Kb. The averaged ZFST values were plotted across the chromosome with the exclusion of regions containing less than 5 SNPs. The top 1% of informative windows were defined as candidate selection signals.

Likewise, a comparison between Cu-susceptible (Scottish Texel, Irish Suffolk and Welsh Mountain Hill flock) and Cu-tolerant (Finnsheep, Scottish Blackface and German Grey Hearth) breed groups for standardised XP-EHH scores were computed with the ies2xpehh function in R package REHH (Gautier and Vitalis, 2012) using haplotype information and default settings. Prior to this, integrated extended haplotype homozygosity (iES) values were determined using scan_hh function in the R "REHH" package with the option 'polarised = FALSE'. Haplotypes were estimated with fastphase 1.4 (Scheet and Stephens, 2006) by applying the following options for each chromosome: -T10 -C25 -Ku40 -Kl10 -Ki5 -Km1000 -H100, where T is the number of the start of EM algorithm, C is the number of iterations of EM algorithm, Ku is the upper limit of number of clusters, Ki is the upper and lower limit of number of clusters, Ki is the interval between values of number of clusters, Km is the number of SNP loci used for cross-validation and H is the number of haplotype samples, respectively. For determination of candidate

selection signals, standardised XP-EHH scores were transformed into pXP-EHH = –log[1–2|ΦXP-EHH – 0.5|] in which Φ (XP-EHH) represents the Gaussian cumulative distribution function, which was determined by the R function "pnorm". We defined potential selection signals as regions with a minimum of four SNPs within the top 1% of the pXP-EHH distribution equivalent to |XP-EHH| score of ± 2.79 and ± 2.77 for datasets 1 and 2, respectively. XP-EHH scores across all autosomes were plotted with the GGPLOT2 package (Wickham, 2016) in R v4.2.3.

Using the quality control data subsets, we performed a genome-wide scan for selection signatures with the hapFLK (Fariello et al., 2013). For this analysis, we calculated Reynolds distance between the groups (Cu-susceptible vs Cu-tolerant) using the *gene.dist* function in the "hierfstat" R package (Goudet, 2005) and converted the result to kinship matrix with available R script from https://forge-dga.jouy.inra.fr/documents/222. Analysis of hapFLK statistics was performed with the hapflk v1.2 software (Fariello et al., 2013) with the inclusion of the kinship matrix and other parameters such as -K 15 (number of clusters as earlier determined from haplotype estimation with fastphase software), --nfit=1 (number of Expectation-Maximisation (EM) runs) and --ncpu=2 (number of central processing units). Furthermore, we performed the scaling as well as *P* value calculation of the hapFLK statistics with the available Python script (scaling_chi2_hapflk.py) obtained from https://forge-dga.jouy.inra.fr/documents/588. The top 1 % of the distribution of the hapFLK statistic was defined as candidate regions of selection signatures. Of these, only regions with a minimum of four significant SNPs were considered as regions under selection.

Gene identification and enrichment analysis

For all methods used in this study, selection signals found in both datasets were scanned for genes in the ovine genome assembly (NCBI: *Ovis aries*, ARS-UI_Ramb_v2.0). Subsequently, we selected genes that overlapped across a minimum of 2 methods for analysis of potential biological significance. We examined the functional enrichment of the selected genes using the Database for Annotation, Visualization and Integrated Discovery (**DAVID**) software (https://david.ncifcrf.gov, accessed on 7 March 2024) (Huang et al., 2009b, 2009a; Sherman et al., 2022). Additionally, we investigated Gene

Ontology (**GO**) and Kyoto encyclopaedia of genes and genomes (**KEGG**) pathway terms. GO terms including biological process, cellular component and molecular function were accessed. Enriched GO and KEGG pathway terms were considered significant at *P*-value ≤ 0.05 and FDR ≤ 0.05 (Benjamini and Hochberg, 1995) before and after correction for multiple testing, respectively. Additionally, a Venn diagram showing a number of jointly and separately identified genes across datasets and methods was constructed with the "ggvenn" package in R v4.2.3 (R Core Team, 2024).

Results

Population structure and phylogenetic tree

In order to investigate the reliability of the grouping of sheep breeds into Cu-susceptible (Scottish Texel, Irish Suffolk and Welsh Mountain Hill flock) and Cu-tolerant (Finnsheep, Scottish Blackface and German Grey Hearth), we analysed the population structure and phylogenetic relationship of the breeds using PCA and neighbour-joining tree. The top two principal components (PC1 and PC2) of the PCA explain 5.95% and 5.08% (Fig. 1a) of the genetic variance for dataset 1, respectively. Similar percentages were obtained for dataset 2 (PC1, 5.45%; PC2, 5.04%) (Fig. 1b). In both PCA plots, PC1 distinguished Irish Suffolk from other breeds whereas Scottish Texel is separated from other breeds by PC2. However, the PCA plots (Fig. 1a and 1b) showed that Cu-tolerant breeds are clustered together, even though the Welsh Mountain Hill flock breed was near this cluster. The neighbour-joining tree for both datasets revealed that all breeds are distinct from each other and are clustered on the neighbour-joining plot in accordance with the Cu status grouping of breeds analysed in this study (Figure 2a and 2b).

Genomic regions and genes under selection

After averaging Z-transformed F_{ST} values and removal of windows with less than five SNPs, we kept a total of 4 662 and 4 668 informative windows with an average of 10.02 and 10.01 SNPs per window (Standard deviation = 2.13 for both datasets) for dataset 1 and 2, respectively. To eliminate spurious regions of selection in our dataset, we compared selection signals between both datasets obtained by each method

(Supplementary Table S3a, S3b, S4a, S4b, S5a and S5b) and selected common regions of selection for further analysis. Following this, overlapping signals of selection were observed in 18, 8 and 3 regions identified by F_{ST}, XP-EHH and hapFLK, respectively (Tables 2, 3 and 4). These regions under selection were found on OAR 1, 2,3,4,5,7,8,11,12,13 14,16 and 20 (Tables 2, 3 and 4). Two regions on OAR 4 and 8 were observed to be jointly identified as selection regions by F_{ST} and XP-EHH methods, and a region on OAR 11 was significant with all methods (Tables 2, 3 and 4; Figure 3a and 3b). A total of 139, 96 and 113 genes are located within overlapping selection regions identified by F_{ST}, XP-EHH and hapFLK methods, respectively (Figure 4a, 4b and 4c). Of these, 54 genes are in regions of selection identified by a minimum of two methods with 40 genes located in regions identified by all methods (Figure 4d).

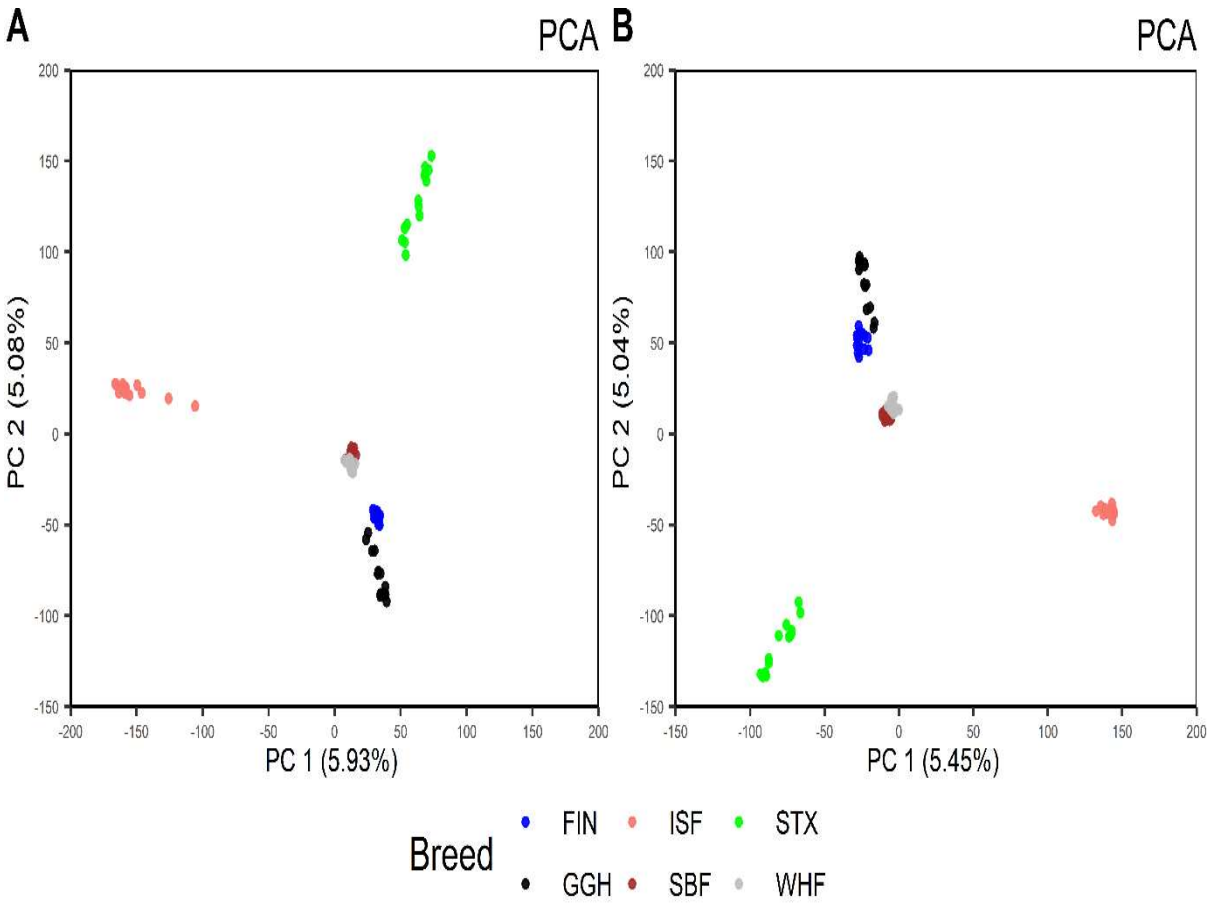

Fig. 1. Principal component analysis (PCA) plots of the 6 sheep breeds: 3 copper-susceptible (STX = Scottish Texel; ISF = Irish Suffolk; WHF = Welsh Mountain Hill flock) and 3 copper-tolerant (FIN = Finnsheep; SBF = Scottish Blackface; GGH = German Grey Hearth) using (a) dataset 1 and (b) dataset 2.

Enrichment analysis of genes under selection

To assess the functional significance of candidate selection genes associated with Cu accretion, all 54 genes (Supplementary Table S6) identified by at least 2 methods were included in a functional enrichment analysis using the DAVID software, which recognised 49 from these genes (Supplementary Table S6). The results show that 19 GO and 1 KEGG pathway terms are significantly enriched (*P*-value ≤ 0.05) (Table 5). Four of the enriched GO terms were significant after *P*-value adjustment (FDR ≤ 0.05) (Table 5). The most significant GO term is associated with lipoxygenase activity (GO:0016165, linoleate 13S-lipoxygenase activity) whereas the significantly enriched KEGG pathway is related to ferroptosis (oas04216, ferroptosis). Other GO terms observed in this study are involved in transcription regulation and repression including GO:0045944 (positive regulation of transcription from RNA polymerase II promoter) and GO:0001227 (transcriptional repressor activity, RNA polymerase II transcription regulatory region sequence-specific binding). Additionally, the 4 GO terms significantly enriched after *P*-value adjustment (FDR ≤ 0.05) include lipoxygenase activity and arachidonic acid metabolism.

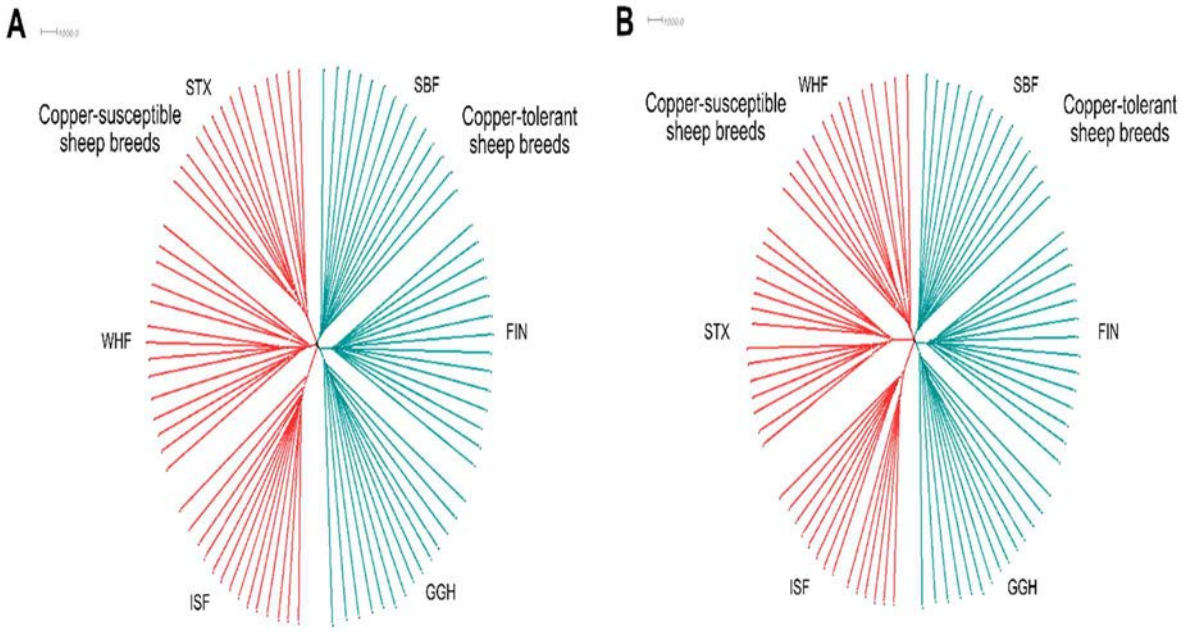

Fig. 2. Neighbour-joining tree plot of the 6 sheep breeds: 3 copper-susceptible (STX = Scottish Texel; ISF = Irish Suffolk; WHF = Welsh Mountain Hill flock) and 3 copper-tolerant (FIN = Finnsheep; SBF = Scottish Blackface; GGH = German Grey Hearth) using (a) dataset 1 and (b) dataset 2.

Table 2. Overlapping regions and genes under selection for copper accretion in sheep detected by F_{ST} for dataset 1 and 2.

Chr	Start[1]	End	Length of region (Kb)	Genes[2]
1	110 858 992	111 331 819	472.83	*VSIG8, CFAP45, TAGLN2, IGSF9, SLAMF9, PIGM, LOC121820658, KCNJ9, KCNJ10, IGSF8, ATP1A2, LOC101118398, CASQ1, PEA15, DCAF8*
1	135 585 935	136 060 808	474.87	*NCAM2*
2	113 644 524	114 107 784	463.26	*HERC2, NIPA1, NIPA2, CYFIP1, TUBGCP5*
3	146 440 774	146 890 350	449.58	*CNTN1, MUC19, LRRK2, LOC121819176, LOC121819177, LOC121819178, LOC121819179*
3	217 657 380	217 963 277	305.90	*MRTFA, MCHR1, SLC25A17, ST13, XPNPEP3, DNAJB7*
4	70 190 366	70 392 090	201.72	*EVX1*
5	58 342 060	58 821 145	479.09	*ABLIM3, LOC105606707, AFAP1L1, GRPEL2, PCYOX1L, IL17B, MIR143, PIGY, CSNK1A1, ARHGEF37, LOC114114896*
7	58 760 956	59 176 863	415.91	*DTWD1, FAM227B, FGF7, GALK2*
7	59 416 935	59 686 761	269.83	*SHC4, EID1, CEP152*
7	100 844 593	101 219 708	375.12	*LOC101115969, LOC114115667, CTDSPL2, EIF3J, SPG11, PATL2, B2M, LOC114108604, LOC121820091, LOC101120839, TERB2, LOC114115674*
8	31 743 299	31 935 827	192.53	*LOC101110768*
9	46 826 171	47 170 495	344.32	*NCOA2*
10	29 071 493	29 545 928	474.44	*FRY, LOC101110773, RXFP2*
11	26 831 470	27 199 959	368.49	*DVL2, PHF23, GABARAP, LOC101118285, CTDNEP1, ELP5, CLDN7, SLC2A4, YBX2, EIF5A, GPS2, LOC105607811, NEURL4, ACAP1, KCTD11, TNK1, PLSCR3, TMEM256, NLGN2, SPEM1, SPEM2, SPEM3, TMEM102, FGF11, CHRNB1, ZBTB4, TMEM95, SLC35G6, POLR2A, LOC101122801, TNFSF13, SENP3, EIF4A1, CD68, MPDU1, SOX15, FXR2, SAT2, SHBG, ATP1B2, TP53*
12	48 869 405	49 280 407	411.00	*MEGF6, ARHGEF16, PRDM16*
13	52 522 167	52 799 399	277.23	*TGM3, STK35*
14	42 817 493	43 231 297	413.80	*CEP89, FAAP24, RHPN2, LOC106991603, GPATCH1, WDR88, LRP3, SLC7A10, CEBPA*
20	17 006 839	17 487 984	481.15	*DLK2, TJAP1, LOC121817410, LRRC73, YIPF3, POLR1C, XPO5, POLH, GTPBP2, LOC101115833, RSPH9, MRPS18A, LOC105603710, VEGFA*

Abbreviations: Chr = Chromosome; F_{ST} = Fixation index; XP-EHH = cross-population extended haplotype homozygosity; hapFLK = haplotype-based FLK,

[1] SNP positions are based on the *Ovis aries* ARS-UI_Ramb_v2.0 genome assembly in NCBI.

[2] The underlined genes were identified by a minimum of two methods (F_{ST}, XP-EHH and hapFLK).

Table 3. Overlapping regions and genes under selection for copper accretion in sheep detected by XP-EHH for dataset 1 and 2.

Chr	Start[1]	End	Length of region (Kb)	Genes[2]
1	111 331 819	111 499 739	167.92	*COPA, NCSTN, NHLH1, VANGL2, SLAMF6*
1	254 851 954	254 931 259	79.31	*EPHB1*
4	50 954 084	51 056 257	102.17	*NRCAM*
4	70 190 366	70 888 570	698.20	*EVX1, HOXA13, LOC105606592, HOXA11, HOXA10, LOC121819410, HOXA9, HOXA7, HOXA3, HOXA5, HOXA6, HOXA4, HOXA2, HOXA1, SKAP2*
8	31 097 538	31 935 827	838.29	*PRDM1, LOC101107359, LOC114116192, LOC101110768*
11	26 588 278	27 199 959	611.68	*ALOX15, LOC114116880, LOC101113251, ALOX12, LOC105607815, RNASEK, C11H17orf49, BCL6B, LOC101114882, SLC16A11, LOC101117600, ASGR2, LOC101116157, DLG4, ACADVL, DVL2, PHF23, LOC101118285, CTDNEP1, ELP5, CLDN7, SLC2A4, YBX2, EIF5A, GPS2, NEURL4, LOC105607811, ACAP1, KCTD11, TMEM95, TNK1, PLSCR3, TMEM256, NLGN2, SPEM1, SPEM2, SPEM3, TMEM102, FGF11, CHRNB1, ZBTB4, SLC35G6, POLR2A, LOC101122801, TNFSF13, SENP3, EIF4A1, CD68, MPDU1, SOX15, FXR2, SAT2, SHBG, ATP1B2, TP53*
13	62 866 739	63 435 585	568.85	*CDK5RAP1, SNTA1, LOC101109899, CBFA2T2, NECAB3, ACTL10, E2F1, PXMP4, ZNF341, LOC105606908, CHMP4B, RALY*
16	33 688 218	33 786 111	97.89	*MROH2B, C7*
16	52 902 038	53 068 320	166.28	*No gene*

Abbreviations: Chr = Chromosome; F_{ST} = Fixation index, XP-EHH = cross-population extended haplotype homozygosity; hapFLK = haplotype-based FLK,

[1] SNP positions are based on the *Ovis aries* ARS-UI_Ramb_v2.0 genome assembly in NCBI.

[2] The underlined genes were identified by a minimum of two methods (F_{ST}, XP-EHH and hapFLK).

Table 4. Overlapping regions and genes under selection for copper accretion in sheep detected by hapFLK statistics for dataset 1 and 2.

Chr	Start[1]	End	Length of region (Kb)	Genes[2]
11	25 809 503	26 772 177	962.67	*NLRP1, LOC105616457, MIS12, DERL2, DHX33, LOC101106021, RPAIN, NUP88, RABEP1, ZFP3, LOC101114793, KIF1C, INCA1, CAMTA2, SPAG7, ENO3, PFN1, RNF167, SLC25A11, GP1BA, CHRNE, LOC105607817, C11H17orf107, MINK1, PLD2, PSMB6, LOC121820578, GLTPD2, VMO1, TM4SF5, ZMYND15, CXCL16, MED11, PELP1, ARRB2, ALOX15, LOC114116880, LOC101113251, ALOX12, LOC105607815, RNASEK, C11H17orf49, BCL6B, LOC101114882, SLC16A11, LOC101117600, ASGR2*
11	26 831 470	27 542 320	710.85	*DVL2, PHF23, LOC101118285, CTDNEP1, ELP5, CLDN7, SLC2A4, YBX2, EIF5A, GPS2, NEURL4, LOC105607811, ACAP1, KCTD11, TMEM95, TNK1, PLSCR3, TMEM256, NLGN2, SPEM1, SPEM2, SPEM3, TMEM102, FGF11, CHRNB1, ZBTB4, SLC35G6, POLR2A, LOC101122801, TNFSF13, SENP3, EIF4A1, CD68, MPDU1, SOX15, FXR2, SAT2, SHBG, ATP1B2, TP53, WRAP53, EFNB3, DNAH2, KDM6B, TMEM88, NAA38, LOC101105010, CHD3, RNF227, KCNAB3, TRAPPC1, CNTROB, GUCY2D, LOC101121185, ALOX12B*
11	27 858 086	28 430 355	572.27	*NDEL1, MYH10, CCDC42, MFSD6L, RPL26, PIK3R6, PIK3R5, NTN1*

Abbreviations: Chr = Chromosome; F_{ST} = Fixation index; XP-EHH = cross-population extended haplotype homozygosity; hapFLK = haplotype-based FLK.

[1] SNP positions are based on the *Ovis aries* ARS-UI_Ramb_v2.0 genome assembly in NCBI.

[2] The underlined genes were identified by a minimum of two methods (F_{ST}, XP-EHH and hapFLK).

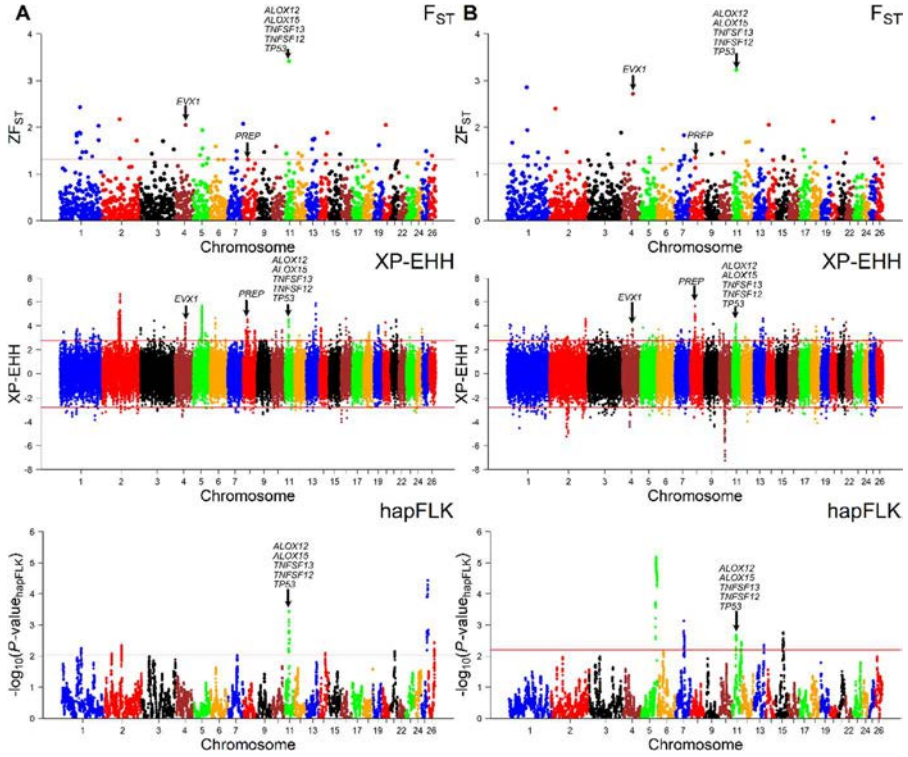

Fig. 3. Manhattan plots for Fixation index (F_{ST}), cross-population extended haplotype homozygosity (XP-EHH) and haplotype-based FLK (hapFLK) analyses of copper-susceptible vs copper-tolerant sheep breeds using (a) dataset 1 and (b) dataset 2. The red lines represent the top 1% of the distribution of each method.

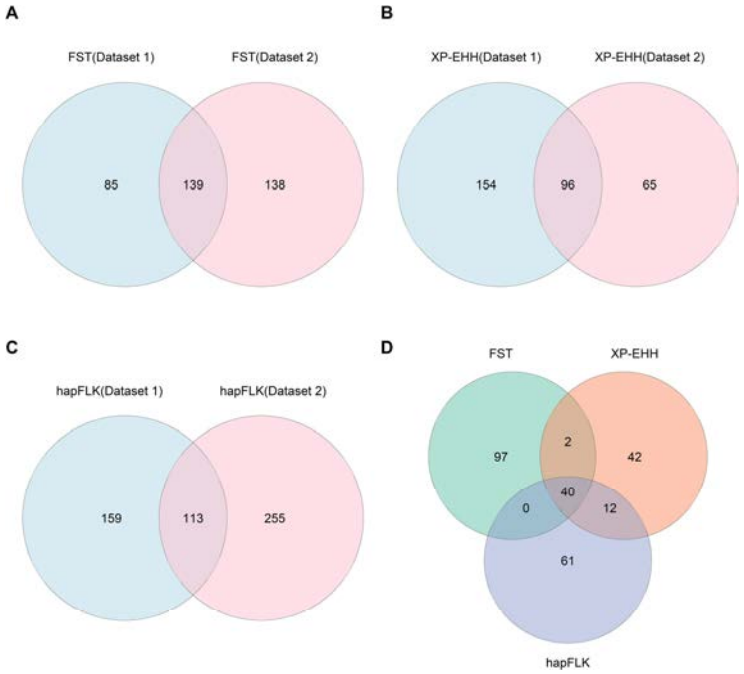

Fig. 4. Venn diagrams show the number of overlapping genes under selection for copper accretion in sheep between dataset 1 and dataset 2 for (a) Fixation index (FST), (b) cross-population extended haplotype homozygosity (XP-EHH), (c) haplotype-based FLK (hapFLK) methods, and (d) across FST, XP-EHH and hapFLK method.

Table 5. Enriched GO and KEGG pathway terms determined by DAVID from genes identified in selection regions associated with copper accretion in sheep by a minimum of 2 methods (F_{ST}, XP-EHH and hapFLK).

Category	Term	Genes	*P*-value	FDR
GOTERM_MF	GO:0016165~linoleate 13S-lipoxygenase activity	*ALOX15, ALOX12, LOC101113251*	0.00	0.00
GOTERM_MF	GO:0004052~arachidonate 12-lipoxygenase activity	*ALOX15, ALOX12, LOC101113251*	0.00	0.00
GOTERM_BP	GO:0019372~lipoxygenase pathway	*ALOX15, ALOX12, LOC101113251*	0.00	0.02
GOTERM_BP	GO:0019369~arachidonic acid metabolic process	*ALOX15, ALOX12, LOC101113251*	0.00	0.04
GOTERM_CC	GO:0071339~MLL1 complex	*EIF4A1, SENP3, C11H17ORF49*	0.00	0.14
GOTERM_MF	GO:0043621~protein self-association	*PLSCR3, DVL2, TP53*	0.00	0.09
KEGG_PATHWAY	oas04216:Ferroptosis	*ALOX15, SAT2, TP53*	0.00	0.43
GOTERM_CC	GO:0016328~lateral plasma membrane	*CLDN7, DVL2, ATP1B2*	0.00	0.17
GOTERM_MF	GO:0050473~arachidonate 15-lipoxygenase activity	*ALOX15, ALOX12*	0.01	0.12
GOTERM_BP	GO:2001303~lipoxin A4 biosynthetic process	*ALOX15, ALOX12*	0.01	0.59
GOTERM_MF	GO:0003743~translation initiation factor activity	*EIF5A, EIF4A1, SENP3*	0.01	0.12
GOTERM_CC	GO:0005737~cytoplasm	*EIF4A1, SOX15, TNFSF13, ALOX12, KCTD11, ATP1B2, SPEM1, ELP5, TP53, SENP3, LOC101113251*	0.01	0.34
GOTERM_BP	GO:0043651~linoleic acid metabolic process	*ALOX15, ALOX12*	0.01	0.70
GOTERM_BP	GO:0007406~negative regulation of neuroblast proliferation	*KCTD11, TP53*	0.01	0.70
GOTERM_MF	GO:0001046~core promoter sequence-specific DNA binding	*POLR2A, TP53*	0.02	0.30

Abbreviations: DAVID = Database for Annotation, Visualization and Integrated Discovery software; F_{ST} = Fixation index; XP-EHH = cross-population extended haplotype homozygosity; hapFLK = haplotype-based FLK; GO = gene ontology; GOTERM = gene Ontology term; GOTERM_MF = molecular function; GOTERM_BP= biological process; GOTERM_CC = cellular component; KEGG_PATHWAY = Kyoto Encyclopedia of Genes and Genomes pathway; FDR = False discovery rate.

Table 5 contd. Enriched GO and KEGG pathway terms determined by DAVID from genes identified in selection regions associated with copper accretion in sheep by a minimum of 2 methods (F_{ST}, XP-EHH and hapFLK).

Category	Term	Genes	*P*-value	FDR
GOTERM_BP	GO:0016926~protein desumoylation	*EIF4A1, SENP3*	0.02	0.85
GOTERM_BP	GO:0045944~positive regulation of transcription from RNA polymerase II promoter	*SOX15, DVL2, GPS2, EVX1, TP53*	0.02	0.85
GOTERM_CC	GO:0005829~cytosol	*FXR2, PLSCR3, ALOX15, TNK1, DVL2, GPS2, ALOX12, SLC2A4, ELP5, ZBTB4, TP53*	0.04	0.77
GOTERM_MF	GO:0005506~iron ion binding	*ALOX15, ALOX12, LOC101113251*	0.04	0.50
GOTERM_MF	GO:0001227~transcriptional repressor activity, RNA polymerase II transcription regulatory region sequence-specific binding	*BCL6B, ZBTB4, TP53*	0.05	0.50

Abbreviations: DAVID = Database for Annotation, Visualization and Integrated Discovery software; F_{ST} = Fixation index; XP-EHH = cross-population extended haplotype homozygosity; hapFLK = haplotype-based FLK; GO = gene ontology; GOTERM = gene Ontology term; GOTERM_MF = molecular function; GOTERM_BP= biological process; GOTERM_CC = cellular component; KEGG_PATHWAY = Kyoto Encyclopedia of Genes and Genomes pathway; FDR = False discovery rate.

Discussion

Variability in Cu accretion between sheep breeds has been discussed and documented extensively, but the underlying genetic factors are not known. In this study, we performed signatures of selection analyses on two separate datasets (Datasets 1 and 2) using three methods (F_{ST}, XP-EHH and hapFLK) to identify candidate regions and genes under selection for Cu accretion in sheep. In the available literature, the Welsh Mountain Hill flock and German Grey Hearth were not compared directly with Texel and Scottish Blackface, respectively, but the reported separate comparisons of Welsh Mountain Hill flock and German Grey Hearth with a known Cu-tolerant (Scottish Blackface) and Cu-susceptible (Texel) breed, respectively, supports our grouping. Moreover, the clustering of these breeds in the neighbour-joining tree (Figure 2a and 2b) confirms the grouping of

sheep breeds applied in this study. However, different regions or genes were recently reported by Adeniyi et al. (2023), who studied within-breed differences in hepatic Cu concentration whereas here we investigate between-breed variations in Cu accumulation. This suggests that differences in Cu accretion within the previously studied breed (Merinoland sheep) are controlled by other genes and pathways than in this study.

Within overlapping regions observed between both datasets used in this study, a candidate region (~ 1 Mb) on OAR11 (26.2-27.2 Mb) was identified as a potential region of selection influencing variation in Cu accretion among sheep breeds by a minimum of two methods. Genes located within this region include solute carrier family 2 member 4 (*SLC2A4*), tumour protein p53 (*TP53*), TNF superfamily member 13 (*TNFSF13*), TNF superfamily member 12 (*LOC101122801* or *TNFSF12*), arachidonate 15-lipoxygenase (*ALOX15*), arachidonate 12-lipoxygenase 12S type (*ALOX12*) and eukaryotic translation initiation factor 5A (*EIF5A*), which are involved in oxidative stress and apoptosis processes. Other candidate regions under selection harbour even-skipped homeobox 1 (*EVX1*) and prolyl endopeptidase (*LOC101110768* or *PREP*) located on OAR4 and OAR8, respectively.

Earlier reports have implicated TP53 in the transcriptional regulation of the synthesis of cytochrome c oxidase 2 (*SCO2*) gene that produces a protein required for Cu transportation to the cytochrome c oxidase (COX) complex (Matoba et al., 2006; Madan et al., 2011; Won et al., 2012). Matoba et al. (2006) showed that the regulation of mitochondrial respiration by TP53 is associated with its impact on SCO2 synthesis. This is not surprising due to the influence of SCO2 on the COX complex, an important site of cellular oxygen consumption during aerobic respiration (Timón-Gómez et al., 2018). In addition, various studies have reported the influence of TP53 on various forms of programmed cell death such as apoptosis (Zuckerman et al., 2009; Aubrey et al., 2018; Wang et al., 2022b) and ferroptosis (Li et al., 2020; Xu et al., 2023).

Ferroptosis is a regulated cell death that is dependent on reactive oxygen species accumulation induced by Fe^{2+}- oxidised lipids (Li et al., 2020). Though Fe is the main ferroptosis-inducing agent, Gao et al. (2021) reported that elesclomol induced

ferroptosis in cells by degradation of ATP7A, which in turn increases the quantity of cellular Cu. The authors observed that increasing Cu accretion led to ROS accumulation and ferroptosis. Genes identified in this study including *TP53*, *ALOX12* and *ALOX15* have been associated with ferroptosis (Xu et al., 2023). This suggests that the sensitivity of cells to ferroptosis is associated with breed differences in Cu accumulation.

Recently, a novel type of cell death termed "cuproptosis" has been associated with Cu homeostasis and mitochondrial respiration (Chen et al., 2022; Li et al., 2022; Tang et al., 2022). Currently, TP53 is considered a potential regulator of pathways influencing cuproptosis (Xiong et al., 2023). According to Xiong et al. (2023), TP53 may facilitate cuproptosis by enhancing mitochondrial metabolism, regulating glutathione (GSH) levels and inhibiting glycolysis in cells. The process resulting in glycolysis inhibition may involve the downregulation of the *GLUT* genes (Kawauchi et al., 2008; Vousden and Ryan, 2009). Interestingly, the gene *SLC2A4* observed within the identified selection signal on OAR 11 is a known *GLUT* gene. Our findings indicate that *TP53* which regulates cuproptosis and SCO2 protein production may have a major effect on variation in Cu homeostasis and accumulation between sheep breeds.

On the other hand, *ALOX15* and *ALOX12* genes encode lipoxygenases that catalyse fatty acid peroxidation in cells resulting inflammation (Chu et al., 2019; Snodgrass and Brüne, 2019; Benatzy et al., 2022). ALOX15 has been identified in the production of pro-resolving mediators that promote inflammation resolution (Wuest et al., 2012; Snodgrass and Brüne, 2019). These findings suggest that genes within the selection region may influence sensitivity to Cu-induced oxidative stress and cell death as observed by Simpson et al. (2006) in liver cells of Cu-susceptible North Ronaldsay sheep. Furthermore, the *TNFSF12* and *TNFSF13* genes identified in this study are associated with induction of apoptosis, regulation of angiogenesis and plasma cell survival (Locksley et al., 2001; Gaur and Aggarwal, 2003). Previous studies have reported that *TNFSF* genes encode inflammatory cytokines that regulate survival, proliferation, apoptosis and immune response of cells (Rath and Aggarwal, 1999; Idriss and Naismith, 2000).

The TNFSF12 also known as TNF-like weak inducer of apoptosis (TWEAK) is recognised by a receptor termed fibroblast growth factor (FGF)-inducible molecule 14 (FN14,

TNFRSF12A). TWEAK is a cytokine that modulates various cellular processes including angiogenesis, apoptosis, proliferation, survival, differentiation and inflammation after binding to FN14 (Winkles, 2008). TWEAK functions by binding to FN14, which is linked to several intracellular signalling pathways including TNFR-associated factor (TRAF), which initiates downstream signalling pathway such as nuclear factor-κB (NF-κB) (Wang et al., 2022a). The TWEAK/FN14 signal has been suggested to affect cellular response to tissue repair following injury (Vince et al., 2008; Dostert et al., 2019). Moreover, Tirnitz-Parker et al. (2010) reported that TWEAK in conjunction with FN14 facilitates hepatic regeneration during chronic injury via the NF-κB pathway. In another report, increased TWEAK and FN14 expression was associated with hepatic stellate cell (HSC) activation and higher levels of liver fibrosis in response to liver injury (Wilhelm et al., 2016). In addition, Wilhelm et al. (2016) found higher FN14 expression in activated HSCs than in quiescent cells. The impact of TWEAK/FN14 interaction has been described as a double-edged sword that facilitates the repair of liver progenitor cells in acute liver damage while contributing to the pathogenesis of chronic liver damage via induction of liver fibrosis (Wang et al., 2022a). Interestingly, hepatic Cu accumulation has been associated with progression in liver fibrosis (Hatano et al., 2000). A comparison of the North Ronaldsay (Cu-susceptible) and Cambridge (Cu-tolerant) sheep revealed that HSCs were activated in liver cells from North Ronaldsay and quiescent in Cambridge after excess Cu intake. Variation in hepatocyte TWEAK/FIN4 expression may be accountable for differences in HSC response to Cu-induced injury, which leads to varying stages of liver fibrosis development, as observed by Haywood et al. (2005). In addition, EIF5A has been identified as a pro-apoptotic protein in TNF-α mediated apoptosis (Taylor et al., 2004) and may regulate the activities of TP53 (Li et al., 2004; Taylor et al., 2007).

The *PREP* gene identified in this study has been associated with hepatic inflammation, oxidative stress and regulation of cathepsin B and D (Jiang et al., 2020; Zhang et al., 2021; Lin et al., 2023). Zhang et al. (2021) suggested that TP53 mediates the influence of PREP on the regulation of oxidative stress status in the liver. Furthermore, a transcriptional regulation of cathepsin B and D expression by PREP has been suggested (Lin et al., 2023). Interestingly, Simpson et al. (2006) reported an increase in cathepsin D for Cu-challenged North Ronaldsay (Cu-susceptible) sheep when compared with Cambridge sheep (Cu-

tolerant). Therefore, we speculate that *TP53*, *TNFSF13*, *TNFSF12*, *ALOX15*, *ALOX12*, *EIF5A* and *PREP* genes have been under selection for Cu accretion in sheep.

Our study reveals that GO and KEGG pathway terms such as arachidonate 15-lipoxygenase activity, arachidonate 12-lipoxygenase activity and ferroptosis were enriched in this study. Genes contributing to these GO and KEGG pathway terms including *TP53*, *ALOX15* and *ALOX12* may influence Cu homeostasis (Madan et al., 2011; Won et al., 2012), programmed cell death (Chen et al., 2022; Xu et al., 2023) and response to inflammation (Snodgrass and Brüne, 2019). Our findings suggest that variability in response to hepatocellular inflammation and apoptosis may be responsible for breed difference in liver Cu accretion in sheep. This is in concordance with the finding that North Ronaldsay sheep (Cu-susceptible) have a higher mitochondrial sensitivity to Cu-induced oxidative stress than Cambridge sheep (Haywood et al., 2005; Simpson et al., 2006). The identified candidate genes and genomic regions responsible for differences in Cu accumulation between sheep breeds may allow the selection within susceptible breeds of individuals with reduced Cu accretion as well as the selection within breeds that are highly prone to deficiency of individuals with an improved Cu retention. This may be supported by an optimisation of the feeding. A limitation of this study was the relatively low number of sheep breeds with sufficient information on Cu accretion as well as available genomic data. To this end, further studies to investigate the Cu accretion status of other sheep breeds with available genomic data are needed to provide additional information on genetic factors influencing breed differences in Cu accumulation.

Conclusions

We compared sheep breeds based on the accumulation of Cu using selection signatures analysis methods including F_{ST}, XP-EHH and hapFLK. For this purpose, we used available ovine genomic SNP data to identify regions and genes associated with variations in Cu accretion between sheep breeds. The findings of this study suggest that OAR 4, 8 and 11 contain potential gene regions involved in Cu accretion. In these regions, we identified *TP53*, *TNFSF13*, *TNFSF12*, *ALOX15*, *ALOX12 EIF5A* and *PREP* as candidate genes that may influence Cu accretion of sheep. Gene enrichment analysis indicated that enriched functions and involved genes regulate processes involving inflammation and cell death.

This study reveals promising regions and genes under selection for further studies to investigate their influence on Cu accretion and potential use in sheep breeding.

Acknowledgements

We thank Shannon M. Clarke for providing SNP data of some Scottish Blackface samples used in this study.

Financial support statement

This research was supported by the Deutsche Forschungsgemeinschaft (DFG, grant no. 62202147).

References

Adeniyi, O.O., Medugorac, I., Grochowska, E., Düring, R.-A., Lühken, G., 2023. Single-Locus and Multi-Locus Genome-Wide Association Studies Identify Genes Associated with Liver Cu Concentration in Merinoland Sheep. Genes 14, 1–14.

Aubrey, B.J., Kelly, G.L., Janic, A., Herold, M.J., Strasser, A., 2018. How does p53 induce apoptosis and how does this relate to p53-mediated tumour suppression? Cell death and differentiation 25, 104–113.

Barry, A.N., Shinde, U., Lutsenko, S., 2010. Structural organization of human Cu-transporting ATPases: learning from building blocks. Journal of biological inorganic chemistry : JBIC : a publication of the Society of Biological Inorganic Chemistry 15, 47–59.

Benatzy, Y., Palmer, M.A., Brüne, B., 2022. Arachidonate 15-lipoxygenase type B: Regulation, function, and its role in pathophysiology. Frontiers in pharmacology 13, 1042420.

Benjamini, Y., Hochberg, Y., 1995. Controlling the False Discovery Rate: A Practical and Powerful Approach to Multiple Testing. Journal of the Royal Statistical Society: Series B (Methodological) 57, 289–300.

Beynon, S.E., Slavov, G.T., Farré, M., Sunduimijid, B., Waddams, K., Davies, B., Haresign, W., Kijas, J., MacLeod, I.M., Newbold, C.J., Davies, L., Larkin, D.M., 2015. Population structure and history of the Welsh sheep breeds determined by whole genome genotyping. BMC genetics 16, 65.

Borobia, M., Villanueva-Saz, S., Ruiz de Arcaute, M., Fernández, A., Verde, M.T., González, J.M., Navarro, T., Benito, A.A., Arnal, J.L., Las Heras, M. de, Ortín, A., 2022. Copper Poisoning, a Deadly Hazard for Sheep. Animals : an open access journal from MDPI 12, 1–16.

Chang, C.C., Chow, C.C., Tellier, L.C., Vattikuti, S., Purcell, S.M., Lee, J.J., 2015. Second-generation PLINK: rising to the challenge of larger and richer datasets. GigaScience 4, 7.

Chen, L., Min, J., Wang, F., 2022. Copper homeostasis and cuproptosis in health and disease. Signal transduction and targeted therapy 7, 378.

Chu, B., Kon, N., Chen, D., Li, T., Liu, T., Le Jiang, Song, S., Tavana, O., Gu, W., 2019. ALOX12 is required for p53-mediated tumour suppression through a distinct ferroptosis pathway. Nature cell biology 21, 579–591.

Dostert, C., Grusdat, M., Letellier, E., Brenner, D., 2019. The TNF Family of Ligands and Receptors: Communication Modules in the Immune System and Beyond. Physiological reviews 99, 115–160.

Dray, S., Dufour, A.-B., 2007. The ade4 Package: Implementing the Duality Diagram for Ecologists. Journal of Statistical Software 22, 1–20.

Eydivandi, S., Roudbar, M.A., Ardestani, S.S., Momen, M., Sahana, G., 2021. A selection signatures study among Middle Eastern and European sheep breeds. Journal of animal breeding and genetics 138, 574–588.

Fariello, M.I., Boitard, S., Naya, H., SanCristobal, M., Servin, B., 2013. Detecting signatures of selection through haplotype differentiation among hierarchically structured populations. Genetics 193, 929–941.

Flori, L., Fritz, S., Jaffrézic, F., Boussaha, M., Gut, I., Heath, S., Foulley, J.-L., Gautier, M., 2009. The genome response to artificial selection: a case study in dairy cattle. PloS one 4, 1-13.

Fry, R.S., Spears, J.W., Lloyd, K.E., O'Nan, A.T., Ashwell, M.S., 2013. Effect of dietary copper and breed on gene products involved in copper acquisition, distribution, and use in Angus and Simmental cows and fetuses1,2. Journal of animal science 91, 861–871.

Wiener, G., Herbert, J.G., Field, A.C., 1976. Variation in liver and plasma copper concentrations of sheep in relation to breed and haemoglobin type. Journal of comparative pathology 86, 101–109.

Gao, W., Huang, Z., Duan, J., Nice, E.C., Lin, J., Huang, C., 2021. Elesclomol induces copper-dependent ferroptosis in colorectal cancer cells via degradation of ATP7A. Molecular oncology 15, 3527–3544.

Gaur, U., Aggarwal, B.B., 2003. Regulation of proliferation, survival and apoptosis by members of the TNF superfamily. Biochemical pharmacology 66, 1403–1408.

Gautier, M., Vitalis, R., 2012. rehh: an R package to detect footprints of selection in genome-wide SNP data from haplotype structure. Bioinformatics (Oxford, England) 28, 1176–1177.

Goudet, J., 2005. HIERFSTAT , a package for R to compute and test hierarchical F -statistics. Molecular Ecology Notes 5, 184–186.

Hatano, R., Ebara, M., Fukuda, H., Yoshikawa, M., Sugiura, N., Kondo, F., Yukawa, M., Saisho, H., 2000. Accumulation of copper in the liver and hepatic injury in chronic hepatitis C. Journal of gastroenterology and hepatology 15, 786–791.

Haywood, S., Simpson, D.M., Ross, G., Beynon, R.J., 2005. The greater susceptibility of North Ronaldsay sheep compared with Cambridge sheep to copper-induced oxidative stress, mitochondrial damage and hepatic stellate cell activation. Journal of comparative pathology 133, 114–127.

Herbert, J.G., Wiener, G., Field, A.C., 1978. The effect of breed and of dried seaweed meal in the diet on the levels of copper in liver, kidney and plasma of sheep fed on a high copper diet. Animal Science 26, 193–201.

Huang, D.W., Sherman, B.T., Lempicki, R.A., 2009a. Bioinformatics enrichment tools: paths toward the comprehensive functional analysis of large gene lists. Nucleic acids research 37, 1–13.

Huang, D.W., Sherman, B.T., Lempicki, R.A., 2009b. Systematic and integrative analysis of large gene lists using DAVID bioinformatics resources. Nature protocols 4, 44–57.

Huson, D.H., Bryant, D., 2006. Application of phylogenetic networks in evolutionary studies. Molecular biology and evolution 23, 254–267.

Idriss, H.T., Naismith, J.H., 2000. TNF? and the TNF receptor superfamily: Structure-function relationship(s). Microscopy Research and Technique 50, 184–195.

Jiang, D.-X., Zhang, J.-B., Li, M.-T., Lin, S.-Z., Wang, Y.-Q., Chen, Y.-W., Fan, J.-G., 2020. Prolyl endopeptidase gene disruption attenuates high fat diet-induced nonalcoholic fatty liver disease in mice by improving hepatic steatosis and inflammation. Annals of translational medicine 8, 218.

Kaler, S.G., 2013. Inborn errors of copper metabolism. Handbook of clinical neurology 113, 1745–1754.

Kawauchi, K., Araki, K., Tobiume, K., Tanaka, N., 2008. p53 regulates glucose metabolism through an IKK-NF-kappaB pathway and inhibits cell transformation. Nature cell biology 10, 611–618.

Kijas, J.W., Lenstra, J.A., Hayes, B., Boitard, S., Porto Neto, L.R., San Cristobal, M., Servin, B., McCulloch, R., Whan, V., Gietzen, K., Paiva, S., Barendse, W., Ciani, E., Raadsma, H., McEwan, J., Dalrymple, B., 2012. Genome-wide analysis of the world's sheep breeds reveals high levels of historic mixture and strong recent selection. PLoS biology 10, e1001258.

Leary, S.C., Kaufman, B.A., Pellecchia, G., Guercin, G.-H., Mattman, A., Jaksch, M., Shoubridge, E.A., 2004. Human SCO1 and SCO2 have independent, cooperative functions in copper delivery to cytochrome c oxidase. Human molecular genetics 13, 1839–1848.

Li, A.-L., Li, H.-Y., Jin, B.-F., Ye, Q.-N., Zhou, T., Yu, X.-D., Pan, X., Man, J.-H., He, K., Yu, M., Hu, M.-R., Wang, J., Yang, S.-C., Shen, B.-F., Zhang, X.-M., 2004. A novel eIF5A complex functions as a regulator of p53 and p53-dependent apoptosis. The Journal of biological chemistry 279, 49251–49258.

Li, J., Cao, F., Yin, H.-L., Huang, Z.-J., Lin, Z.-T., Mao, N., Sun, B., Wang, G., 2020. Ferroptosis: past, present and future. Cell death & disease 11, 88.

Li, S.-R., Bu, L.-L., Cai, L., 2022. Cuproptosis: lipoylated TCA cycle proteins-mediated novel cell death pathway. Signal transduction and targeted therapy 7, 158.

Lin, S.-Z., Wu, W.-J., Cheng, Y.-Q., Zhang, J.-B., Jiang, D.-X., Ren, T.-Y., Ding, W.-J., Liu, M., Chen, Y.-W., Fan, J.-G., 2023. Prolyl endopeptidase remodels macrophage function as a novel transcriptional coregulator and inhibits fibrosis. Experimental & molecular medicine 55, 1437–1450.

Locksley, R.M., Killeen, N., Lenardo, M.J., 2001. The TNF and TNF Receptor Superfamilies: Integrating Mammalian Biology. Cell 104, 487–501.

Lutsenko, S., 2010. Human copper homeostasis: a network of interconnected pathways. Current opinion in chemical biology 14, 211–217.

Lutsenko, S., Barnes, N.L., Bartee, M.Y., Dmitriev, O.Y., 2007. Function and regulation of human copper-transporting ATPases. Physiological reviews 87, 1011–1046.

Madan, E., Gogna, R., Bhatt, M., Pati, U., Kuppusamy, P., Mahdi, A.A., 2011. Regulation of glucose metabolism by p53: Emerging new roles for the tumor suppressor. Oncotarget 2.

Manichaikul, A., Mychaleckyj, J.C., Rich, S.S., Daly, K., Sale, M., Chen, W.-M., 2010. Robust relationship inference in genome-wide association studies. Bioinformatics (Oxford, England) 26, 2867–2873.

Matoba, S., Kang, J.-G., Patino, W.D., Wragg, A., Boehm, M., Gavrilova, O., Hurley, P.J., Bunz, F., Hwang, P.M., 2006. p53 Regulates Mitochondrial Respiration. Science (New York, N.Y.) 312, 1650–1653.

Meyer, H., Coenen, M., 1994. Observations of the liver-Cu-concentrations in sheep in Northwest ´Germany. Deutsche tierärztliche Wochenschrift, 1–40.

Paradis, E., Claude, J., Strimmer, K., 2004. APE: Analyses of Phylogenetics and Evolution in R language. Bioinformatics (Oxford, England) 20, 289–290.

R Core Team, 2024. R: A Language and Environment for Statistical Computing, Vienna, Austria. https://www.R-project.org/. Accessed 27 August, 2024.

Rath, P.C., Aggarwal, B.B., 1999. TNF-Induced Signaling in Apoptosis. Journal of Clinical Immunology 19, 350–364.

Sabeti, P.C., Varilly, P., Fry, B., Lohmueller, J., Hostetter, E., Cotsapas, C., Xie, X., Byrne, E.H., McCarroll, S.A., Gaudet, R., Schaffner, S.F., Lander, E.S., The International HapMap Consortium., 2007. Genome-wide detection and characterization of positive selection in human populations. Nature 449, 913–918.

Saravanan, K.A., Panigrahi, M., Kumar, H., Bhushan, B., Dutt, T., Mishra, B.P., 2020. Selection signatures in livestock genome: A review of concepts, approaches and applications. Livestock Science 241, 104257.

Scheet, P., Stephens, M., 2006. A fast and flexible statistical model for large-scale population genotype data: applications to inferring missing genotypes and haplotypic phase. American journal of human genetics 78, 629–644.

Sherman, B.T., Hao, M., Qiu, J., Jiao, X., Baseler, M.W., Lane, H.C., Imamichi, T., Chang, W., 2022. DAVID: a web server for functional enrichment analysis and functional annotation of gene lists (2021 update). Nucleic acids research 50, W216-W221.

Simpson, D.M., Mobasheri, A., Haywood, S., Beynon, R.J., 2006. A proteomics study of the response of North Ronaldsay sheep to copper challenge. BMC veterinary research 2, 36.

Snodgrass, R.G., Brüne, B., 2019. Regulation and Functions of 15-Lipoxygenases in Human Macrophages. Frontiers in pharmacology 10, 719.

Suttle, N.F., 2010. Mineral nutrition of livestock, 4th ed. CABI, Wallingford, Cambridge, UK, 255-305.

Suttle, N.F., Field, A.C., 1983. Effects of dietary supplements of thiomolybdates on copper and molybdenum metabolism in sheep. Journal of comparative pathology 93, 379–389.

Suttle, N.F., Lewis, R.M., Small, J.N.W., 2002. Effects of breed and family on rate of copper accretion in the liver of purebred Charollais, Suffolk and Texel lambs. Anim. Sci. 75, 295–302.

Tang, D., Chen, X., Kroemer, G., 2022. Cuproptosis: a copper-triggered modality of mitochondrial cell death. Cell research 32, 417–418.

Tao, T.Y., Gitlin, J.D., 2003. Hepatic copper metabolism: insights from genetic disease. Hepatology (Baltimore, Md.) 37, 1241–1247.

Taylor, C.A., Senchyna, M., Flanagan, J., Joyce, E.M., Cliche, D.O., Boone, A.N., Culp-Stewart, S., Thompson, J.E., 2004. Role of eIF5A in TNF-alpha-mediated apoptosis of lamina cribrosa cells. Investigative ophthalmology & visual science 45, 3568–3576.

Taylor, C.A., Sun, Z., Cliche, D.O., Ming, H., Eshaque, B., Jin, S., Hopkins, M.T., Thai, B., Thompson, J.E., 2007. Eukaryotic translation initiation factor 5A induces apoptosis in colon cancer cells and associates with the nucleus in response to tumour necrosis factor alpha signalling. Experimental cell research 313, 437–449.

Timón-Gómez, A., Nývltová, E., Abriata, L.A., Vila, A.J., Hosler, J., Barrientos, A., 2018. Mitochondrial cytochrome c oxidase biogenesis: Recent developments. Seminars in cell & developmental biology 76, 163–178.

Tirnitz-Parker, J.E.E., Viebahn, C.S., Jakubowski, A., Klopcic, B.R.S., Olynyk, J.K., Yeoh, G.C.T., Knight, B., 2010. Tumor necrosis factor-like weak inducer of apoptosis is a mitogen for liver progenitor cells. Hepatology (Baltimore, Md.) 52, 291–302.

van der Berg, R., Levels, F.H., van der Schee, W., 1983. Breed differences in sheep with respect to the accumulation of copper in the liver. The veterinary quarterly 5, 26–31.

Vince, J.E., Chau, D., Callus, B., Wong, W.W.-L., Hawkins, C.J., Schneider, P., McKinlay, M., Benetatos, C.A., Condon, S.M., Chunduru, S.K., Yeoh, G., Brink, R., Vaux, D.L., Silke, J., 2008. TWEAK-FN14 signaling induces lysosomal degradation of a cIAP1-TRAF2 complex to sensitize tumor cells to TNFalpha. The Journal of cell biology 182, 171–184.

Vousden, K.H., Ryan, K.M., 2009. p53 and metabolism. Nature reviews. Cancer 9, 691–700.

Wang, S., Li, L., Cook, C., Zhang, Y., Xia, Y., Liu, Y., 2022a. A potential fate decision landscape of the TWEAK/Fn14 axis on stem and progenitor cells: a systematic review. Stem cell research & therapy 13, 270.

Wang, Y.-C., Wang, L.-T., Hung, T.I., Hong, Y.-R., Chen, C.-H., Ho, C.-J., Wang, C., 2022b. Severe cellular stress drives apoptosis through a dual control mechanism independently of p53. Cell death discovery 8, 282.

Wickham, H., 2016. ggplot2: Elegant Graphics for Data Analysis, 2nd ed. Springer International Publishing.

Wiener, G., 1979. Review of genetic aspects of mineral metabolism with particular reference to copper in sheep. Livestock Production Science 6, 223–232.

Wiener, G., Field, A.C., 1969. Copper concentrations in the liver and blood of sheep of different breeds in relation to swayback history. Journal of comparative pathology 79, 7–14.

Wilhelm, A., Shepherd, E.L., Amatucci, A., Munir, M., Reynolds, G., Humphreys, E., Resheq, Y., Adams, D.H., Hübscher, S., Burkly, L.C., Weston, C.J., Afford, S.C., 2016.

Interaction of TWEAK with Fn14 leads to the progression of fibrotic liver disease by directly modulating hepatic stellate cell proliferation. The Journal of pathology 239, 109–121.

Winkles, J.A., 2008. The TWEAK-Fn14 cytokine-receptor axis: discovery, biology and therapeutic targeting. Nature reviews. Drug discovery 7, 411–425.

Won, K.Y., Lim, S.-J., Kim, G.Y., Kim, Y.W., Han, S.-A., Song, J.Y., Lee, D.-K., 2012. Regulatory role of p53 in cancer metabolism via SCO2 and TIGAR in human breast cancer. Human pathology 43, 221–228.

Woolliams, J.A., Suttle, N.F., Wiener, G., Field A. C., Woolliams, C., 1982. The effect of breed of sire on the accumulation of copper in lambs, with particular reference to copper toxicity. Animal Production 35, 299–307.

Wuest, S.J.A., Crucet, M., Gemperle, C., Loretz, C., Hersberger, M., 2012. Expression and regulation of 12/15-lipoxygenases in human primary macrophages. Atherosclerosis 225, 121–127.

Xiong, C., Ling, H., Hao, Q., Zhou, X., 2023. Cuproptosis: p53-regulated metabolic cell death? Cell death and differentiation 30, 876–884.

Xu, R., Wang, W., Zhang, W., 2023. Ferroptosis and the bidirectional regulatory factor p53. Cell death discovery 9, 197.

Zhang, J., Jiang, D., Lin, S., Cheng, Y., Pan, J., Ding, W., Chen, Y., Fan, J., 2021. Prolyl endopeptidase disruption reduces hepatic inflammation and oxidative stress in methionine-choline-deficient diet-induced steatohepatitis. Life sciences 270, 119131.

Zuckerman, V., Wolyniec, K., Sionov, R.V., Haupt, S., Haupt, Y., 2009. Tumour suppression by p53: the importance of apoptosis and cellular senescence. The Journal of pathology 219, 3–15.

APPENDIX

Supplementary Table S1. Overview of sheep breeds and SNPs included in the study.

Breed	Group	Number of samples before	Number of samples after merging and removal of related individuals (IBD > 0.30)	Sources
Finnsheep	TOL	96	78	Kijas et al. (2012)
German Grey Heath	TOL	14	14	J.A Lenstra; S. Mastrangelo
Irish Suffolk	SUS	55	28	Kijas et al. (2012)
Scottish Blackface	TOL	99	75	Kijas et al. (2012); Shannon Clarke
ScottishTexel	SUS	80	20	Kijas et al. (2012)
Welsh Mountain Hill flock	SUS	24	14	Beynon et al. (2015)
Total number of samples (Total number of autosomal SNPs)		368	229 (45 640)	

Abbreviations: SNP = single nucleotide polymorphism; SUS = copper-susceptible; TOL = copper-tolerant; IBD = Identity by descent.

Supplementary Table S2. Information on the number of sheep samples and SNPs for datasets 1 and 2.

Data	Total number of samples[1]	Total number of SNPs autosomal	Total number of samples after QC	Total number of SNPs after QC	Total number of SNPs after LD prunning	Analyses
Dataset 1	84	45 640	84	45 080	42 107	PCA, NJ tree, FST, XPEHH and hapFLK
Dataset 2	84	45 640	84	45 076	42 150	PCA, NJ tree, FST, XPEHH and hapFLK

Abbreviations: SNP = single nucleotide polymorphism; QC = Quality Control; LD = linkage disequilibrium; PCA = princpal component analysis; NJ tree = neighbour-joining tree; ; FST = Fixation index; XP-EHH = cross population extended haplotype homozygosity; hapFLK = haplotype-based FLK.

[1] 14 samples each from 3 copper-susceptible and 3 copper-tolerant sheep breeds.

Supplementary Table S3a. Regions of selection signatures identified in sheep from the top 1% of the distribution of the FST statistic for Dataset 1.

Chr	Start[1]	End	Length of region (Kb)	Genes
1	110 327 162	110 791 037	463.88	*LOC101114228, LOC101122569, LOC11411759, APCS, LOC114113241, LOC101115495*
1	110 858 992	111 331 819	472.83	*VSIG8, CFAP45, TAGLN2, IGSF9, SLAMF9, PIGM, LOC121820658, KCNJ9, KCNJ10, IGSF8, ATP1A2, LOC101118398, CASQ1, PEA15, DCAF8*
1	111 384 492	111 747 212	362.72	*NHLH1, VANGL2, SLAMF6, CD84, SLAMF1*
1	129 226 770	129 560 710	333.94	*No gene*
1	132 623 354	133 057 319	433.97	*No gene*
1	135 585 935	136 060 808	474.87	*NCAM2*
1	136 717 011	137 072 044	355.03	*No gene*
1	148 618 586	148 877 772	259.19	*No gene*
1	171 795 801	172 250 108	454.31	*No gene*
1	212 398 558	212 742 441	343.88	*NAALADL2*
1	253 996 472	254 203 939	207.47	*No gene*
1	254 791 747	255 224 981	433.23	*EPHB1*
2	113 644 524	114 107 784	463.26	*HERC2, NIPA1, NIPA2, CYFIP1, TUBGCP5*
2	114 161 052	114 548 023	386.97	*CCDC115, IMP4, PTPN18, AMER3, ARHGEF4*
2	224 564 634	224 988 509	423.88	*SGPP2, FARSB, MOGAT1*
3	72 788 190	73 207 953	419.76	*No gene*
3	146 440 774	146 890 350	449.58	*CNTN1, MUC19, LRRK2, LOC121819176, LOC121819177, LOC121819178, LOC121819179*
3	217 657 380	217 963 277	305.90	*MRTFA, MCHR1, SLC25A17, ST13, XPNPEP3, DNAJB7*
4	70 190 366	70 392 090	201.72	*EVX1*
5	43 936 080	44 302 774	366.69	*DDX46, C5H5orf24, TXNDC15, PCBD2, CATSPER3, PITX1, LOC114114877*
5	58 342 060	58 821 145	479.09	*ABLIM3, LOC105606707, AFAP1L1, GRPEL2, PCYOX1L, IL17B, MIR143, PIGY, CSNK1A1, ARHGEF37, LOC114114896*
5	58 904 072	59 257 097	353.03	*PPARGC1B, PDE6A, SLC26A2, TIGD6, HMGXB3, CSF1R, PDGFRB*
5	95 383 543	95 782 931	399.39	*RGMB, CHD1*

6	38 330 994	38 772 831	441.84	*No gene*
6	55 385 404	55 760 667	375.26	*No gene*
6	90 220 372	90 539 188	318.82	*BTC*
7	58 760 956	59 176 863	415.91	*DTWD1, FAM227B, FGF7, GALK2*
7	59 416 935	59 686 761	269.83	*SHC4, EID1, CEP152*
7	100 844 593	101 219 708	375.12	*LOC101115969, LOC114115667, CTDSPL2, EIF3J, SPG11, PATL2, B2M, LOC114108604, LOC121820091, LOC101120839, TERB2, LOC114115674*
8	31 743 299	31 935 827	192.53	*LOC101110768*
9	46 826 171	47 170 495	344.32	*NCOA2*
10	29 071 493	29 545 928	474.44	*FRY, LOC101110773, RXFP2*
11	10 201 618	10 621 416	419.80	*DHX40, CLTC, PTRH2, VMP1, MIR21, TUBD1, RPS6KB1, RNFT1*
11	26 831 470	27 199 959	368.49	*DVL2, PHF23, GABARAP, LOC101118285, CTDNEP1, ELP5, CLDN7, SLC2A4, YBX2, EIF5A, GPS2, LOC105607811, NEURL4, ACAP1, KCTD11, TNK1, PLSCR3, TMEM256, NLGN2, SPEM1, SPEM2, SPEM3, TMEM102, FGF11, CHRNB1, ZBTB4, TMEM95, SLC35G6, POLR2A, LOC101122801, TNFSF13, SENP3, EIF4A1, CD68, MPDU1, SOX15, FXR2, SAT2, SHBG, ATP1B2, TP53*
12	26 714 010	27 207 046	493.04	*NVL, CNIH4, WDR26, CNIH3*
12	48 869 405	49 280 407	411.00	*MEGF6, ARHGEF16, PRDM16*
13	36 850 552	37 479 043	628.49	*LOC443027, LOC121816323, LOC121816037, LOC121816324, LOC101119236, LOC114117473, BFSP1*
13	38 559 254	38 982 514	423.26	*SLC24A3, LOC121816197, RIN2*
13	46 001 246	46 423 175	421.93	*LARP4B, DIP2C*
13	52 522 167	52 799 399	277.23	*TGM3, STK35*
14	42 817 493	43 231 297	413.80	*CEP89, FAAP24, RHPN2, LOC106991603, GPATCH1, WDR88, LRP3, SLC7A10, CEBPA*
14	52 378 137	52 680 321	302.18	*BCAM, NECTIN2, TOMM40, APOE, APOC2, APOC4, CLPTM1, RELB, CLASRP, ZNF296, GEMIN7, PPP1R37, NKPD1, TRAPPC6A, BLOC1S3*
15	73 427 776	73 808 876	381.10	*CD82, TSPAN18*
19	31 606 961	32 025 911	418.95	*MITF*
20	17 006 839	17 487 984	481.15	*DLK2, TJAP1, LOC121817410, LRRC73, YIPF3, POLR1C, XPO5, POLH, GTPBP2, LOC101115833, RSPH9, MRPS18A, LOC105603710, VEGFA*
25	26 121 091	26 401 023	279.93	*ADAMTS14, TBATA, SGPL1, PCBD1*
26	19 986 788	20 471 449	484.66	*REEP3*

Abbreviations: SNP = single nucleotide polymorphism; Chr = Chromosome; FST = Fixation index.

[1] SNP positions are based on the Ovis aries ARS-UI_Ramb_v2.0 genome assembly in NCBI.

Supplementary Table S3b. Regions of selection signatures identified in sheep from the top 1% of the distribution of the FST statistic for Dataset 2.

Chr	Start[1]	End	Length of region (Kb)	Genes
1	33 322 815	33 783 248	460.43	*MYSM1, JUN*
1	110 858 992	111 331 819	472.83	*VSIG8, CFAP45, TAGLN2, IGSF9, SLAMF9, PIGM, LOC121820658, KCNJ9, KCNJ10, IGSF8, ATP1A2, LOC101118398, CASQ1, PEA15, DCAF8*
1	129 226 770	129 560 710	333.94	*No gene*
1	132 623 354	133 057 319	433.97	*No gene*
1	135 585 935	136 060 808	474.87	*NCAM2*
1	202 757 387	203 195 923	438.54	*C1H3orf70, VPS8*
1	268 782 525	269 234 392	451.87	*SETD4, LOC101114408, LOC101114663, LOC114110594, LOC101115172, LOC101115420, DOP1B(DOPEY2), MORC3*
2	37 727 498	38 146 810	419.31	*AQP3, AQP7, NFX1, CHMP5, BAG1, SPINK4, LOC105607270, B4GALT1, LOC101118252, SMU1, DNAJA1, APTX, LOC121818609*
2	113 644 524	114 107 784	463.26	*HERC2, NIPA1, NIPA2, CYFIP1, TUBGCP5*
2	196 569 965	196 999 882	429.92	*No gene*
3	04 140 079	04 481 046	340.97	*AK8, GTF3C4, DDX31, BARHL1, CFAP77, TTF1*
3	132 313 207	132 720 905	407.70	*SMUG1, LOC105611011, HOXC4, HOXC5, HOXC6, HOXC8, HOXC9, HOXC10, HOXC11, HOXC12, HOXC13*
3	146 440 774	146 890 350	449.58	*CNTN1, MUC19, LRRK2, LOC121819176, LOC121819177, LOC121819178, LOC121819179*
3	217 657 380	217 963 277	305.90	*MRTFA, MCHR1, SLC25A17, XPNPEP3, ST13, DNAJB7*
4	70 190 366	70 392 090	201.72	*EVX1*
4	78 678 288	79 025 880	347.59	*CAMK2B, YKT6, GCK, MYL7, POLD2, AEBP1, POLM, BLVRA, LOC101118606*
5	58 342 060	58 821 145	479.09	*ABLIM3, LOC105606707, AFAP1L1, GRPEL2, PCYOX1L, IL17B, MIR143, PIGY, CSNK1A1, ARHGEF37, LOC114114896*
5	59 361 964	59 809 942	447.98	*CAMK2A, ARSI, TCOF1, CD74, RPS14, NDST1, SYNPO, MYOZ3*
6	38 330 994	38 772 831	441.84	*No gene*
7	34 715 155	35 178 697	463.54	*INO80, EXD1, LOC114108769, CHP1, LOC105615677, OIP5, NUSAP1, NDUFAF1, RTF1, ITPKA, LTK, RPAP1, TYRO3*
7	58 760 956	59 176 863	415.91	*DTWD1, FAM227B, FGF7, GALK2*
7	59 416 935	59 686 761	269.83	*SHC4, EID1, CEP152*

7	62 485 809	62 671 324	185.52	*No gene*
7	100 844 593	101 219 708	375.12	*LOC101115969, LOC114115667, CTDSPL2, EIF3J, SPG11, PATL2, B2M, LOC114108604, LOC121820091, LOC101120839, TERB2, LOC114115674*
8	31 743 299	31 935 827	192.53	*LOC101110768*
9	46 826 171	47 170 495	344.32	*NCOA2*
10	29 071 493	29 545 928	474.44	*FRY, LOC101110773, RXFP2*
11	26 831 470	27 199 959	368.49	*DVL2, PHF23, GABARAP, LOC101118285, CTDNEP1, ELP5, CLDN7, SLC2A4, YBX2, EIF5A, GPS2, LOC105607811, NEURL4, ACAP1, KCTD11, TNK1, PLSCR3, TMEM256, NLGN2, SPEM1, SPEM2, SPEM3, TMEM102, FGF11, CHRNB1, ZBTB4, TMEM95, SLC35G6, POLR2A, LOC101122801, TNFSF13, SENP3, EIF4A1, CD68, MPDU1, SOX15, FXR2, SAT2, SHBG, ATP1B2, TP53*
12	28 307 594	28 660 263	352.67	*SDE2, LOC121820769, H3F3A, LOC106991444, ACBD3, MIXL1, LIN9, PARP1*
12	32 252 789	32 669 043	416.25	*ZBTB18, AKT3*
12	48 869 405	49 280 407	411.00	*MEGF6, ARHGEF16, PRDM16*
13	52 522 167	52 799 399	277.23	*TGM3, STK35*
14	14 181 859	14 486 971	305.11	*FANCA, SPIRE2, TCF25, MC1R, DEF8, LOC101113004, LOC101113264, DBNDD1, GAS8, LOC101109035, SHCBP1*
14	42 817 493	43 231 297	413.80	*CEP89, FAAP24, RHPN2, LOC106991603, GPATCH1, WDR88, LRP3, SLC7A10, CEBPA*
15	50 739 399	51 094 107	354.71	*CLPB, PDE2A, ARAP1, LOC121816699, STARD10, ATG16L2*
15	51 119 800	51 596 412	476.61	*FCHSD2, LOC106991638, P2RY2, P2RY6, ARHGEF17*
16	23 673 409	24 082 155	408.75	*SLC38A9, LOC121816765, PLPP1, MTREX, LOC101115571, DHX29*
17	24 986 903	25 452 635	465.73	*PCDH10, LOC114108793*
17	33 045 040	33 507 035	462.00	*ANKRD50*
18	26 820 627	27 221 033	400.41	*PCSK6, SNRPA1, LOC106991733, LOC105603132*
20	17 006 839	17 487 984	481.15	*DLK2, TJAP1, LOC121817410, LRRC73, YIPF3, POLR1C, XPO5, POLH, GTPBP2, LOC101115833, RSPH9, MRPS18A, LOC105603710, VEGFA*
21	36 788 282	37 227 081	438.80	*MYRF, TMEM258, FEN1, FADS1, FADS2, FADS3, RAB3IL1, BEST1, FTH1, LOC114110147, LOC101110719, LOC101110982*
22	02 528 052	02 986 738	458.69	*ZWINT*
25	24 166 506	24 414 864	248.36	*TET1, CCAR1, LOC101103781, STOX1, DDX50*
25	36 066 005	36 527 160	461.16	*NRG3*
26	01 994 897	02 371 815	376.92	*CSMD1*
26	11 985 048	12 446 044	461.00	*TENM3*

Abbreviations: SNP = single nucleotide polymorphism; Chr = Chromosome; FST = Fixation index.

[1] SNP positions are based on the Ovis aries ARS-UI_Ramb_v2.0 genome assembly in NCBI.

Supplementary Table S4a. Regions of selection signatures identified in sheep from the top 1% of the distribution of the XPEHH statistic for Dataset 1.

Chr	Start[1]	End	Length of region (Kb)	Genes
1	110 627 634	110 791 037	163.40	*CRP*
1	111 331 819	111 499 739	167.92	*COPA, NCSTN, NHLH1, VANGL2, SLAMF6*
1	220 657 684	220 834 397	176.71	*SERPINI2, ZBBX*
1	254 851 954	254 931 259	79.31	*EPHB1*
2	109 376 189	110 366 984	990.80	*No gene*
2	110 398 238	111 377 507	979.27	*LOC114113035, LOC105608622, LOC114113036, LOC101121661, MFAP3L*
2	111 409 427	112 205 243	795.82	*CLCN3, NEK1, SH3RF1, CBR4, PALLD*
2	114 107 784	114 491 252	383.47	*TUBGCP5, CCDC115, IMP4, PTPN18, AMER3, ARHGEF4*
2	116 653 173	117 630 781	977.61	*LOC114113042, HS6ST1, UGGT1, LOC105608734, SAP130, LOC105601854, AMMECR1L, POLR2D*
2	117 664 977	118 625 704	960.73	*WDR33, SFT2D3, LIMS2, GPR17, MYO7B, IWS1, PROC, MAP3K2, LOC106990950, ERCC3, LOC101118856, BIN1*
2	118 678 184	119 641 141	962.96	*NEMP2, MFSD6, INPP1, HIBCH, C2H2orf88, MSTN, PMS1, ORMDL1, OSGEPL1, ANKAR*
2	119 758 540	120 391 153	632.61	*SLC40A1, LOC105608837, WDR75, COL5A2, COL3A1*
3	90 701 567	90 886 631	185.06	*LTBP1*
3	111 903 256	112 013 877	110.62	*LOC121819084*
4	50 954 084	51 056 257	102.17	*NRCAM*
4	70 057 842	71 059 051	1 001.21	*HIBADH, EVX1, HOXA13, LOC105606592, HOXA11, HOXA10, LOC121819410, HOXA9, HOXA7, HOXA3, HOXA5, HOXA6, HOXA4, HOXA2, HOXA1, SKAP2*
5	57 291 739	58 264 628	972.89	*LOC121819654, LOC101108915, LOC121819736, LOC101116828, SPINK13, SPINK7, SPINK9, FBXO38, HTR4, ADRB2, SH3TC2*
5	58 404 713	59 257 097	852.38	*ABLIM3, LOC105606707, AFAP1L1, GRPEL2, PCYOX1L, IL17B, LOC114114896, MIR143, CSNK1A1, ARHGEF37, PPARGC1B, PDE6A, SLC26A2, TIGD6, HMGXB3, CSF1R, PDGFRB*
6	39 132 138	39 353 698	221.56	*No gene*
8	21 075 370	21 160 278	84.91	*FAM162B, KPNA5, ZUP1*
8	31 076 230	31 935 827	859.60	*PRDM1, LOC101107359, LOC114116192, LOC101110768*

8	79 035 112	79 237 295	202.18	*LOC101105418, LOC101105666, SCAF8*
11	26 211 634	27 199 959	988.33	*ZFP3, KIF1C, INCA1, CAMTA2, SPAG7, ENO3, PFN1, RNF167, SLC25A11, GP1BA, LOC105607817, CHRNE, C11H17orf107, MINK1, PLD2, LOC121820578, PSMB6, GLTPD2, VMO1, TM4SF5, ZMYND15, CXCL16, MED11, PELP1, ARRB2, ALOX15, LOC114116880, LOC101113251, ALOX12, LOC105607815, RNASEK, C11H17orf49, BCL6B, LOC101114882, SLC16A11, LOC101117600, ASGR2, LOC101116157, DLG4, ACADVL, DVL2, PHF23, LOC101118285, CTDNEP1, ELP5, CLDN7, SLC2A4, YBX2, EIF5A, GPS2, NEURL4, LOC105607811, ACAP1, KCTD11, TMEM95, TNK1, PLSCR3, TMEM256, NLGN2, SPEM1, SPEM2, SPEM3, TMEM102, FGF11, CHRNB1, ZBTB4, SLC35G6, POLR2A, LOC101122801, TNFSF13, SENP3, EIF4A1, CD68, MPDU1, SOX15, FXR2, SAT2, SHBG, ATP1B2, TP53*
13	46 776 915	47 079 387	302.47	*RASSF2, SLC23A2, TMEM230, PCNA, CDS2*
13	62 842 323	63 435 585	593.26	*LOC101116754, CDK5RAP1, SNTA1, LOC101109899, CBFA2T2, NECAB3, ACTL10, E2F1, PXMP4, ZNF341, LOC105606908, CHMP4B, RALY*
14	13 557 704	14 227 536	669.83	*CDT1, APRT, GALNS, TRAPPC2L, PABPN1L, CBFA2T3, ACSF3, CDH15, SLC22A31, ANKRD11, SPG7, RPL13, CPNE7, LOC121816363, DPEP1, CHMP1A, CDK10, SPATA2L, ZNF276, VPS9D1, FANCA, SPIRE2*
16	33 688 218	33 786 111	97.89	*MROH2B, C7*
16	52 902 038	53 068 320	166.28	*No gene*
18	39 103 558	40 099 817	996.26	*SCFD1, COCH, STRN3, AP4S1, HECTD1, HEATR5A, LOC121817107, DTD2, GPR33, NUBPL*
19	31 691 651	32 159 727	468.08	*MITF, FRMD4B*

Abbreviations: SNP = single nucleotide polymorphism; Chr = Chromosome; FST = Fixation index.

[1] SNP positions are based on the Ovis aries ARS-UI_Ramb_v2.0 genome assembly in NCBI.

Supplementary Table S4b. Regions of selection signatures identified in sheep from the top 1% of the distribution of the XPEHH statistic for Dataset 2.

Chr	Start[1]	End	Length of region (Kb)	Genes
1	81 800 770	81 897 012	96.24	*No gene*
1	111 331 819	111 936 524	604.71	*COPA, NCSTN, NHLH1, VANGL2, SLAMF6, CD84, SLAMF1, LOC114117625, LOC114118728, LOC114117626, SLAMF7*
1	250 885 969	251 125 611	239.64	*PIK3CB*
1	254 851 954	254 931 259	79.31	*EPHB1*
1	269 081 834	269 234 392	152.56	*DOP1B, MORC3*
2	113 100 863	113 859 766	758.90	*LGSN, OCA2, HERC2, NIPA1*
2	122 921 016	123 378 419	457.40	*LOC114113605, LOC114113058*
2	124 296 458	124 485 938	189.48	*No gene*
2	236 169 959	236 460 574	290.62	*NKAIN1, PUM1, SDC3*
4	50 954 084	51 056 257	102.17	*NRCAM*
4	70 190 366	70 888 570	698.20	*EVX1, HOXA13, LOC105606592, HOXA11, HOXA10, LOC121819410, HOXA9, HOXA7, HOXA3, HOXA5, HOXA6, HOXA4, HOXA2, HOXA1, SKAP2*
7	43 137 634	43 304 654	167.02	*NID2*
8	31 097 538	31 935 827	838.29	*PRDM1, LOC101107359, LOC114116192, LOC101110768*
8	32 348 128	32 853 633	505.51	*LIN28B, HACE1*
9	68 716 217	69 037 250	321.03	*EMC2*
10	38 619 849	39 063 627	443.78	*No gene*
10	39 169 734	39 603 890	434.16	*No gene*
10	42 322 459	42 792 907	470.45	*No gene*
10	43 563 187	44 056 987	493.80	*No gene*

11	26 588 278	27 617 555	1 029.28	*ALOX15, LOC114116880, LOC101113251, ALOX12, LOC105607815, RNASEK, C11H17orf49, BCL6B, LOC101114882, SLC16A11, LOC101117600, ASGR2, LOC101116157, DLG4, ACADVL, DVL2, PHF23, LOC101118285, CTDNEP1, ELP5, CLDN7, SLC2A4, YBX2, EIF5A, GPS2, NEURL4, LOC105607811, ACAP1, KCTD11, TMEM95, TNK1, PLSCR3, TMEM256, NLGN2, SPEM1, SPEM2, SPEM3, TMEM102, FGF11, CHRNB1, ZBTB4, SLC35G6, POLR2A, LOC101122801, TNFSF13, SENP3, EIF4A1, CD68, MPDU1, SOX15, FXR2, SAT2, SHBG, ATP1B2, TP53, WRAP53, EFNB3, DNAH2, KDM6B, TMEM88, NAA38, LOC101105010, CHD3, RNF227, KCNAB3, TRAPPC1, CNTROB, GUCY2D, LOC101121185, ALOX12B, ALOXE3, HES7, LOC105607806, PER1, VAMP2*
13	62 866 739	63 435 585	568.85	*CDK5RAP1, SNTA1, LOC101109899, CBFA2T2, NECAB3, ACTL10, E2F1, PXMP4, ZNF341, LOC105606908, CHMP4B, RALY*
15	02 947 956	03 107 687	159.73	*No gene*
16	33 688 218	33 786 111	97.89	*MROH2B, C7*
16	52 902 038	53 068 320	166.28	*No gene*
16	65 348 064	65 509 391	161.33	*MTRR, FASTKD3, C16H5orf49, ADCY2*
18	29 659 661	29 935 223	275.56	*SCAPER, RCN2, PSTPIP1*
18	36 216 126	36 441 983	225.86	*No gene*
19	31 691 651	32 025 911	334.26	*MITF*
21	16 145 695	16 251 909	106.21	*PAK1*
21	36 383 303	36 856 591	473.29	*DDB1, TKFC, LOC101106637, TMEM138, TMEM216, CPSF7, SDHAF2, PPP1R32, LRRC10B, SYT7, DAGLA, MYRF, TMEM258, FEN1, FADS1*
25	10 567 955	10 763 877	195.92	*No gene*

Abbreviations: SNP = single nucleotide polymorphism; Chr = Chromosome; FST = Fixation index.

[1] SNP positions are based on the Ovis aries ARS-UI_Ramb_v2.0 genome assembly in NCBI.

Supplementary Table S5a. Regions of selection signatures identified in sheep from the top 1% of the distribution of the hapFLK statistic for Dataset 1.

Chr	Start[1]	End	Length of region (Kb)	Genes
1	128 464 999	128 852 507	387.51	*No gene*
1	130 276 885	131 143 177	866.29	*CYYR1, LOC105613472, LOC101111593*
2	116 794 775	117 630 781	836.01	*LOC114113042, HS6ST1, UGGT1, LOC105608734, SAP130, LOC105601854, AMMECR1L, POLR2D*
2	117 664 977	118 028 588	363.61	*WDR33, SFT2D3, LIMS2, GPR17, MYO7B, IWS1*
11	24 841 134	25 689 737	848.60	*SPNS2, SPNS3, MYBBP1A, GGT6, TEKT1, SMTNL2, FBXO39, XAF1, SLC13A5, C11H17orf100, MED31, TXNDC17, KIAA0753, AIPL1, WSCD1*
11	25 809 503	26 772 177	962.67	*NLRP1, LOC105616457, MIS12, DERL2, DHX33, LOC101106021, RPAIN, NUP88, RABEP1, ZFP3, LOC101114793, KIF1C, INCA1, CAMTA2, SPAG7, ENO3, PFN1, RNF167, SLC25A11, GP1BA, CHRNE, LOC105607817, C11H17orf107, MINK1, PLD2, PSMB6, LOC121820578, GLTPD2, VMO1, TM4SF5, ZMYND15, CXCL16, MED11, PELP1, ARRB2, ALOX15, LOC114116880, LOC101113251, ALOX12, LOC105607815, RNASEK, C11H17orf49, BCL6B, LOC101114882, SLC16A11, LOC101117600, ASGR2*
11	26 831 470	27 723 413	891.94	*DVL2, PHF23, LOC101118285, CTDNEP1, ELP5, CLDN7, SLC2A4, YBX2, EIF5A, GPS2, NEURL4, LOC105607811, ACAP1, KCTD11, TMEM95, TNK1, PLSCR3, TMEM256, NLGN2, SPEM1, SPEM2, SPEM3, TMEM102, FGF11, CHRNB1, ZBTB4, SLC35G6, POLR2A, LOC101122801, TNFSF13, SENP3, EIF4A1, CD68, MPDU1, SOX15, FXR2, SAT2, SHBG, ATP1B2, TP53, WRAP53, EFNB3, DNAH2, KDM6B, TMEM88, NAA38, LOC101105010, CHD3, RNF227, KCNAB3, TRAPPC1, CNTROB, GUCY2D, LOC101121185, ALOX12B, ALOXE3, HES7, LOC105607806, PER1, VAMP2, TMEM107, BORCS6, AURKB, CTC1, PFAS, RANGRF*
11	27 858 086	28 764 983	906.90	*NDEL1, MYH10, CCDC42, MFSD6L, RPL26, PIK3R6, PIK3R5, NTN1, STX8, CFAP52, USP43*
11	28 879 166	29 741 523	862.36	*GAS7, LOC121820584, MYH13, MYH8, LOC101111980, MYH1, MYH2, LOC101113252, LOC121820586, LOC101113508, ADPRM, TMEM220, LOC101114033, TMEM238L, PIRT*
11	29 945 096	30 161 819	216.72	*SHISA6, DNAH9*
14	41 852 295	42 612 559	760.26	*ZNF507, DPY19L3, PDCD5, ANKRD27*
21	27 491 406	28 469 578	978.17	*KIRREL3*
21	28 554 397	29 526 911	972.51	*ETS1*
21	29 581 660	29 953 215	371.56	*FLI1, KCNJ1, KCNJ5, ARHGAP32*

25	35 077 078	36 066 005	988.93	*LOC121816022, LOC101104438, PAG11, LOC101105540, LOC114110058, LOC101105788, LOC121817495, PAG9, LOC101106045, LOC101104869, PAG6, LOC101106809, LOC443348*
25	36 140 533	37 073 280	932.75	*NRG3*
25	37 158 289	38 108 536	950.25	*No gene*
25	38 193 143	39 184 223	991.08	*CDHR1, LRIT1, LRIT2, RGR, CCSER2*
25	39 328 632	40 337 856	1 009.22	*GRID1, WAPL*
25	40 378 469	41 336 137	957.67	*LDB3, BMPR1A, MMRN2, SNCG, ADIRF, FAM25A, GLUD1, SHLD2, SYT15, GPRIN2, NPY4R2, LOC101114082, LOC105605095, LOC105605098, ZNF488, RBP3, GDF2, GDF10*
25	41 381 526	42 360 896	979.37	*PTPN20, FRMPD2, MAPK8, ARHGAP22, WDFY4, LRRC18, VSTM4*
25	42 383 515	43 315 920	932.41	*FAM170B, TMEM273, C25H10orf71, DRGX, ERCC6, LOC114110835, SLC18A3, CHAT, C25H10orf53, OGDHL, PARG, LOC101118849, NCOA4, MSMB, LOC121817975, LOC105605067, WASHC2C, ZFAND4, MARCHF8*
25	43 361 406	44 271 417	910.01	*LOC101117644, ZNF22, RASSF4, DEPP1, TMEM72, CXCL12*
25	44 402 487	44 693 592	291.11	*ZNF32, ZNF236, TFAM, AGT, COG2*
26	38 773 429	39 738 322	964.89	*LOC105605263, LOC106991954, OXSM, NGLY1, TOP2B*
26	39 925 747	40 797 959	872.21	*RARB*
26	40 928 712	41 608 372	679.66	*THRB, NR1D2, RPL15, NKIRAS1, UBE2E1, LOC121818053*

Abbreviations: SNP = single nucleotide polymorphism; Chr = Chromosome; FST = Fixation index.

[1] SNP positions are based on the Ovis aries ARS-UI_Ramb_v2.0 genome assembly in NCBI.

Supplementary Table S5b. Regions of selection signatures identified in sheep from the top 1% of the distribution of the hapFLK statistic for Dataset 2.

Chr	Start[1]	End	Length of region (Kb)	Genes
5	93 089 061	93 368 694	279.63	*LOC114115026, PCSK1*
5	93 425 926	94 359 760	933.83	*CAST, ERAP1, ERAP2, LOC101102729, LOC114114973, LIX1, RIOK2*
5	94 412 163	95 335 172	923.01	*LOC121819705*
5	95 383 543	96 347 297	963.75	*RGMB, CHD1*
5	96 385 046	97 308 627	923.58	*LOC121819707*
5	97 378 514	98 354 942	976.43	*FAM174A, ST8SIA4*
5	98 393 605	99 359 273	965.67	*SLCO4C1, SLCO6A1, PAM*
5	99 405 973	100 367 657	961.68	*LOC105609307, GIN1, PPIP5K2, MACIR, LOC114114917, LOC114115030, LOC114115031, NUDT12*
5	100 406 735	101 320 890	914.16	*LOC121819687*
5	101 385 920	102 265 620	879.70	*No gene*
7	55 753 741	56 683 228	929.49	*ONECUT1, FAM214A, ARPP19, MYO5A, MYO5C, GNB5, BCL2L10, MAPK6, LOC121819980, LEO1, LOC105607297, TMOD3*
7	56 717 443	57 905 205	1 187.76	*TMOD2, LYSMD2, SCG3, DMXL2, GLDN, CYP19, TNFAIP8L3, AP4E1, SPPL2A, TRPM7*
7		59 755 693	915.18	*FAM227B, FGF7, GALK2, COPS2, SECISBP2L, SHC4, EID1, CEP152*
7	59 801 172	60 138 604	337.43	*FBN1*
11	25 667 220	26 772 177	1 104.96	*NLRP1, LOC105616457, MIS12, DERL2, DHX33, LOC101106021, RPAIN, NUP88, RABEP1, ZFP3, LOC101114793, KIF1C, INCA1, CAMTA2, SPAG7, ENO3, PFN1, RNF167, SLC25A11, GP1BA, CHRNE, LOC105607817, C11H17orf107, MINK1, PLD2, PSMB6, LOC121820578, GLTPD2, VMO1, TM4SF5, ZMYND15, CXCL16, MED11, PELP1, ARRB2, ALOX15, LOC114116880, LOC101113251, ALOX12, LOC105607815, RNASEK, C11H17orf49, BCL6B, LOC101114882, SLC16A11, LOC101117600, ASGR2, LOC10111615, DLG4, ACADVL, DVL2, PHF23, LOC101118285, CTDNEP1, ELP5, CLDN7, SLC2A4, YBX2, EIF5A, GPS2, NEURL4, LOC105607811, ACAP1, KCTD11, TMEM95, TNK1, PLSCR3, TMEM256, NLGN2, SPEM1, SPEM2, SPEM3, TMEM102, FGF11, CHRNB1, ZBTB4, SLC35G6, POLR2A, LOC101122801, TNFSF13, SENP3, EIF4A1, CD68, MPDU1, SOX15, FXR2, SAT2, SHBG, ATP1B2, TP53, WRAP53, EFNB3, DNAH2, KDM6B, TMEM88, NAA38, LOC101105010, CHD3, RNF227, KCNAB3, TRAPPC1, CNTROB, GUCY2D, LOC101121185, ALOX12B*

11	26 831 470	27 542 320	710.85	*DVL2, PHF23, LOC101118285, CTDNEP1, ELP5, CLDN7, SLC2A4, YBX2, EIF5A, GPS2, NEURL4, LOC105607811, ACAP1, KCTD11, TMEM95, TNK1, PLSCR3, TMEM256, NLGN2, SPEM1, SPEM2, SPEM3, TMEM102, FGF11, CHRNB1, ZBTB4, SLC35G6, POLR2A, LOC101122801, TNFSF13, SENP3, EIF4A1, CD68, MPDU1, SOX15, FXR2, SAT2, SHBG, ATP1B2, TP53, WRAP53, EFNB3, DNAH2, KDM6B, TMEM88, NAA38, LOC101105010, CHD3, RNF227, KCNAB3, TRAPPC1, CNTROB, GUCY2D, LOC101121185, ALOX12B*
11	27 617 555	28 430 355	812.80	*TMEM107, BORCS6, AURKB, CTC1, PFAS, RANGRF, SLC25A35, ARHGEF15, ODF4, KRBA2, RPL26, LOC114116876, RNF222, NDEL1, MYH10, CCDC42, MFSD6L, PIK3R6, PIK3R5, NTN1*
11	57 672 247	58 302 855	630.61	*SLC39A11, SOX9, LOC121820667*
11	58 423 899	59 362 586	938.69	*No gene*
11	59 411 330	60 283 688	872.36	*LOC121820669, KCNJ2, KCNJ16, LOC114116812*
11	60 377 667	61 353 084	975.42	*MAP2K6, LOC105610551, ABCA5, ABCA10, ABCA6, LOC121820672, LOC101115808, LOC101108503, FAM20A, PRKAR1A, WIPI1, ARSG, SLC16A6, AMZ2, GNA13, RGS9*
11	61 406 066	61 806 640	400.57	*AXIN2, LOC12182068, CEP112, APOH*
13	68 390 271	68 935 669	545.40	*LOC114108774*
15	45 468 361	46 396 437	928.08	*LOC114118611, LOC101107816, LOC114118262, LOC101114303, LOC101108077, LOC101108337, LOC101108600, LOC101108857, LOC101114553, LOC101114807, LOC101115061, LOC101115307, LOC101115567, LOC101115822, LOC101109119, LOC101109079, LOC101109388, LOC101116085, MRPL17, DCHS1, TPP1, TAF10, ILK, RRP8, DNHD1, TIMM10B, ARFIP2, TRIM3, HPX, APBB1, SMPD1*
15	46 453 879	47 507 050	1 053.17	*CAVIN3, CCKBR, CNGA4, FHIP1B, C15H11orf42, LOC101119417, LOC101111226, LOC101119668, LOC101112258, LOC101112512, LOC101112762, LOC101113528, LOC101119931, LOC101113790, LOC101114052, LOC101120190, LOC101114304, LOC101120691, LOC101114809, LOC101115064, LOC101120948, LOC101115569, LOC101115825, LOC105606072, LOC101121198, LOC101121706, LOC101122214, LOC101113314, LOC101116860, LOC101117105, LOC101117361, LOC101122721, LOC114118417, LOC101117874, LOC121816645, LOC101123233, LOC101123492, LOC101101917, LOC101102173, LOC101102419, LOC101118638, LOC101118897, LOC114118420, LOC105614607, LOC101119159, LOC114118423, TRIM34*
15	47 564 310	47 821 307	257.00	*LOC101119670, LOC105602420, UBQLNL, UBQLN3, LOC101120692, LOC101120949, LOC101121200, LOC101121708, LOC101103421, LOC101122462, LOC101103669, LOC101122723, LOC101122977, LOC114118376, LOC114118271, LOC114118272*

15	49 212 696	50 239 969	1 027.27	*LOC101111655, LOC101111902, LOC101112158, LOC101119847, LOC101112671, LOC101113096, TRIM68, LOC114118279, LOC101120356, LOC101113881, LOC101120602, LOC101114136, LOC101114385, LOC114118502, LOC101121373, LOC101121627, TRIM21, LOC101121883, LOC101122626, LOC101115155, LOC101115400, LOC114118287, LOC101123149, LOC101123408, RRM1, STIM1, RHOG, PGAP2, NUP98, LOC101123662, LOC114118292, LOC114118428, LOC114118523, LOC114118522, LOC114118429, LOC101102334, LOC101117960, LOC101102587*
15	50 275 839	51 252 656	976.82	*LOC121816696, RNF121, LOC101118903, NUMA1, LRRC51, LAMTOR1, TOMT, ANAPC15, FOLR3, FOLR1, FOLR2, INPPL1, PHOX2A, CLPB, PDE2A, ARAP1, STARD10, LOC121816699, ATG16L2, FCHSD2*
15	51 303 852	52 005 522	701.67	*P2RY2, LOC105601843, P2RY6, ARHGEF17, RELT, FAM168A, LOC101108352, LOC114108780, RAB6A, MRPL48*

Abbreviations: SNP = single nucleotide polymorphism; Chr = Chromosome; FST = Fixation index.

[1] SNP positions are based on the Ovis aries ARS-UI_Ramb_v2.0 genome assembly in NCBI.

Supplementary Table S6. List of genes from sheep genome annotation used in gene enrichment analysis.

Official gene symbol[1]	Name	Specie	Recognition status in DAVID
POLR2A	RNA polymerase II subunit A	*Ovis aries*	Recognised
ATP1B2	ATPase Na+/K+ transporting subunit beta 2	*Ovis aries*	Recognised
EIF4A1	eukaryotic translation initiation factor 4A1	*Ovis aries*	Recognised
SHBG	sex hormone binding globulin	*Ovis aries*	Recognised
SAT2	spermidine/spermine N1-acetyltransferase family member 2	*Ovis aries*	Recognised
DVL2	dishevelled segment polarity protein 2	*Ovis aries*	Recognised
TP53	tumor protein p53	*Ovis aries*	Recognised
SOX15	SRY-box transcription factor 15	*Ovis aries*	Recognised
EVX1	even-skipped homeobox 1	*Ovis aries*	Recognised
CD68	CD68 molecule	*Ovis aries*	Recognised
YBX2	Y-box binding protein 2	*Ovis aries*	Recognised
NEURL4	neuralized E3 ubiquitin protein ligase 4	*Ovis aries*	Recognised
ELP5	elongator acetyltransferase complex subunit 5	*Ovis aries*	Recognised
SLC16A11	solute carrier family 16 member 11	*Ovis aries*	Recognised
EIF5A	eukaryotic translation initiation factor 5A	*Ovis aries*	Recognised
LOC101113251	polyunsaturated fatty acid (12S)/(13S)-lipoxygenase, epidermal-type-like	*Ovis aries*	Recognised
LOC101117600	C-type lectin domain family 10 member A	*Ovis aries*	Recognised
TMEM95	transmembrane protein 95	*Ovis aries*	Recognised
FXR2	FMR1 autosomal homolog 2	*Ovis aries*	Recognised
MPDU1	mannose-P-dolichol utilization defect 1	*Ovis aries*	Recognised
ALOX15	arachidonate 15-lipoxygenase	*Ovis aries*	Recognised
SENP3	SUMO specific peptidase 3	*Ovis aries*	Recognised
CLDN7	claudin 7	*Ovis aries*	Recognised
SPEM3	SPEM family member 3	*Ovis aries*	Recognised
LOC105607811	uncharacterized *LOC105607811*	*Ovis aries*	Recognised
CHRNB1	cholinergic receptor nicotinic beta 1 subunit	*Ovis aries*	Recognised
TMEM102	transmembrane protein 102	*Ovis aries*	Recognised

NLGN2	neuroligin 2	*Ovis aries*	Recognised
SLC2A4	solute carrier family 2 member 4	*Ovis aries*	Recognised
LOC105607815	DNA-directed RNA polymerase III subunit RPC6-like	*Ovis aries*	Recognised
CTDNEP1	CTD nuclear envelope phosphatase 1	*Ovis aries*	Recognised
TMEM256	transmembrane protein 256	*Ovis aries*	Recognised
ACAP1	ArfGAP with coiled-coil, ankyrin repeat and PH domains 1	*Ovis aries*	Recognised
BCL6B	BCL6B transcription repressor	*Ovis aries*	Recognised
ALOX12	arachidonate 12-lipoxygenase, 12S type	*Ovis aries*	Recognised
KCTD11	potassium channel tetramerization domain containing 11	*Ovis aries*	Recognised
SPEM2	SPEM family member 2	*Ovis aries*	Recognised
GPS2	G protein pathway suppressor 2	*Ovis aries*	Recognised
SPEM1	spermatid maturation 1	*Ovis aries*	Recognised
PHF23	PHD finger protein 23	*Ovis aries*	Recognised
PLSCR3	phospholipid scramblase 3	*Ovis aries*	Recognised
RNASEK	ribonuclease K	*Ovis aries*	Recognised
TNK1	tyrosine kinase non receptor 1	*Ovis aries*	Recognised
C11H17orf49	chromosome 11 C17orf49 homolog	*Ovis aries*	Recognised
SLC35G6	solute carrier family 35 member G6	*Ovis aries*	Recognised
TNFSF13	TNF superfamily member 13	*Ovis aries*	Recognised
FGF11	fibroblast growth factor 11	*Ovis aries*	Recognised
ASGR2	asialoglycoprotein receptor 2	*Ovis aries*	Recognised
ZBTB4	zinc finger and BTB domain containing 4	*Ovis aries*	Recognised
LOC101114882	solute carrier family 16 member 13	*Ovis aries*	Unrecognised
LOC101118285	GABA type A receptor-associated protein	*Ovis aries*	Unrecognised
LOC114116880		*Ovis aries*	Unrecognised
LOC101110768	prolyl endopeptidase	*Ovis aries*	Unrecognised
LOC101122801	TNF superfamily member 12	*Ovis aries*	Unrecognised

Abbreviation:DAVID = Database for Annotation, Visualization and Integrated Discovery software.

[1] Gene anotation is based on the Ovis aries ARS-UI_Ramb_v2.0 genome assembly in NCBI.

4. Comparative transcriptome analysis reveals genes associated with variation in liver copper concentration in Polish-Merino sheep

Olusegun Olaniyi Adeniyi[1], Ewa Grochowska[2], Zexi Cai[3], Gesine Lühken[1]

[1]Institute of Animal Breeding and Genetics, Justus Liebig University, Giessen 35390, Germany.

[2]Department of Oncology, Faculty of Health Sciences, Collegium Medicum, Nicolaus Copernicus University, Łukasiewicza 1 St., 85-821 Bydgoszcz, Poland.

[3] Center for Quantitative Genetics and Genomics, Aarhus University, C. F. Møllers Allé 3, Aarhus, Denmark.

Prepared for submission:

Abstract

Economic gain for sheep farmers is continually affected by incidences of copper intoxication and deficiency. This study assessed the ovine genome for differentially expressed genes (DEGs) influencing within-breed variation in hepatic copper content in Polish Merino sheep. To this end, we compared whole genome RNA sequence expression data from 12 female Polish Merino sheep liver samples (dataset 1) selected and grouped equally into high liver copper (HLC) and low liver copper (LLC) groups. Likewise, a subset of dataset 1 (dataset 2) with 3 samples each in the HLC and LLC groups was analyzed. The DEG analyses of HLC vs LLC groups for both datasets revealed a lower number of significant DEGs for dataset 1(n = 64) when compared to dataset 2 (n = 252). Of the significant DEGs, 53 were jointly identified with both datasets. Identified DEGs downregulated in the HLC group including *MVD*, *DHCR7*, *LOC101113583* and *ERG28* are implicated in cholesterol synthesis, whereas *AKR1B10* and *CYP26A1* are associated with retinoic acid synthesis. Moreover, this study revealed enriched gene ontologies including cholesterol biosynthetic process (GO:0006695), as well as Kyoto encyclopedia of genes and genomes pathways such as retinol metabolism (oas00830). Our findings provide new information on candidate genes associated with within-breed differences in hepatic copper concentration.

Keywords transcriptome analysis, genes, liver, copper, sheep

Introduction

Sheep are more susceptible to copper (Cu) intoxication when compared with other ruminants such as cattle and goats (Gooneratne et al., 1989; Clarkson et al., 2020). Cu is an important trace mineral that is involved in many biological processes. It is a part of many copper-dependent enzymes including cytochrome c oxidase (CCO), ferroxidase II, tyrosinase, superoxide dismutase 1 (SOD1) and superoxide dismutase 2 (SOD2) that play essential roles in mitochondrial respiration, iron oxidation, pigmentation and anti-oxidation of free radicals, respectively (Suttle, 2010).

Within-breed variability of hepatic Cu levels, under the same feeding condition, have been reported in earlier studies (Woolliams et al., 1986; Suttle et al., 2002; Sivertsen and

Løvberg, 2014). Sivertsen and Løvberg (2014) found Cu concentration ranges of 89–221 µg/g wet weight (ww) and 87–186 µg/g ww in the livers of Norwegian Dala ewes kept on pasture at different seasons. Recently, we published a work that supported the within-breed variability in liver Cu content in Merinoland sheep (Adeniyi et al., 2023). In this report, hepatic Cu ranges of 67–273 mg/kg DM and 20–188 mg/kg DM for two herds of Merinoland sheep kept in Bavaria. In addition to the variability in liver Cu concentration, we estimated a heritability of 0.67 (s.e 0.29) for this trait (Adeniyi et al. 2023). This is comparable to the heritability of 0.60 (s.e 0.32) estimated by Judson et al. (1994) in Merino sheep. All these findings point to a significant influence of genetic factors.

Existing documentation provides evidence of the involvement of some genes in hepatic Cu transport and homeostasis (Lutsenko, 2010; Clarkson et al., 2020). Among them are cyclooxygenase 17 (*COX17*), copper transporter 1 (*CTR1*), copper chaperone for superoxide dismutase (*CCS*), antioxidant-1 (*ATOX1*), metallothionein (*MT*), copper-transporting ATPase 2 (*ATP7B*), cytochrome c oxidase (*CCO*) and superoxide dismutase 1 (*SOD1*). The *CTR1*, *ATOX1* and *ATP7B* genes function in import, transport and efflux of hepatic Cu into, within and out of hepatocytes, respectively (Prohaska, 2008). Other Cu-related genes including *CCS* and *COX17* are involved in Cu transport to SOD1 and CCO target proteins, respectively (Lutsenko, 2010).

In recent years, advancement in high-throughput technologies such as DNA microarray and RNA sequencing (RNA-seq) have been keys in the development of methods used to measuring genome-wide gene expression patterns (Toro-Domínguez et al., 2021). Previous studies on the expression of genes associated with hepatic Cu levels have revealed potential candidate genes associated with differences in liver Cu concentration (Song and Freedman, 2005; Muller et al., 2007; Ranches et al., 2021). Using human HepG2 cells and microarray analysis, Muller et al. (2007) reported changes in gene expression patterns of liver cells after Cu overload. Furthermore, the authors found that Cu overload in liver cells resulted in the upregulation of genes such as *MT1A, HMOX1, TXNRD1, IL8* and *GCLM* involved in heavy-metal detoxification, oxidative stress, electron transport, signaling and glutathione biosynthesis, respectively (Muller et al., 2007). Similarly, a recent study by Jin et al. (2024) revealed that genes including *ACTN2* and *GHRHR* were upregulated during Cu supplemented feeding, while *FOXO3* and *TPSB2*

were upregulated during Cu deficient feeding of Wu Ranke sheep using RNA-seq technology. In the study by Jin et al. (2024), expression patterns of liver cells from sheep fed deficient or supplemented Cu were compared with sheep on a control diet.

In our study, we hypothesized that gene expression in hepatic tissue with low and high Cu content from sheep kept under similar feeding and environmental conditions differ significantly. For this purpose, we analyzed liver Cu content of Polish-Merino sheep kept under similar treatment conditions. Liver samples of selected sheep with the lowest and highest liver Cu concentration were compared in a genome-wide gene expression study to identify differences in gene expression patterns associated with varying liver Cu levels in Polish Merino sheep.

Results

Statistics of liver Cu concentration and age

After analysis of samples for hepatic Cu content, our results show that liver Cu concentration for all samples ranged from 62.00 to 522.61 mg/kg DM with a mean hepatic Cu concentration of 231.07 mg/kg DM. Mean liver Cu concentration of samples in the low liver Cu (LLC) group and samples in the high liver Cu (HLC) group for dataset 1 were 130.12 and 372.76 mg/kg DM, respectively (Table 1). For dataset 2, average liver Cu levels for the LLC and HLC groups were 100.19 and 318.45 mg/kg DM, respectively. Moreover, significant difference in means between the LLC and HLC groups was observed ($P < 0.05$) for dataset 1 (Table 1). Regarding the age, we observed a range of 250 to 315 days with a mean of 288 days (Table 1) for all samples. Table 1 shows that the ages of samples in the LLC groups for datasets 1 and 2 averaged 282.83 and 296.33 days, respectively. On the other hand, mean values for samples in the HLC groups for datasets 1 and 2 were 304.17 and 299.67 days, respectively. Analysis for dataset 1 shows that ages of the LLC group were significantly lower than that of the HLC group ($P < 0.05$) (Table 1).

Principal components

The principal component 1 (PC1) and PC2 for dataset 1 explained approximately 16.5% and 13.7% of the variability between samples, respectively (Figure 1a). Although the PC1

did not separate the samples into distinct groups (LLC and HLC) in the PCA plots, the PC2 separated most of the samples according to their liver Cu (LC) groups. Using dataset 2, a second PCA plot showing PC1 and PC2 was constructed with samples clearly separated by PC1 which accounted for 32% of the sample variation (Figure 1b). Moreover, PC2 explained 19.3% of the sample difference for dataset 2. Of the two PCA plots, the PCA plot for dataset 2 showed the better clustering of samples into LC groups (Figure 1a and 1b).

TABLE 1 | Descriptive and inferential statistics of liver Cu concentration and age of complete dataset and liver copper (LC) groups for datasets 1 and 2. LLC = low liver copper; HLC = high liver copper.

Sample groups	**Number**	**Liver Cu concentration**				**Age**			
		Mean Cu (mg/kg DM) ± SEM	**Min**	**Max**	**P-value**	**Mean (age in days)**	**Min**	**Max**	**P-value**
All	38	231.07 ± 13.70	62.00	522.61		288.00 ± 3.29	250.00	315.00	
Dataset 1									
LLC	6	130.12 ± 16.17	62.00	179.69	0.00	282.83 ± 7.38	264.00	309.00	0.04
HLC	6	372.76 ± 35.60	296.39	522.61		304.17 ± 4.83	278.00	311.00	
Dataset 2									
LLC	3	100.19 ± 13.48	62.00	142.58		296.33 ± 6.47	274.00	309.00	
HLC	3	318.45 ± 6.40	296.39	331.46		299.67 ± 6.26	278.00	311.00	

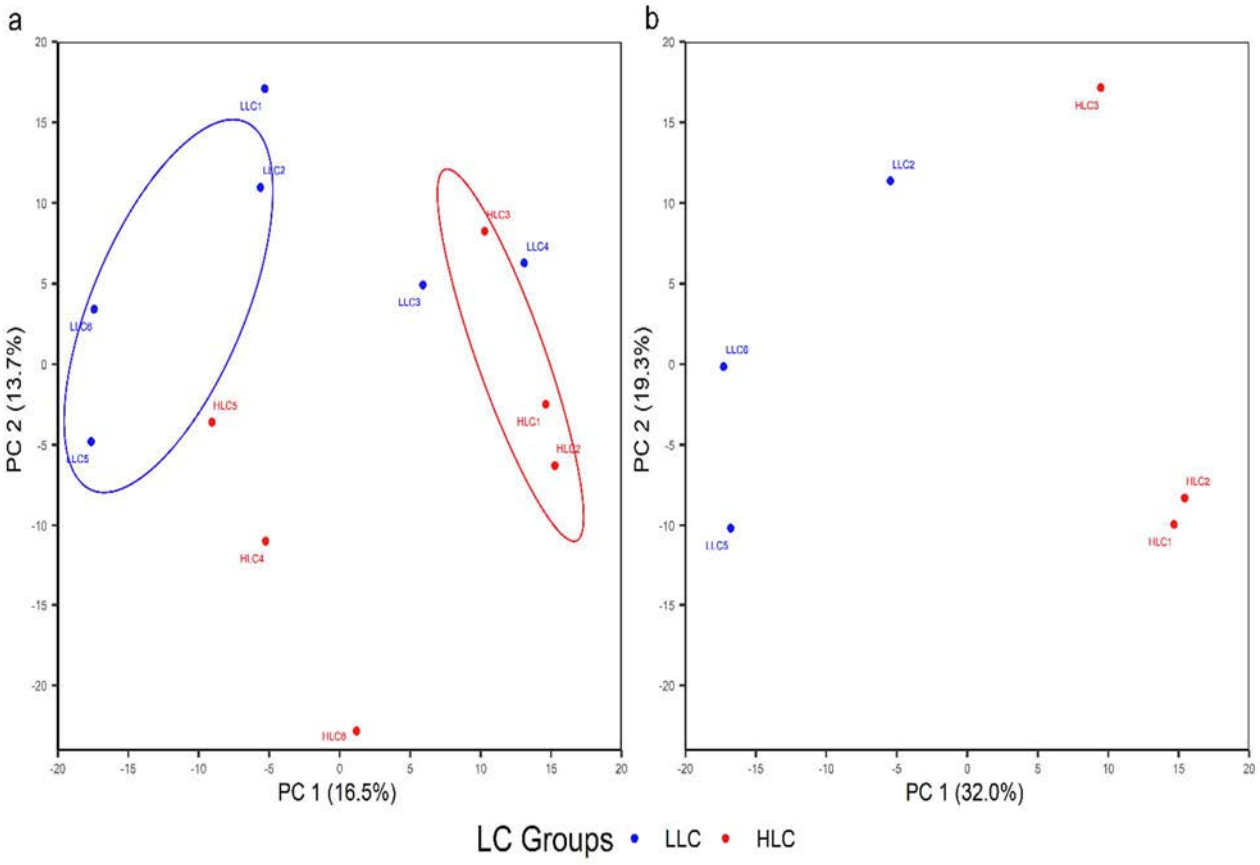

FIGURE 1 | PCA plots of principal component 1 (PC 1) vs PC 2 for datasets 1(a) and 2 (a). LC = liver copper; LLC = low liver copper; HLC = high liver copper; encircled samples = samples selected into dataset 2.

Identified DEGs and enriched functions

After mapping and quality control, 30,186 expressed genes were available for differentially expressed genes (DEGs) analysis. In this study, analysis of dataset 1 revealed that 120 genes were differentially expressed for HLC vs LLC groups, whereas 421 genes were differentially expressed between the groups in dataset 2. However, differences were significant only for 64 and 252 genes at FDR ≤ 0.05 (adjusted P-value) and |log2foldchange| ≥ 1 (Supplementary Table S3a and S3b) for datasets 1 and 2, respectively. Of these DEGs, our results reveal that 31 and 33 DEGs (Figure 2a, Supplementary Table S3a) were significantly upregulated and downregulated in HLC samples for datasets 1, respectively. On the other hand, 103 DEGs and 149 DEGs (Figure 2b, Supplementary Table S3b) were upregulated and downregulated in the HLC group for datasets 2, respectively. For clarity, all significantly upregulated genes in the HLC group were downregulated in the LLC group, and vice versa.

For both datasets, the volcano plots show the significantly upregulated or downregulated genes associated with the HLC group (Figure 2a and 2b, Supplementary Table S3a and S3b), whereas the heatmap plots reveal the degree of expression for significantly up- or downregulated DEGs between the HLC and LLC groups in this study (Figure 3a and 3b). A total of 53 significant DEGs were jointly identified for both datasets. The results of functional enrichment analysis for dataset 1 show that 11 GO and 3 KEGG pathway terms were significantly enriched at P-value ≤ 0.05. Additionally, 2 GO and 1 KEGG pathway terms were significantly enriched at FDR ≤ 0.05 (Figure 4a). Regarding dataset 2, our results show that 41 GO and 20 KEGG pathway terms were significantly enriched at P-value ≤ 0.05 with 14 (8 GO and 6 KEGG pathway) terms significantly enriched after P-value adjustment at FDR ≤ 0.05 (Figure 4b).

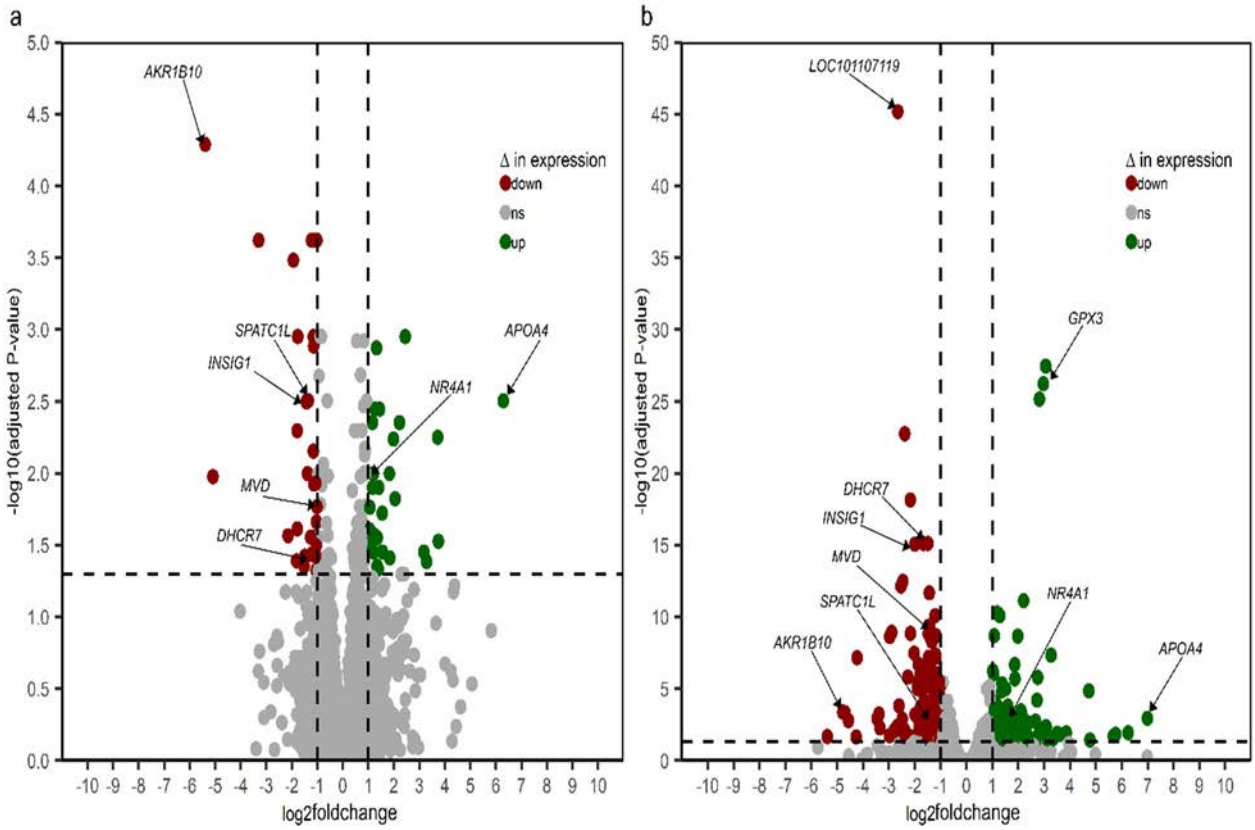

FIGURE 2 | Volcano plots of significantly (FDR ≤ 0.05; |log2foldchange| ≥ 1) up- or down-regulated differentially expressed genes (DEGs) in the HLC group for datasets 1 (a) and 2 (b).

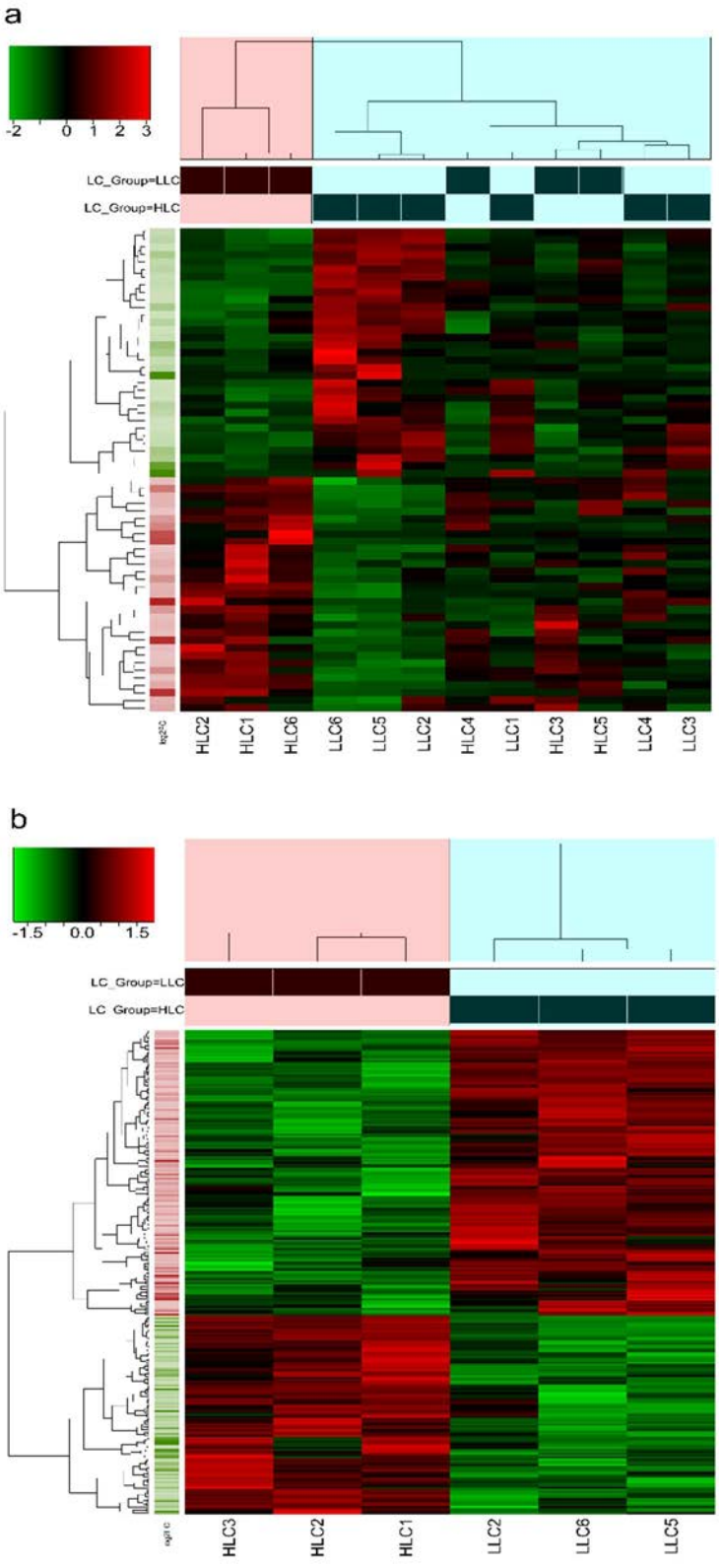

FIGURE 3 | Heatmap plots of the degree of expression of significantly (FDR ≤ 0.05; |log2foldchange (log2FC)| ≥ 1) up- or down-regulated differentially expressed genes (DEGs) for datasets 1 (a) and 2 (b). LC = liver copper; LLC = low liver copper; HLC = high liver copper.

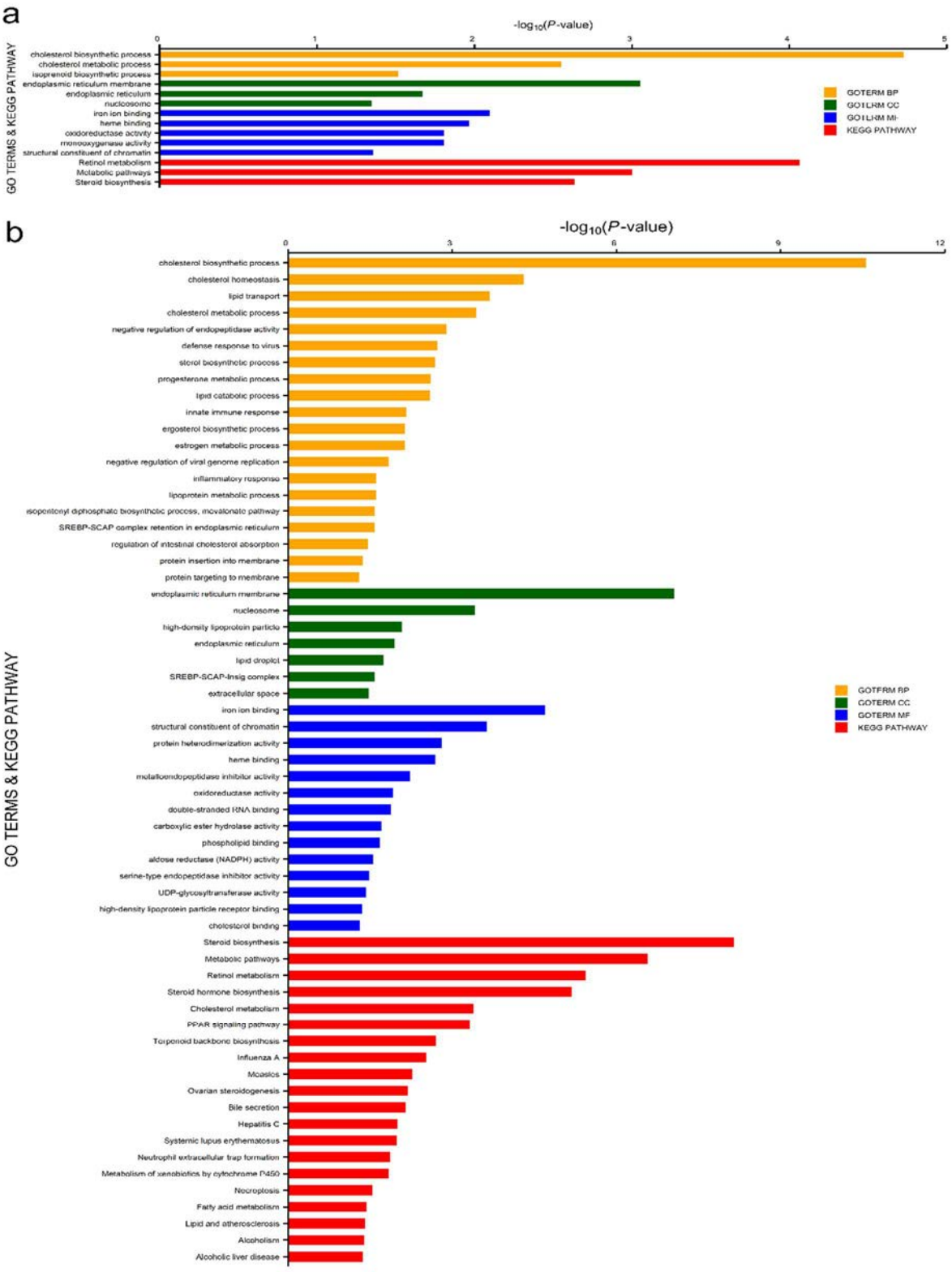

FIGURE 4 | Enriched Gene Ontology (GO) and Kyoto encyclopaedia of genes and genomes (KEGG) pathway terms of significantly up- or down-regulated DEGs for datasets 1 (a) and 2 (b). GOTERMs: BP = biological process; CC = cellular component; MF = molecular function.

Validation of RNAseq data by RT-qPCR

A selection of differentially expressed genes observed in both LC groups using RNAseq data was validated by reverse transcription-quantitative polymerase chain reaction (RT-qPCR). For dataset 1, the direction of the gene expression was observed to be similar to that detected with RNAseq data for all genes (*APOA4, FMN2, NIPAL1, ALDH1A3, CYP1A1, SPATC1L, FDPS, MVD, DHC*R7) with the exception of *NR4A1* (Figure 5a). This exception was not observed for dataset 2 with the direction of the gene expression found to be like the RNAseq data expression (Figure 5b). Furthermore, the magnitude of the gene expression for both methods was observed to be similar in some genes for both datasets. The similarity in magnitude of the gene expression improved in dataset 2 when compared to dataset 1 (Figures 6a and 6b).

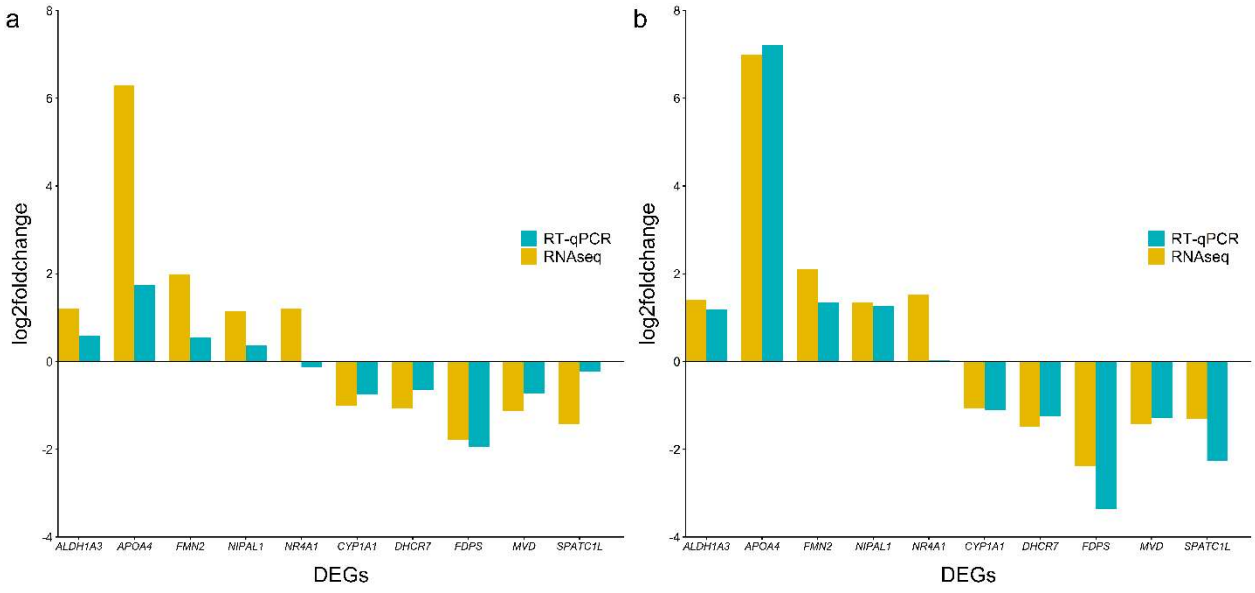

FIGURE 5 | Comparison of reverse transcription-quantitative polymerase chain reaction (RT-qPCR) and RNAseq measured expression of selected significantly (FDR ≤ 0.05; |log2foldchange| ≥ 1) up- or down-regulated differentially expressed genes (DEGs) in the HLC group for datasets 1 (a) and 2 (b).

Discussion

This study evaluated differences in gene expression of hepatic tissue with high and low liver Cu concentration in Polish Merino sheep. As expected, variation in hepatic Cu levels were evident in the sampled sheep reared under similar conditions as seen in Table 1. An

earlier study in Merino sheep kept under similar rearing conditions by Judson et al. (1994) found values of 6.7 and ±2.6 as mean and standard deviation of liver Cu, respectively. Findings by Judson et al. (1994) equates to a 37.3% coefficient of variation for the liver Cu values and supports evidence of within-breed variation in liver Cu concentration in sheep. Additionally, our result supports recent findings by Adeniyi et al. (2023) on within-breed variations in liver Cu accretion in Merinoland sheep when kept under similar feeding and environmental conditions. Some samples selected for transcriptome analysis did not clearly separate in a PCA plot (Figure 1a) according to LC groups. Therefore, a subset of dataset 1 (dataset 2) was reanalyzed with better clustering in the PCA plot (Figure 1b). A comparison of the DEG analyses with the two different data sets show that the number of significant DEGs was lower for dataset 1 (n = 64) when compared to dataset 2 (n = 252) suggesting an improvement in significant DEGs discovery. This may be due to higher similarity in expression patterns of samples in each LC groups for dataset 2 as evidenced by the better sample clustering seen in the second heatmap plot (Figure 3b). The selected significant DEGs observed with RNAseq data were successfully validated using RT-qPCR.

In this study, the expression of 33 and 149 genes was significantly downregulated in the HLC group for datasets 1 and 2, respectively. Of these, 5 downregulated genes jointly identified for both datasets are directly involved in the cholesterol biosynthesis pathway including mevalonate diphosphate decarboxylase (*MVD*), squalene epoxidase (*SQLE*), 7-dehydrocholesterol reductase (*DHCR7*), farnesyl diphosphate synthase (*FDPS*) and lanosterol 14-alpha demethylase (*LOC101113583*) (Cerqueira et al., 2016; Luo et al., 2020). In addition to this, many more cholesterol-related genes including mevalonate kinase (*MVK*), 3-hydroxy-3-methylglutaryl-CoA synthase 1 (*HMGCS1*) and NAD(P) dependent steroid dehydrogenase-like (*NSDHL*) were significantly downregulated for dataset 2. An association between Cu concentration and cholesterol biosynthesis has been suggested in earlier studies (Huster et al., 2006; Huster et al., 2007; Huster and Lutsenko, 2007). In these studies, it was observed that cholesterol biosynthesis was downregulated in ATP7B-deficient mice resulting from increased copper levels. Likewise, reviews by other authors indicate that a possible relationship exist between Cu homeostasis and lipid metabolism (Engle, 2011; Lutsenko, 2014; Blades et al., 2021). Similarly to the cholesterol synthesis-related genes, the ergosterol biosynthetic protein

28 homolog (*LOC101110679*) gene was downregulated in the HLC group. A recent study by Capell-Hattam et al. (2022) shows the involvement of ERG28 protein in cholesterol synthesis via activation of SREP2. Moreover, we also identified the FUN14 domain-containing protein 2 (*LOC114118711*) gene, known to aid triglyceride homeostasis via *SREBP1c* upregulation (Gao et al., 2015; Yang et al., 2018), as a downregulated gene in the HLC group. In line with the review of earlier studies by Blades et al. (2021), our results confirm that cholesterol biosynthesis is upregulated in hepatic tissue with low Cu concentration and downregulated in hepatic cells with high Cu concentration, respectively.

Furthermore, this study identified the insulin induced gene 1 (*INSIG1*) as an upregulated gene in the LLC group. The INSIG1 protein has been identified as an important protein involved in the regulation of cholesterol synthesis via sterol regulatory element-binding proteins (SREBPs) and 3-hydroxy-3-methylglutaryl coenzyme A reductase (HMG-CoA reductase) (Dong et al., 2012). The SREBPs are membrane bound transcription factors that modulate the expression of genes involved in lipid synthesis, while HMG-CoA reductase is a rate-limiting enzyme involved in the cholesterol synthesis pathway (Luo et al., 2020; Chandrasekaran and Weiskirchen, 2024). The INSIG1 protein forms a complex with SREBP cleavage-activating protein (SCAP) and SREBPs in the endoplasmic reticulum (ER), leading to the inhibition of cholesterol synthesis occasioned by preventing SREBPs transport to the Golgi apparatus (Dong et al., 2012; Shimano and Sato, 2017). Likewise, INSIG1 protein binds directly to HMG-CoA reductase resulting in the accelerated degradation of the enzyme followed by suppression of cholesterol synthesis (Dong et al., 2012). Though INSIG1 functions in the reduction of cholesterol levels, it is possible that the significantly higher expression of *INSIG1* gene observed in the LLC group indicates a feedback response to high cholesterol levels in the hepatocytes. In this study, we noted that these cholesterol-related genes were significantly downregulated in the HLC group for both datasets. This suggests that genes associated with cholesterol synthesis are downregulated in liver cells with high liver Cu concentration and upregulated in hepatocytes with low liver content. However, these results do not explain the cause for within-breed variation in hepatic Cu levels in the liver samples because changes in cholesterol biosynthesis is considered an outcome of changes in Cu concentration levels as reviewed by Blades et al. (2021) and Engle (2011).

Four genes involved in retinoic acid metabolism including aldo-keto reductase family 1 member B10 (*LOC101107697 or AKR1B10*), cytochrome P450 26A1 (*LOC101103439 or CYP26A1*), aldehyde dehydrogenase 1 family member A3 (*ALDH1A3*) and nuclear receptor 4A1 (*NR4A1*) genes (Thatcher and Isoherranen, 2009; Endo et al., 2021) were significantly expressed differently. Of these, *AKR1B10* and *CYP26A1* were downregulated, while *ALDH1A3* and *NR4A1* were upregulated in the HLC group. Retinoic acid has been associated with intrinsic apoptotic pathways that occur after mitochondrial permeation occasioned by the modulation of proapoptotic (e.g. Bax) and anti-apoptotic (e.g. Bcl-2) proteins that mediate mitochondrial-based apoptosis (Noy, 2010). Additionally, retinoic acid has also been indicated in the regulation of the expression of caspases that mediate inflammatory responses and apoptosis (Noy, 2010; Julien and Wells, 2017).

AKR1B10 catalyzes the reversible step in retinoid metabolism by converting retinal (substrate for retinoic acid production) to retinol, whereas CYP26A1 regulates retinoic acid levels by conversion to its hydroxy- and/or oxo-metabolites (Zhang et al., 2015; Endo et al., 2021). These findings suggest that AKR1B10 and CYP26A1 assist with the reduction of retinoic acid concentration with the attendant effect on retinoic acid signaling. Conversely, the aldehyde dehydrogenase 1 family member A3 (*ALDH1A3*) and nuclear receptor 4A1 (*NR4A1*) genes associated with retinoic acid production and signaling were upregulated in the HLC group. ALDH1A3 is an enzyme that catalyzes the conversion of retinal to retinoic acid leading to increased retinoic acid production (Thompson et al., 2019), whereas NR4A1 is a transcription factor for the regulation of gene expression associated with retinoic acid signaling (Zhang et al., 2015). Notably, reports have shown that NR4A1 induces mitochondrial related apoptosis by targeting Bcl-2 located on the mitochondria (Li et al., 2000; Lin et al., 2004), and interacts with another gene that was upregulated in the HLC group in this study known as apolipoprotein A4 (*APOA4*) to downregulate gluconeogenesis in mice and human hepatocytes (Li et al., 2014; Li et al., 2015). Thus, genes associated with an increase in retinoic acid synthesis and signaling are upregulated in the HLC group, while genes associated with decreased retinoic acid synthesis were downregulated.

Similar to our observation regarding cholesterol biosynthesis and retinoic acid activity, a report by Muchenditsi et al. (2021) on gene expression in *ATP7B* deficient mice showing the Wilson disease phenotype with increased Cu accumulation found that cholesterol biosynthesis and liver X receptor/retinoid X receptor (LXR/RXR) activation were downregulated and upregulated, respectively. Furthermore, the spermatogenesis and centriole associated 1 like (*SPATC1L*) gene located 148.7 Kilobases (Kb) from a SNP (rs427314005) that was identified in our previous genome-wide association study on genes influencing liver Cu concentration in Merinoland sheep was downregulated in the HLC group (Adeniyi et al., 2023). The SPATC1L protein reportedly associates with the regulatory subunit of protein kinase A, whereas its involvement in Cu homeostasis is unknown. A look at the recent sheep genome annotation (Ovis aries ARS-UI_Ramb_v2.0 genome assembly in NCBI) reveals that a gene known as lanosterol synthase (*LSS*) is located approximately 35 Kb from the *SPATC1L* gene. This implies that both genes are linked within the genome, though no interaction has been established between their proteins. The *LSS* gene has been implicated in the catalysis of a reaction that produces a substrate within the cholesterol biosynthesis pathway named lanosterol. This suggests that the *SPATC1L* and *LSS* genes may be associated with variation in liver copper accumulation in Polish Merino sheep. Interestingly, the *LSS* gene was differentially expressed at FDR ≤ 0.05 in this study but not significant due to a |log2foldchange| less than 1 (|log2foldchange| for *LSS* = 0.999). Further studies need to be conducted to ascertain the effect or not of these genes on hepatic Cu levels.

In this study, some significantly enriched GO terms including cholesterol biosynthetic process (GO:0006695), endoplasmic reticulum membrane (GO:0005789) and cholesterol metabolic process (GO:0008203) were jointly identified for both datasets with involved genes including *INSIG1*, *APOA4*, *MVD* and *DHCR*. Besides, some KEGG pathway terms including retinol metabolism (oas00830), metabolic pathways(oas01100) and steroid biosynthesis (oas00100) were enriched for both datasets in this study. Genes such as *LOC101107697, ALDH1A3* and *LOC101103439* were involved in the enrichment of these KEGG pathway terms. Other significantly enriched KEGG pathway terms identified for dataset 2 in this study include PPAR signaling pathway (oas03320) and cholesterol metabolism (oas04979). Our findings suggest that cholesterol and retinol metabolism processes are associated with variations in hepatic Cu levels in Polish

Merino sheep. This study has some limitations such as the relative low number of samples used in transcriptome analysis as well as the slight variation in age at slaughter (included as a factor in the DEGs analysis) among the samples. Additionally, an inclusion of male lambs in a new study may aid our understanding of sex influence on gene expression associated with within-breed differences in hepatic Cu concentration.

Conclusions

A total of 53 significantly up- or downregulated genes were jointly observed for both datasets. Of these, we identified that some downregulated genes in the HLC group including *MVD*, *SQLE*, *DHCR7*, *FDPS*, *LOC101113583* and *ERG28* are associated with cholesterol synthesis. Likewise, this study revealed 4 genes including *AKR1B10, CYP26A1*, *ALDH1A3* and *NR4A1* that are implicated in retinoic acid synthesis. Moreover, GO and KEGG pathway enrichment highlighted processes involving cholesterol biosynthesis, endoplasmic reticulum membrane, steroid biosynthesis and retinol metabolism. A gene (*SPATC1L*) located near a SNP identified in our previous study was significantly downregulated in the HLC group. Our findings deliver possible candidate genes and processes that may influence or serve as an indicator for difference in within-breed liver Cu concentration in sheep, and may aid in breeding improvements for reduction in the occurrence of Cu intoxication or deficiency in sheep farming.

Materials and methods

All lambs of the Polish Merino breed were raised for lamb meat production on a commercial farm in Poland. Lambs were slaughtered in a commercial abattoir and carcasses were prepared for sale. Biological samples were collected post-mortem from these carcasses. As this was a standard and routine farming procedure not related to our research, the approval for procedures involving animals from the Local Ethics Committee for Animal Experimentation was not compulsory.

Sample collection

Lambs were raised indoors. All sheep had free access to drinking water and were fed *ad libitum* on the same diet of hay, pellet concentrate, silage and whole oats grains. Lambs

were fasted 24 h before slaughter. Samples of liver tissue from the *lobus caudatus* region were collected from 38 lambs immediately after slaughter into FixRNA (Eurx, Gdańsk, Poland), stored for 24 h in this buffer at 4 ^{0}C, and subsequently frozen in cryotubes in -80 ^{0}C for long-term storage. In addition, samples were collected from the *lobus caudatus* region of the liver, and frozen at -20 ^{0}C for the determination of liver Cu content. Sex and ages at slaughter were recorded for all lambs.

Determination of liver Cu content and grouping of samples

All 38 liver samples were freeze-dried, crushed and stored in tubes. Analysis of liver Cu concentration was performed with an inductively coupled plasma-optical emission spectrometer (ICP-OES; Agilent 720ES, Darmstadt, Germany) at a wavelength of 327.4 nm after microwave digestion as described by Adeniyi et al. (2023). Furthermore, mineral concentration of feed samples was determined by a nutrient analysis laboratory (Intertek Food Services GmbH, Linden, Germany) (Supplementary Table S1). Liver copper concentration values were reported in mg/kg DM. Of the 38 samples analyzed for liver Cu concentration, a subset of 12 samples (dataset 1) from ewes with the lowest (n = 6) and highest (n = 6) Cu concentration were selected into two liver Cu (LC) groups (LLC = low liver Cu; HLC = high liver Cu) for RNA sequencing and analysis.

RNA extraction

Total RNA was extracted from the selected liver samples (dataset 1; n = 12) using a Universal RNA Purification Kit (Eurx, Gdańsk, Poland) according to the manufacturer's protocol for animal tissues with the use of RNA Extracol reagent (Eurx, Gdańsk, Poland). RNA quantity and purity were assessed on a Nanodrop 2000 spectrophotometer (Thermo Scientific, Waltham, MA, USA). RNA integrity was evaluated on an Agilent Bioanalyzer 2100 system (Agilent Technologies, Santa Clara, CA, USA) using an RNA Nano 6000 Assay Kit RNA (Agilent Technologies, Santa Clara, CA, USA). RNA degradation and contamination were monitored on 1% agarose gel. All the samples passed the quality control requirements (RNA integrity number (RIN) ≥ 7.5) and were processed for downstream applications.

RNA sequencing and cDNA mapping

Firstly, ribosomal RNA was removed from total RNA using TruSeq Stranded Total RNA Library Prep (Illumina, San Diego, CA, USA). RNA-seq libraries were prepared using Novogene NGS Stranded RNA Library Prep Set (PT044). All cDNA libraries were sequenced using a paired-end strategy with a reading length of 150 bps on an Illumina NovaSeq 6000 sequencing platform (Illumina, San Diego, CA, USA) at a depth of 50 million reads per sample by Novogene (Beijing, China). These raw data were processed using fastp software (Chen et al., 2018) to remove adapter sequences and trim low-quality reads to obtain clean data for downstream analysis. The paired-end reads that passed the quality control were mapped to the sheep reference genome (NCBI: Ovis aries, ARS-UI_Ramb_v2.0, annotation release 105) using STAR v2.7.9a aligner (Dobin et al., 2013).

Principal component analysis

Using the count matrix, a principal component analysis (PCA) was performed with dataset 1 using prcomp package in Rv3.3.3 software (R Core Team, 2024) after count matrix data transformation with the *rlog* function in R "DESeq2" package (Love et al., 2014). Subsequently, a PCA plot comparing the first principal component (PC 1) against PC 2 was drawn with the ggplot package in R. Due to incomplete clustering of the samples, a subset of dataset 1 (dataset 2) consisting of 6 individuals (LLC: n = 3; HLC: n = 3) with the best possible clustering of samples into LC groups according to PC 1 of the first PCA plot was selected. As described for dataset 1, a second PC analysis was performed for dataset 2 with the construction of a PCA plot showing the first two PCs.

Statistical analysis

A t-test and Mann-Whitney U test to compare means of LC groups for liver Cu concentration and age were performed for dataset 1 using the *t.test* and *wilcox.test* functions in R "stats" package, respectively (R Core Team, 2024). Prior to this, data on liver Cu concentration and age were tested for fulfillment of parametric test assumptions using the *shapiro.test* and *var.test* functions in the above-mentioned package in R. No statistical analysis was carried out for dataset 2 due to low sample size. Descriptive

statistics of all samples and LC groups of datasets 1 and 2 were calculated using the dplyr package in R (Wickham et al., 2023).

Analysis of differentially expressed genes (DEGs analysis)

Using dataset 1, a comparison of the reads per gene for both LC groups was analysed for determination of differentially expressed genes (DEGs) using DESeq2 package in R (Love et al., 2014). The DEGs analysis of HLC vs LLC was performed with a model that included age as factor with two categories (less or more than 300 days), respectively. The DEGs were identified as significant at FDR ≤ 0.05 (adjusted P-value) (Benjamini, Y. and Hochberg, Y., 1995) and |log2foldchange| ≥ 1. Result of the DEGs analysis was used in the construction of a volcano plot to show significantly up- or down regulated DEGs using ggplot2 package in R (Wickham, 2016). Furthermore, a heatmap plot showing differences in the expression profile of significantly up- or down regulated DEGs for LLC and HLC samples was drawn using heatmap3 package in R (Zhao et al., 2014). Prior to the construction of the heatmap plot, count data was normalized using the *vst* function in R "DESeq2" package. Using similar parameters, DEGs analysis and heatmap plotting was repeated for dataset 2 with the results of DEGs analysis plotted in a volcano plot.

DEGs identification and enrichment analysis

Differentially expressed genes identified as significant in the analyses of datasets 1 and 2 were separately included in functional enrichment analysis using the Database for Annotation, Visualization and Integrated Discovery (DAVID) software (https://david.ncifcrf.gov, accessed on 12 September 2024) (Huang et al., 2009b, 2009a; Sherman et al., 2022). The gene list was analyzed by selecting the ovine gene annotations. The gene ontology (GO) and pathways terms including biological process (BP), cellular component (CC), molecular function (MF) and Kyoto encyclopedia of genes and genomes (KEGG), were investigated in this study. Enriched GO and KEGG pathway terms were considered significant at P-value ≤ 0.05 and FDR ≤ 0.05 (Benjamini und Hochberg 1995) before and after correction for multiple testing, respectively.

Reverse transcription-quantitative PCR analysis

From extracted RNA, first-strand cDNAs were synthesized using smART First Strand cDNA Synthesis kit (Eurx, Gdańsk, Poland) according to the manufacturer's instructions. SYBER Green chemistry was used to measure the gene expression levels on a Bio-Rad CFX Opus 96 Real-Time PCR System. The primers were designed using Primer-BLAST software (Ye et al., 2012). The glyceraldehyde-3-phosphate dehydrogenase gene (*GAPDH*) and actin beta (*ACTB*) genes were used as endogenous controls with primer information sourced from Schulze et al. (2017) and French et al. (2006), respectively. The qPCRs were performed in triplicate in a final volume of 20 µl containing 50 ng cDNA, 10 µl SG qPCR Master Mix (Eurx, Gdańsk, Poland), 5 pmol of each primer (forward and reverse) (Supplementary Table S2), 0.2 U uracil-N-glycosylase (UNG) and nuclease-free water. The qPCR program was started with UNG pre-treatment at 50 °C for 2 min., followed by initial denaturation at 95 °C for 10 min., 40 cycles of 94 °C for 15 s, 60 °C for 30 s, 72 °C for 30 s, and ended with a final stage of melting curve analysis, which was carried out using following conditions: 94 °C for 5 s, 70 °C for 5 s and then a gradual increase in temperature to 95 °C at a ramp rate of 0.5 °C/5 s to ensure that single product was amplified in each reaction. All qPCR reactions showed a single peak on the dissociation curve confirming the specific amplification of PCR products. The average cycle threshold (Ct) values of the genes were normalized to the geometric means of the controls. The delta delta Ct method was used to analyze the relative expression levels of the studied genes. After which log2foldchange was calculated from the relative expression.

Funding

This study was financially supported by the Deutsche Forschungsgemeinschaft (DFG, grant no. 62202147).

References

Adeniyi, O.O., Medugorac, I., Grochowska, E., Düring, R.-A., Lühken, G., 2023. Single-Locus and Multi-Locus Genome-Wide Association Studies Identify Genes Associated with Liver Cu Concentration in Merinoland Sheep. Genes 14, 1–14.

Benjamini, Y. and Hochberg, Y., 1995. Controlling the False Discovery Rate: A Practical and Powerful Approach to Multiple Testing. Journal of the Royal Statistical Society. Series B (Methodological) 57, 289–300.

Blades, B., Ayton, S., Hung, Y.H., Bush, A.I., La Fontaine, S., 2021. Copper and lipid metabolism: A reciprocal relationship. Biochimica et biophysica acta. General subjects 1865, 129979.

Capell-Hattam, I.M., Fenton, N.M., Coates, H.W., Sharpe, L.J., Brown, A.J., 2022. The Non Catalytic Protein ERG28 has a Functional Role in Cholesterol Synthesis and is Coregulated Transcriptionally. Journal of lipid research 63, 100295.

Cerqueira, N.M.F.S.A., Oliveira, E.F., Gesto, D.S., Santos-Martins, D., Moreira, C., Moorthy, H.N., Ramos, M.J., Fernandes, P.A., 2016. Cholesterol Biosynthesis: A Mechanistic Overview. Biochemistry 55, 5483–5506.

Chandrasekaran, P., Weiskirchen, R., 2024. The Role of SCAP/SREBP as Central Regulators of Lipid Metabolism in Hepatic Steatosis. International journal of molecular sciences 25.

Chen, S., Zhou, Y., Chen, Y., Gu, J., 2018. fastp: an ultra-fast all-in-one FASTQ preprocessor. Bioinformatics (Oxford, England) 34, i884-i890.

Clarkson, A.H., Paine, S., Martín-Tereso, J., Kendall, N.R., 2020. Copper physiology in ruminants: trafficking of systemic copper, adaptations to variation in nutritional supply and thiomolybdate challenge. Nutrition research reviews 33, 43–49.

Dobin, A., Davis, C.A., Schlesinger, F., Drenkow, J., Zaleski, C., Jha, S., Batut, P., Chaisson, M., Gingeras, T.R., 2013. STAR: ultrafast universal RNA-seq aligner. Bioinformatics (Oxford, England) 29, 15–21.

Dong, X.-Y., Tang, S.-Q., Chen, J.-D., 2012. Dual functions of Insig proteins in cholesterol homeostasis. Lipids in Health and Disease 11, 173.

Endo, S., Matsunaga, T., Nishinaka, T., 2021. The Role of AKR1B10 in Physiology and Pathophysiology. Metabolites 11.

Engle, T.E., 2011. Copper and lipid metabolism in beef cattle: a review. Journal of animal science 89, 591–596.

French, M.C., Littlejohn, R.P., Greer, G.J., Bain, W.E., McEwan, J.C., Tisdall, D.J., 2006. Growth hormone and ghrelin receptor genes are differentially expressed between genetically lean and fat selection lines of sheep. Journal of animal science 84, 324–331.

Gao, L.-L., Li, M., Wang, Q., Liu, S.-A., Zhang, J.-Q., Cheng, J., 2015. HCBP6 Modulates Triglyceride Homeostasis in Hepatocytes Via the SREBP1c/FASN Pathway. Journal of cellular biochemistry 116, 2375–2384.

Gooneratne, S.R., Buckley, W.T., Christensen, D.A., 1989. REVIEW OF COPPER DEFICIENCY AND METABOLISM IN RUMINANTS. Canadian Journal of Animal Science 69, 819–845.

Huang, D.W., Sherman, B.T., Lempicki, R.A., 2009a. Bioinformatics enrichment tools: paths toward the comprehensive functional analysis of large gene lists. Nucleic acids research 37, 1–13.

Huang, D.W., Sherman, B.T., Lempicki, R.A., 2009b. Systematic and integrative analysis of large gene lists using DAVID bioinformatics resources. Nature protocols 4, 44–57.

Huster, D., Finegold, M.J., Morgan, C.T., Burkhead, J.L., Nixon, R., Vanderwerf, S.M., Gilliam, C.T., Lutsenko, S., 2006. Consequences of copper accumulation in the livers of the Atp7b-/- (Wilson disease gene) knockout mice. The American journal of pathology 168, 423–434.

Huster, D., Lutsenko, S., 2007. Wilson disease: not just a copper disorder. Analysis of a Wilson disease model demonstrates the link between copper and lipid metabolism. Molecular bioSystems 3, 816–824.

Huster, D., Purnat, T.D., Burkhead, J.L., Ralle, M., Fiehn, O., Stuckert, F., Olson, N.E., Teupser, D., Lutsenko, S., 2007. High copper selectively alters lipid metabolism and cell cycle machinery in the mouse model of Wilson disease. The Journal of biological chemistry 282, 8343–8355.

Jin, X., Meng, L., Qi, Z., Mi, L., 2024. Transcriptomics and metabolomics analysis reveal the dietary copper deficiency and supplementation effects of liver gene expression and metabolite change in grazing sheep. BMC genomics 25, 220.

Judson, G.J., Walkley, J. R. W. , James Peter J., Kleemann David O., Ponzoni R. W., 1994. Genetic variation in trace element status of Merino sheep. Proceedings of the of the Australian Society of Animal Production 20, 438.

Julien, O., Wells, J.A., 2017. Caspases and their substrates. Cell death and differentiation 24, 1380–1389.

Li, H., Kolluri, S.K., Gu, J., Dawson, M.I., Cao, X., Hobbs, P.D., Lin, B., Chen, G., Lu, J., Lin, F., Xie, Z., Fontana, J.A., Reed, J.C., Zhang, X., 2000. Cytochrome c Release and Apoptosis Induced by Mitochondrial Targeting of Nuclear Orphan Receptor TR3. Science (New York, N.Y.) 289, 1159–1164.

Li, X., Xu, M., Wang, F., Ji, Y., Davidson, W.S., Li, Z., Tso, P., 2015. Interaction of ApoA-IV with NR4A1 and NR1D1 Represses G6Pase and PEPCK Transcription: Nuclear Receptor-Mediated Downregulation of Hepatic Gluconeogenesis in Mice and a Human Hepatocyte Cell Line. PloS one 10, e0142098.

Li, X., Xu, M., Wang, F., Kohan, A.B., Haas, M.K., Yang, Q., Lou, D., Obici, S., Davidson, W.S., Tso, P., 2014. Apolipoprotein A-IV reduces hepatic gluconeogenesis through nuclear receptor NR1D1. The Journal of biological chemistry 289, 2396–2404.

Lin, B., Kolluri, S.K., Lin, F., Liu, W., Han, Y.-H., Cao, X., Dawson, M.I., Reed, J.C., Zhang, X., 2004. Conversion of Bcl-2 from Protector to Killer by Interaction with Nuclear Orphan Receptor Nur77/TR3. Cell 116, 527–540.

Love, M.I., Huber, W., Anders, S., 2014. Moderated estimation of fold change and dispersion for RNA-seq data with DESeq2. Genome biology 15, 550.

Luo, J., Yang, H., Song, B.-L., 2020. Mechanisms and regulation of cholesterol homeostasis. Nature reviews. Molecular cell biology 21, 225–245.

Lutsenko, S., 2010. Human copper homeostasis: a network of interconnected pathways. Current opinion in chemical biology 14, 211–217.

Lutsenko, S., 2014. Modifying factors and phenotypic diversity in Wilson's disease. Annals of the New York Academy of Sciences 1315, 56–63.

Muchenditsi, A., Talbot, C.C., Gottlieb, A., Yang, H., Kang, B., Boronina, T., Cole, R., Wang, L., Dev, S., Hamilton, J.P., Lutsenko, S., 2021. Systemic deletion of Atp7b modifies the hepatocytes' response to copper overload in the mouse models of Wilson disease. Scientific reports 11, 5659.

Muller, P., van Bakel, H., van de Sluis, B., Holstege, F., Wijmenga, C., Klomp, L.W.J., 2007. Gene expression profiling of liver cells after copper overload in vivo and in vitro reveals new copper-regulated genes. Journal of biological inorganic chemistry : JBIC : a publication of the Society of Biological Inorganic Chemistry 12, 495–507.

Noy, N., 2010. Between death and survival: retinoic acid in regulation of apoptosis. Annual review of nutrition 30, 201–217.

Prohaska, J.R., 2008. Role of copper transporters in copper homeostasis. The American journal of clinical nutrition 88, 826S-829S.

R Core Team, 2024. R: A Language and Environment for Statistical Computing, Vienna, Austria. https://www.R-project.org/. Accessed 27 August, 2024.

Ranches, J., Alves, R., Vedovatto, M., Palmer, E.A., Moriel, P., Arthington, J.D., 2021. Differences in copper and selenium metabolism between Angus (Bos taurus) and Brahman (Bos indicus) cattle. Journal of animal science 99.

Schulze, F., Malhan, D., El Khassawna, T., Heiss, C., Seckinger, A., Hose, D., Rösen-Wolff, A., 2017. A tissue-based approach to selection of reference genes for quantitative real-time PCR in a sheep osteoporosis model. BMC genomics 18, 975.

Sherman, B.T., Hao, M., Qiu, J., Jiao, X., Baseler, M.W., Lane, H.C., Imamichi, T., Chang, W., 2022. DAVID: a web server for functional enrichment analysis and functional annotation of gene lists (2021 update). Nucleic acids research 50, W216-W221.

Shimano, H., Sato, R., 2017. SREBP-regulated lipid metabolism: convergent physiology - divergent pathophysiology. Nature reviews. Endocrinology 13, 710–730.

Sivertsen, T., Løvberg, K.E., 2014. Seasonal and individual variation in hepatic copper concentrations in a flock of Norwegian Dala sheep. Small Ruminant Research 116, 57–65.

Song, M.O., Freedman, J.H., 2005. Expression of copper-responsive genes in HepG2 cells. Molecular and cellular biochemistry 279, 141–147.

Suttle, N.F., 2010. Mineral nutrition of livestock, 4th ed. CABI, Wallingford, Cambridge, UK, 255-305.

Suttle, N.F., Lewis, R.M., Small, J.N.W., 2002. Effects of breed and family on rate of copper accretion in the liver of purebred Charollais, Suffolk and Texel lambs. Anim. Sci. 75, 295–302.

Thatcher, J.E., Isoherranen, N., 2009. The role of CYP26 enzymes in retinoic acid clearance. Expert opinion on drug metabolism & toxicology 5, 875–886.

Thompson, B., Katsanis, N., Apostolopoulos, N., Thompson, D.C., Nebert, D.W., Vasiliou, V., 2019. Genetics and functions of the retinoic acid pathway, with special emphasis on the eye. Human genomics 13, 61.

Toro-Domínguez, D., Villatoro-García, J.A., Martorell-Marugán, J., Román-Montoya, Y., Alarcón-Riquelme, M.E., Carmona-Sáez, P., 2021. A survey of gene expression meta-analysis: methods and applications. Briefings in bioinformatics 22, 1694–1705.

Wickham, H., 2016. ggplot2: Elegant Graphics for Data Analysis, 2nd ed. Springer International Publishing.

Wickham, H., François, R., Henry Lionel, Müller Kirill, Vaughan Davis, 2023. dplyr: A Grammar of Data Manipulation. https://dplyr.tidyverse.org.

Woolliams, C., Suttle, N.F., Woolliams, J.A., Jones, D.G., Wiener, G., 1986. Studies on lambs from lines genetically selected for low and high copper status 1. Differences in mortality. Anim. Sci. 43, 293–301.

Yang, X., Han, M., Liu, S., Yuan, X., Liu, X., Feng, S., Zhou, L., Li, Y., Lu, H., Cheng, J., Lin, S., 2018. HCBP6 upregulates human SREBP1c expression by binding to C/EBPβ-binding site in the SREBP1c promoter. BMB reports 51, 33–38.

Ye, J., Coulouris, G., Zaretskaya, I., Cutcutache, I., Rozen, S., Madden, T.L., 2012. Primer-BLAST: A tool to design target-specific primers for polymerase chain reaction. BMC Bioinformatics 13, 134.

Zhang, R., Wang, Y., Li, R., Chen, G., 2015. Transcriptional Factors Mediating Retinoic Acid Signals in the Control of Energy Metabolism. International journal of molecular sciences 16, 14210–14244.

Zhao, S., Guo, Y., Sheng, Q., Shyr, Y., 2014. Heatmap3: an improved heatmap package with more powerful and convenient features. BMC Bioinformatics 15.

APPENDIX

Supplementary Table S1. Mineral content of hay, concentrate, silage and oat grains fed to Polish Merino sheep.

Mineral* (mg/kg DM)	Hay	Pellets Concentrate	Silage	Whole Oat grains
Cu	7.10	11.20	5.40	5.60
Zn	27.60	115.00	31.70	37.90
Fe	88.80	554.00	1040.00	95.40
Mo	0.47	0.98	0.36	0.75
Mn	95.40	217.00	37.90	47.00

Supplementary Table S2. Real-time quantitative polymerase chain reaction primer sequences.

Gene	5'-3' forward primer sequence	5'-3' reverse primer sequence	References
GAPDH	GGTCGGAGTGAACGGATTTG	TGGCAACGATGTCCACTTTG	Schulze et al. (2017)
ACTB	GCAGATGTGGATCAGCAAGC	GGGTGTAACGCAGCTAACAG	French et al. (2006)
ALDH1A3	CTCGATAAAGCACTGAAGCTG	CCAGCGCATATTCACCTAGTTC	This study
APOA4	GATGTTCCTAAAGGCTGTGGTC	CTTGGAAGAGGGTGTTGAGC	This study
FMN2	AGAAAGACCTGAGAGCCTGTG	TCTCCGTCAGTGAGTTCTCC	This study
NIPAL1	TGTCACTAGAGCTGGACAAGG	TGGCAGGAGCGAAAGCATA	This study
NR4A1	CAAAGGCTTCTTCAAGCGCA	TCCTTTCAGGCTGTCTGTCC	This study
CYP1A1	CATCCCACACAGTACCACA	CTCAGATGGATCCTCCCATAG	This study
DHCR7	GAGGTTGGAGGGCCCAAT	ACGAAGTAGTACACGATGAAGGG	This study
FDPS	GGATCTTGGCAGATTCACAGAAA	CATCAATGCCCGCCATATACA	This study
MVD	GTCCTGATCCTCGTGGTGA	AACTGGTTGCTATCCTTCATGGT	This study
SPATC1L	GGAGGAGCTACTACCTGAAT	GACTTGATGGACGTCTGTTT	This study

Supplementary Table S3a Significantly (FDR ≤ 0.05 and |log2foldchange| ≥ 1) up- and downregulated differentially expressed genes in the HLC group for dataset 1.

Gene symbol	log2foldchange	lfcSE	FDR	Expression
PPDPFL	2.447	0.486	0.001	upregulated
PPP1R27	1.322	0.272	0.001	upregulated
APOA4	6.287	1.361	0.003	upregulated
ZNF585B	1.264	0.278	0.004	upregulated
AGBL2	1.441	0.317	0.004	upregulated
COL28A1	2.221	0.495	0.004	upregulated
TTC21A	1.162	0.259	0.004	upregulated
SLC30A8	3.721	0.845	0.006	upregulated
FMN2	1.985	0.452	0.006	upregulated
NR4A1	1.197	0.284	0.010	upregulated
LOC105610560	1.826	0.433	0.010	upregulated
EXD1	1.406	0.342	0.013	upregulated
LOC105603471	1.167	0.284	0.013	upregulated
LOC105602776	2.046	0.504	0.015	upregulated
LOC121816519	1.059	0.264	0.017	upregulated
SLC45A3	1.545	0.388	0.019	upregulated
LMNTD1	1.051	0.270	0.025	upregulated
LOC114114831	1.148	0.297	0.027	upregulated
C1H3orf85	1.241	0.322	0.027	upregulated
SLC15A2	1.022	0.267	0.028	upregulated
NIPAL1	1.151	0.301	0.028	upregulated
SNAI2	1.347	0.352	0.028	upregulated
LOC101119765	3.743	0.985	0.030	upregulated
C18H14orf132	1.096	0.289	0.030	upregulated
SERPINI2	3.171	0.849	0.035	upregulated
ALDH1A3	1.197	0.320	0.035	upregulated
ASB5	1.549	0.415	0.035	upregulated
LOC114117878	1.840	0.500	0.039	upregulated
SYT1	3.283	0.899	0.041	upregulated
KIF14	1.341	0.370	0.044	upregulated
LOC105614854	1.388	0.385	0.046	upregulated
LOC101107697	-5.390	0.908	0.000	downregulated
FCRL3	-3.303	0.602	0.000	downregulated
LOC101110679	-1.223	0.222	0.000	downregulated
CYP1A1	-1.013	0.187	0.000	downregulated
DCDC2	-1.023	0.190	0.000	downregulated
LOC101114456	-1.934	0.365	0.000	downregulated
KCNT2	-1.160	0.233	0.001	downregulated
LOC101103439	-1.768	0.357	0.001	downregulated
LOC121820074	-1.142	0.234	0.001	downregulated
SPATC1L	-1.424	0.308	0.003	downregulated
CUX2	-1.354	0.294	0.003	downregulated
INSIG1	-1.428	0.311	0.003	downregulated
FDPS	-1.793	0.405	0.005	downregulated
LOC101122347	-1.157	0.267	0.007	downregulated

SQLE	-1.384	0.329	0.010	downregulated
LOC114118711	-5.089	1.218	0.011	downregulated
H1-5	-1.061	0.256	0.012	downregulated
MVD	-1.139	0.275	0.012	downregulated
LOC105604659	-1.012	0.252	0.017	downregulated
CA3	-1.035	0.263	0.022	downregulated
LOC105606875	-1.786	0.458	0.024	downregulated
NEFH	-2.147	0.558	0.027	downregulated
LOC105605730	-1.072	0.280	0.028	downregulated
LOC101112029	-1.263	0.330	0.028	downregulated
LOC101113583	-1.179	0.309	0.028	downregulated
PSPH	-1.039	0.276	0.032	downregulated
PEMT	-1.238	0.333	0.037	downregulated
LOC101118484	-1.092	0.294	0.037	downregulated
DHCR7	-1.062	0.287	0.038	downregulated
IL9R	-1.491	0.403	0.038	downregulated
SSTR5	-1.816	0.497	0.041	downregulated
COL6A5	-1.516	0.418	0.044	downregulated
TSPO	-1.046	0.291	0.047	downregulated

Supplementary Table S3b Significantly (FDR ≤ 0.05 and |log2foldchange| ≥ 1) up- and downregulated differentially expressed genes in the HLC groupfor dataset 2.

Gene symbol	log2foldchange	lfcSE	FDR	Expression
LOC101120103	3.062	0.260	0.000	upregulated
GPX3	2.971	0.258	0.000	upregulated
PPDPFL	2.821	0.250	0.000	upregulated
LOC114117878	2.204	0.282	0.000	upregulated
LOC101115927	1.181	0.156	0.000	upregulated
CPQ	1.282	0.171	0.000	upregulated
APOA1	1.071	0.153	0.000	upregulated
ERICH4	1.982	0.284	0.000	upregulated
ELAVL2	3.265	0.502	0.000	upregulated
GABRG1	1.860	0.298	0.000	upregulated
AIG1	1.020	0.168	0.000	upregulated
LOC105616317	1.046	0.175	0.000	upregulated
SERPINI2	2.752	0.469	0.000	upregulated
CHMP4C	1.873	0.322	0.000	upregulated
GRIK2	1.364	0.240	0.000	upregulated
NUDT8	1.507	0.274	0.000	upregulated
LDHB	1.365	0.251	0.000	upregulated
LOC101119765	4.729	0.871	0.000	upregulated
LOC105608837	2.724	0.531	0.000	upregulated
APOC3	1.030	0.203	0.000	upregulated
LOC114115030	1.131	0.224	0.000	upregulated
MFSD2A	1.594	0.324	0.000	upregulated
ODC1	1.264	0.261	0.000	upregulated
SNAI2	1.577	0.329	0.000	upregulated
HTATIP2	1.070	0.223	0.000	upregulated
FMN2	2.102	0.443	0.000	upregulated
GPAT3	1.800	0.394	0.001	upregulated
LOC101120408	2.156	0.477	0.001	upregulated
ATP8B4	1.532	0.340	0.001	upregulated
ZNF585B	1.574	0.350	0.001	upregulated
LOC101106471	1.073	0.240	0.001	upregulated
TTC21A	1.571	0.353	0.001	upregulated
APOA4	6.993	1.573	0.001	upregulated
ZDBF2	2.670	0.617	0.002	upregulated
KEF53_t22	1.236	0.290	0.002	upregulated
LOC121820079	2.393	0.563	0.002	upregulated
ASAH2	1.253	0.299	0.003	upregulated
LOC114117546	2.156	0.516	0.003	upregulated
NEK10	1.184	0.286	0.003	upregulated
CCNA1	2.104	0.509	0.004	upregulated
LOC114109131	1.525	0.370	0.004	upregulated
HTR4	1.529	0.375	0.004	upregulated
KCNH5	3.077	0.757	0.004	upregulated
DCHS2	3.044	0.751	0.005	upregulated
SLC45A3	1.752	0.436	0.005	upregulated

LOC114117254	1.072	0.268	0.005	upregulated
MEIOB	1.271	0.320	0.006	upregulated
LOC105602763	1.243	0.314	0.006	upregulated
CFAP206	1.398	0.354	0.006	upregulated
LOC105603471	1.410	0.360	0.007	upregulated
NR4A1	1.528	0.391	0.007	upregulated
LOC105612174	1.254	0.323	0.008	upregulated
SLCO2A1	1.463	0.377	0.008	upregulated
APOD	1.268	0.327	0.008	upregulated
LOC114114851	1.273	0.329	0.008	upregulated
LOC105607270	1.515	0.394	0.008	upregulated
COL28A1	1.751	0.455	0.008	upregulated
FOS	1.245	0.324	0.009	upregulated
ALDH1A3	1.413	0.369	0.009	upregulated
PRUNE2	1.064	0.279	0.009	upregulated
ARHGEF19	2.014	0.530	0.010	upregulated
TRIQK	1.324	0.352	0.011	upregulated
LOC114109666	3.093	0.822	0.011	upregulated
LOC121819085	2.070	0.552	0.011	upregulated
RFX8	6.247	1.669	0.012	upregulated
LOC114113251	3.855	1.034	0.012	upregulated
MIOX	3.507	0.942	0.012	upregulated
CFAP44	1.190	0.320	0.013	upregulated
C1H3orf85	1.345	0.363	0.013	upregulated
KIF14	1.116	0.301	0.013	upregulated
LOC105602776	2.799	0.755	0.013	upregulated
EXD1	1.680	0.454	0.013	upregulated
RPH3AL	1.228	0.334	0.014	upregulated
LMNTD1	1.284	0.350	0.014	upregulated
SPATA48	5.763	1.571	0.014	upregulated
LAMA2	1.078	0.294	0.015	upregulated
NIPAL1	1.351	0.371	0.015	upregulated
LOC121816057	3.586	0.987	0.016	upregulated
LOC101102122	1.311	0.368	0.020	upregulated
LOC121818292	2.377	0.668	0.020	upregulated
LOC105606890	5.676	1.596	0.020	upregulated
LOC114109434	2.279	0.645	0.021	upregulated
LOC114113915	1.232	0.352	0.024	upregulated
PEX11A	1.060	0.306	0.026	upregulated
LOC121816946	1.011	0.293	0.027	upregulated
ZNF382	1.098	0.319	0.028	upregulated
LOC114108786	1.143	0.334	0.029	upregulated
SLC15A2	1.150	0.337	0.030	upregulated
FANCD2	3.118	0.914	0.030	upregulated
LOC121818051	3.349	0.982	0.030	upregulated
LOC121818302	1.404	0.412	0.030	upregulated
C21H11orf86	1.125	0.332	0.032	upregulated
KRT77	4.771	1.430	0.037	upregulated
SPTB	1.090	0.332	0.043	upregulated

SLC22A4	2.214	0.675	0.044	upregulated
C12H1orf105	2.659	0.811	0.044	upregulated
ARMC12	1.039	0.318	0.045	upregulated
LOC114116062	2.104	0.644	0.045	upregulated
SH3GL2	1.851	0.569	0.047	upregulated
LOC101118310	2.502	0.770	0.047	upregulated
ASB5	1.827	0.565	0.049	upregulated
LOC106990846	1.071	0.331	0.049	upregulated
LOC121819726	1.226	0.379	0.049	upregulated
LOC101107119	-2.655	0.178	0.000	downregulated
FDPS	-2.392	0.222	0.000	downregulated
TM7SF2	-2.173	0.224	0.000	downregulated
DHCR7	-1.494	0.167	0.000	downregulated
LOC101112029	-1.663	0.186	0.000	downregulated
INSIG1	-1.995	0.224	0.000	downregulated
CSAD	-2.461	0.299	0.000	downregulated
LOC114108618	-2.533	0.312	0.000	downregulated
LOC101119509	-1.438	0.180	0.000	downregulated
NSDHL	-1.215	0.163	0.000	downregulated
MVD	-1.435	0.198	0.000	downregulated
CDHR5	-2.891	0.407	0.000	downregulated
FASN	-2.163	0.306	0.000	downregulated
PLK4	-1.482	0.210	0.000	downregulated
DDX58	-1.184	0.169	0.000	downregulated
GUCA2B	-2.966	0.426	0.000	downregulated
LOC121820074	-1.388	0.201	0.000	downregulated
ACSS2	-1.332	0.195	0.000	downregulated
SLC17A8	-2.027	0.309	0.000	downregulated
LOC101115576	-1.188	0.183	0.000	downregulated
NOSTRIN	-1.467	0.228	0.000	downregulated
LOC105605730	-1.182	0.184	0.000	downregulated
LOC114117773	-4.226	0.658	0.000	downregulated
RTP4	-1.394	0.220	0.000	downregulated
LOC101110679	-1.404	0.224	0.000	downregulated
LOC101104700	-1.870	0.299	0.000	downregulated
LOC101109915	-1.609	0.264	0.000	downregulated
SQLE	-1.568	0.260	0.000	downregulated
MIF	-1.175	0.196	0.000	downregulated
PARP3	-1.791	0.300	0.000	downregulated
HSD17B7	-1.261	0.212	0.000	downregulated
OCIAD2	-2.267	0.385	0.000	downregulated
PEG3	-1.771	0.302	0.000	downregulated
DHCR24	-1.192	0.205	0.000	downregulated
LOC121818477	-1.865	0.324	0.000	downregulated
RNF213	-1.049	0.183	0.000	downregulated
LOC105614373	-1.884	0.332	0.000	downregulated
KCNT2	-1.111	0.199	0.000	downregulated
TNFRSF9	-1.548	0.277	0.000	downregulated
ZNFX1	-1.256	0.226	0.000	downregulated

MVK	-1.035	0.188	0.000	downregulated
LOC101123417	-1.864	0.338	0.000	downregulated
MX1	-1.893	0.344	0.000	downregulated
DCDC2	-1.229	0.224	0.000	downregulated
CYP1A1	-1.070	0.199	0.000	downregulated
XPNPEP2	-1.254	0.238	0.000	downregulated
HAPLN3	-1.049	0.203	0.000	downregulated
ANO1	-1.158	0.224	0.000	downregulated
PEMT	-1.635	0.320	0.000	downregulated
LDLR	-1.137	0.223	0.000	downregulated
VCAN	-1.305	0.258	0.000	downregulated
EPSTI1	-1.467	0.291	0.000	downregulated
FADS1	-1.313	0.261	0.000	downregulated
BST-2A	-1.463	0.291	0.000	downregulated
MSMO1	-1.030	0.205	0.000	downregulated
SSTR5	-2.609	0.529	0.000	downregulated
LOC105609869	-1.079	0.220	0.000	downregulated
LOC114112219	-1.342	0.274	0.000	downregulated
HERC6	-1.779	0.365	0.000	downregulated
RETSAT	-1.110	0.228	0.000	downregulated
LOC101113583	-1.261	0.259	0.000	downregulated
IFI44L	-1.167	0.241	0.000	downregulated
RDH11	-1.175	0.246	0.000	downregulated
LOC101107697	-4.780	1.018	0.000	downregulated
LOC101110189	-4.698	1.003	0.000	downregulated
HMGCS1	-1.048	0.227	0.001	downregulated
LOC114108679	-3.386	0.733	0.001	downregulated
FABP1	-1.233	0.268	0.001	downregulated
LOC101120447	-1.989	0.433	0.001	downregulated
LOC114117873	-1.081	0.240	0.001	downregulated
TSPO	-1.379	0.311	0.001	downregulated
SCD	-3.454	0.778	0.001	downregulated
EP4C	-2.482	0.562	0.001	downregulated
IRF9	-1.076	0.244	0.001	downregulated
RSAD2	-1.071	0.243	0.001	downregulated
LOC101107809	-1.089	0.248	0.001	downregulated
TSPAN15	-1.293	0.297	0.002	downregulated
LOC101110467	-1.320	0.303	0.002	downregulated
LOC101118189	-4.558	1.049	0.002	downregulated
LOC101103439	-1.790	0.417	0.002	downregulated
MROH6	-1.120	0.262	0.002	downregulated
DHX58	-1.016	0.241	0.003	downregulated
H1-5	-1.342	0.320	0.003	downregulated
CTSZ	-1.089	0.260	0.003	downregulated
LOC121817401	-1.263	0.303	0.003	downregulated
ARFIP2	-1.063	0.256	0.003	downregulated
LOC101112122	-1.819	0.438	0.003	downregulated
NTAN1	-1.081	0.261	0.003	downregulated
NMRAL1	-1.217	0.294	0.004	downregulated

LOC101117763	-1.224	0.298	0.004	downregulated
LOC101108781	-1.828	0.449	0.004	downregulated
LOC105603000	-1.082	0.266	0.004	downregulated
LOC101118224	-2.690	0.661	0.004	downregulated
IL9R	-1.729	0.425	0.004	downregulated
FETUB	-1.120	0.275	0.004	downregulated
MCEMP1	-1.687	0.418	0.005	downregulated
LOC101102344	-1.833	0.454	0.005	downregulated
FCRL3	-3.344	0.836	0.005	downregulated
PDK4	-1.233	0.308	0.005	downregulated
TMEM132B	-1.672	0.418	0.005	downregulated
LOC105606875	-2.603	0.653	0.006	downregulated
ALDH1L1	-1.074	0.270	0.006	downregulated
LOC101112936	-1.200	0.302	0.006	downregulated
IL1B	-1.691	0.428	0.006	downregulated
SPATC1L	-1.309	0.333	0.007	downregulated
LOC114109532	-2.403	0.613	0.007	downregulated
RTP3	-1.331	0.341	0.007	downregulated
BST-2B	-1.129	0.290	0.007	downregulated
SLC12A1	-1.016	0.261	0.007	downregulated
PSPH	-1.139	0.293	0.007	downregulated
PTPRR	-1.170	0.302	0.008	downregulated
LOC114113098	-2.793	0.724	0.008	downregulated
FADS2	-1.209	0.314	0.008	downregulated
LOC101114456	-1.598	0.416	0.009	downregulated
LOC105604659	-1.063	0.280	0.010	downregulated
PFKFB4	-1.326	0.353	0.011	downregulated
IKBKE	-1.291	0.346	0.012	downregulated
LOC105608279	-1.070	0.288	0.013	downregulated
S1PR3	-1.828	0.495	0.014	downregulated
LOC101121216	-1.018	0.277	0.014	downregulated
XAF1	-1.046	0.286	0.015	downregulated
KCTD14	-1.086	0.297	0.015	downregulated
LOC106990414	-1.373	0.376	0.015	downregulated
LOC100101238	-1.074	0.295	0.015	downregulated
EIF2AK2	-1.017	0.279	0.016	downregulated
HK3	-1.048	0.290	0.017	downregulated
LOC101119572	-2.980	0.831	0.018	downregulated
SLC51B	-1.220	0.342	0.020	downregulated
LOC101118999	-1.110	0.311	0.020	downregulated
LOC101122347	-1.414	0.398	0.020	downregulated
ABCA12	-5.379	1.522	0.021	downregulated
LOC114117911	-2.171	0.615	0.021	downregulated
LOC114118711	-4.260	1.213	0.023	downregulated
TSKU	-2.349	0.672	0.024	downregulated
LOC106991529	-1.207	0.347	0.025	downregulated
COL6A5	-1.791	0.517	0.026	downregulated
NOX5	-1.571	0.454	0.026	downregulated
LOC114109692	-1.595	0.464	0.028	downregulated

CA3	-1.034	0.301	0.028	downregulated
LOC101116841	-1.183	0.346	0.029	downregulated
ITGAM	-1.040	0.305	0.030	downregulated
LOC101118484	-1.446	0.427	0.032	downregulated
LRRC23	-1.321	0.391	0.033	downregulated
RNASE6	-2.057	0.609	0.033	downregulated
DLK1	-1.971	0.586	0.034	downregulated
MUC5AC	-1.478	0.441	0.036	downregulated
LOC105604782	-1.512	0.458	0.042	downregulated
FBN3	-1.523	0.471	0.049	downregulated
LOC114112057	-1.909	0.592	0.050	downregulated

5. GENERAL DISCUSSION AND CONCLUSIONS

Liver Cu accumulation in sheep is of vital importance as it affects Cu levels and can result in intoxication or deficiency. The present study focused on unravelling the genetic architecture influencing within-breed variation in liver Cu concentration in sheep as well as between-breed differences in liver Cu accretion. For this purpose, we employed GWAS for the first time on a dataset of 130 liver Cu concentration assessed male lambs from two farms. Furthermore, a comparative whole genome scan for selection signature was performed between 3 Cu-susceptible and 3 Cu-tolerant sheep breeds. Finally, a genome-wide transcriptome analysis comparing liver samples of 12 female lambs with low and high hepatic Cu concentration was conducted.

Structure and heritability estimate of liver Cu concentration status within farms

All animals used in studies 1 and 3 originated from 3 farms (2 in Germany and 1 in Poland). The mean liver Cu concentration varied across all farms as expected since dietary Cu levels were different across farms (Table 2). In study 1, the average liver Cu concentration was lower in Farm 2 when compared to Farm 1. This may be because on Farm 2, sheep were kept solely on pasture with a Cu content of 9.6 mg/kg DM compared to Farm 1 fed grass with a Cu concentration of 11.8 mg/kg DM (Table S1b, Appendix of chapter 2). Moreover, the pasture grass also had the highest Mo content (3.78 mg/kg DM) which may further reduce Cu availability. This supports earlier report by Knowles et al. (1998) that found higher liver Cu concentration in flocks of Romney sheep with access to higher dietary Cu levels.

Table 2. Average liver copper (Cu) concentration of farms included in study1 and 3.

Farm Location/Breed	**Number of samples**	**Mean liver Cu (mg/kg DM) ± SEM**	**SD**	**CV %**
Germany/Merinoland	89	159.54 ± 5.22	49.245	30.9
Germany/Merinoland	41	79.05 ± 6.80	43.541	55.1
Poland/Polish Merino	38	231.07 ± 13.70	84.452	36.5

In addition, the coefficient of variation (CV) for liver Cu concentration data from the three farms was 30.9%, 55.1% and 36.5% (Table2). This agrees with a report by Suttle et al. (2002) that found a CV of 40% and 34 % for liver Cu concentration in Suffolk and Texel sheep, respectively. This indicates that significant within-breed variation in liver Cu concentration occurs in sheep flocks. The within-breed variability observed may be the reason for Cu-intoxication or deficiency only in some but not all sheep within a flock. Reducing within-breed variability in liver Cu accretion in sheep will be an important goal to improve the welfare and optimize mineral supplementation for sheep.

With regards to heritability, we observed a high SNP heritability of 0.67 (s.e 0.29) which is slightly higher than the 0.60 observed in Merino (Judson et al., 1994) and Suffolk and Texel combined (Suttle et al., 2002). Accuracy was slightly better than previous studies with s.e. of 0.29 compared to 0.33 and 0.32 by Suttle et al. (2002) and Judson et al. (1994), respectively. This indicates that the conditions are good for selection within sheep breeds for higher or lower Cu accretion. In comparison with the heritabilities for performance traits such as milk yield with reported values of 0.10 (Sutera et al., 2021b), 0.29 (Haile et al., 2019) and 0.38 (Marshall et al., 2024) in sheep, as well as the heritabilies for functional traits in sheep namely somatic cell score ranging from 0.07 to 0.13 (Rupp et al., 2003) with recent values of 0.20 observed in a study by Marshall et al. (2024), the heritability estimate for liver Cu concentration confirmed in our study is higher with a good chance for the inclusion of this trait in practical sheep breeding.

Within-breed genome-wide analysis for associated SNPs and genes

The first study assessed ovine marker association with liver Cu concentration in the Merinoland sheep breed using single-locus and multi-locus GWAS methods. A total of 130 Merinoland sheep from two farms were analyzed with the adjustment for the fixed effects of farm and age as well as the polygenic effect of the genetic relationship matrix. Results revealed possible markers associated with liver Cu concentration using both methods. However, only two markers were significant above the suggestive level of significance for the SL-GWAS, whereas 13 SNP markers were significant for the ML-GWAS. It has been noted that identified SNPs from association studies are usually not located within genes but may be very close to genes that influence the trait. To the best of our knowledge, this is the first GWAS on liver Cu concentration in sheep with insight

into the nature of this trait. Though heritability was high as observed in other studies, the inability to identify a highly significant region with Bonferroni level of significance in the SL-GWAS is an indication for the polygenic status of this trait. In addition, the relatively low number of samples (n = 130) and SNPs (n = 45,511) may also limit the detection of associated SNPs. We scanned regions of 500 Kb up-and downstream of identified SNPs for genes associated with cellular transport and excretion. No known gene that is obviously functionally associated with Cu metabolism, transport or excretion was observed in all these regions. However, some identified genes such as *VPS35*, *SLC38A9* and *CHMP1A* are reportedly involved in cellular transport and excretion (Woodman, 2016; Wyant et al., 2017; Chen et al., 2019). Other identified genes including *SPG7* and *ATP5MF* genes are involved in the opening of the mitochondrial permeability transition pore (PTP) which leads to mitochondrial swelling and cell death (Bonora et al., 2013; Shanmughapriya et al., 2015; Bonora et al., 2022). Moreover, this study identified enriched gene ontology (GO) terms such as lysosomal membrane and mitochondrial inner membrane.

To further support the GWAS analysis, we performed RNA-seq expression analysis study (study 3) using Polish Merino liver samples (n = 12) with high and low liver copper concentration. Findings of this study revealed that GO and Kyoto encyclopaedia of genes and genomes (KEGG) pathway terms including cholesterol synthesis and retinoic acid synthesis are associated with within-breed variation in liver Cu levels. Expression in liver samples with high liver content showed that cholesterol-related genes were significantly downregulated. Moreover, genes associated with retinoic acid production and signaling were upregulated while genes that aid the reduction of retinoic acid levels were downregulated in the HLC group. These findings are in agreement with a study by Muchenditsi et al. (2021) that reported upregulation of pathways related to liver X receptor/ retinoid X receptor (LXR/RXR) activities in hepatocyte specific *ATP7B* deficient mice, whereas downregulation of cholesterol synthesis was observed in the global *ATP7B* deficient mice. Since both mice are ATP*7B* deficient, they exhibit Cu metabolism dysfunction with the attendant high hepatic Cu levels like the HLC group in the expression study.

Furthermore, a SNP (rs427314005) observed in the first study was found near (148.7 Kb) a significant differentially expressed gene named spermatogenesis and centriole associated 1 Like (*SPATC1L*). Though there is currently no known association of this gene with liver Cu levels, it is possible that this gene alongside a nearby cholesterol-related gene (*LSS*) may influence within-breed variation in hepatic Cu levels.

Between-breed genome-wide scan for genes and genomic regions

After assessing within-breed differences, a second study was conducted to assess the ovine genome for selection signatures associated with variation in Cu accretion using groups of Cu-susceptible (STX = Scottish Texel; ISF = Irish Suffolk; WHF = Welsh Mountain Hill flock) and Cu-tolerant (FIN = Finnsheep; SBF = Scottish Blackface; GGH = German Grey Hearth) sheep breeds. We selected breeds based on available published information on differences in Cu accretion status, and sourced SNP genotype data for the selected breeds. The second study employed the F_{ST}, XP-EHH and hapFLK methods to analyze selection signatures, and considered selection signals identified by a minimum of two methods as significant to eliminate false signals. We found regions on OAR 4, 8 and 11 containing 54 candidate genes under selection for Cu accretion. Genes involved in regulating inflammation and cell death including *PREP, TP53, TNFSF13, TNFSF12, ALOX15, ALOX12* and *EIF5A* were observed within significant selection regions. Notably, the *TP53* gene has been associated with the regulation of a novel form of cell death named “cuproptosis” (Xiong et al., 2023). Cuproptosis is a form of cell death associated with Cu homeostasis and mitochondrial respiration (Chen et al., 2022; Li et al., 2022). This suggests that between-breed difference in Cu accretion may be influenced by variability in response to inflammation and apoptosis. This is in harmony with a higher mitochondrial sensitivity to Cu-induced oxidative stress observed in North Ronaldsay sheep (Cu-suceptible) when compared to Cambridge sheep (Cu-tolerant) (Haywood et al., 2005; Simpson et al., 2006).

Limitations and challenges

Regarding the first study, selection of samples for phenotyping must be done with care to avoid variables such as dietary Cu and environmental conditions. Moreover, the challenge of measuring precise dietary Cu intake of individual animals necessitates the

provision of animals with ad-libitum access to feed. Therefore, lambs that are from the same farm with similar dietary Cu levels and environmental conditions should be sampled. To do this, farms with large flocks of sheep should be targeted. However, the unavailability of many sheep breeds reared as large single flocks limited breed and farm selection for this study. Additionally, it is yet unclear to what extent age influences liver Cu levels. The study by Suttle et al. (2002) showed that liver Cu accumulation increases linearly with age for Texel and Suffolk with a peak at 22 weeks for Suffolk only. This implies that the relationship between age and liver Cu concentration may vary across breeds with the age of sample collection. In all analysis for study 1, age was included as a covariate since liver samples were collected after slaughter of lambs. Though the age at slaughter for lambs is more similar than for adults, the age at slaughter of lambs is more dependent on target weight and therefore differs not only within but even more between breeds. Similar to GWAS, age was considered a variable that could affect transcriptomic analysis. Therefore, we also adjusted for age in the transcriptome study.

Currently, analysis of selection signatures for breed differences in Cu accretion can only be performed with a few breeds due to inadequate and unavailable information on the Cu accumulation status of many breeds despite the availability of genotyping data. On the other hand, there is insufficient genomic data on certain breeds such as North Ronaldsay with a known Cu accretion status. These circumstances limited the number of breeds that could be selected for analysis of selection signals influencing breed-variation in Cu accretion in sheep.

Prospects for further studies on genes influencing liver Cu concentration

Our findings show that further studies need to be conducted to improve our knowledge on the genetic architecture influencing liver Cu concentration in sheep. Additional GWASs using similar or different sheep breeds should be performed to support or oppose identified markers or genes. Reassessment of the heritability for this trait should also be performed before its use in breeding value estimation. Better results can be achieved with a higher number of samples and SNPs. Likewise, further studies to investigate already identified genes or genetic regions can be conducted.

Inter-departmental collaboration between departments of animal breeding, animal nutrition and veterinary medicine should be encouraged to achieve success in further studies. Using the transcriptomic study as an example, the inclusion of liver Cu concentration and histopathological analyses in selection for lambs may improve accuracy in identifying animals with similar transcriptome patterns.

Furthermore, the Cu accretion status of several sheep breeds is yet to be elucidated. The second study sheds light on the need for information regarding liver Cu accumulation in both local and foreign sheep breeds. This will enable further studies on between-breed differences in Cu accumulation to be conducted with already available genotyping data.

Ways to apply our findings in practical sheep breeding

Considering the relatively high heritability of this trait in Merinoland sheep, it can be successfully included in practical breeding programs. The trait can be relatively estimated for individual sheep (e.g. sire) by phenotyping offspring (e.g. half-sibs) after slaughter. Following this, pedigree-based best linear unbiased prediction can be performed for estimating breeding value of this trait as is currently used for Merino sheep breeding in Germany Martin et al. (2024). Currently, genomic selection which has been widely implemented in other animal species including cattle is yet be employed in sheep breeding in Germany (Martin et al., 2024). Martin et al. (2024) in a recently conducted simulation study on genomic selection strategies for German Merino sheep breed reported marginal gains in estimated breeding value prediction using genomic-based best linear unbiased prediction when compared with pedigree-based selection. In addition to the high heritability of liver Cu concentration, the polygenic nature of this trait makes it a good candidate for genomic selection. The goals of selection for this trait should be targeted at either improving the ability to retain Cu with the hope of reducing Cu supplementation and incidence of Cu deficiency in Merinoland sheep or reducing the ability to retain Cu with the hope of grazing Merinoland sheep flocks on Cu-rich pasture while minimizing the risk of Cu intoxication.

6. SUMMARY

The continuous economic and health impact of Cu intoxication and deficiency in sheep farming necessitates the need to understand the influence of the ovine genome on within- and between-breed differences in liver Cu concentration in sheep. Within-breed variation in liver Cu concentration is responsible for incidences of Cu intoxication and deficiency in some sheep flocks despite feeding recommended levels of Cu. In our studies, within-breed variations in liver Cu concentration observed in flocks under similar dietary and environmental conditions ranged from 30% to 55%. The heritability estimate and accuracy (0.67 ± 0.29) observed in our study was similar to values of 0.60± 0.32 found in previous studies. Therefore, it can be concluded that this trait is most likely heritable, and it is influenced by genetic factors.

To this end, we tested the probability that certain SNP markers of the ovine genome may be associated with variability in liver Cu concentration in sheep using single- and multi-locus GWAS methods. The results revealed that a total of 13 markers, identified using ML-GWAS, were associated with variability in liver Cu concentration in the Merinoland sheep. Functional enrichment analysis also revealed enriched GO terms such as lysosomal membrane and mitochondrial inner membrane.

To support this finding, a comparative transcriptome analysis between Polish Merino liver samples with low and high hepatic Cu concentration was performed. Among other differentially expressed genes, the expression analysis revealed the *SPATC1L* gene located 148.7 Kb from a SNP (rs427314005) identified by GWAS before. Enriched GO and KEGG pathway terms including cholesterol and retinoic acid syntheses were identified. Furthermore, we performed selection signature analysis to identify genomic regions under selection between Cu-susceptible and Cu-tolerant sheep breeds. Findings from this study showed that regions on OAR 4, 8 and 11 are under selection for this trait. In addition, lipoxygenase and ferroptosis pathways were identified among others as enriched GO and KEGG pathway terms.

The results of the present study point to a polygenic nature of within- and between-breed differences in liver Cu concentration. Additionally, our study suggests that pathways responsible for within-breed variation differ from those affecting between-breed variation in liver Cu concentration for sheep. Further studies need to be conducted to confirm

identified regions, genes or markers associated with variability in liver Cu concentration and potential use in animal breeding.

7. REFERENCES OF THE GENERAL PARTS

Arredondo, M., Muñoz, P., Mura, C.V., Nùñez, M.T., 2003. DMT1, a physiologically relevant apical Cu1+ transporter of intestinal cells. American journal of physiology. Cell physiology 284, C1525-30.

Asadollahpour Nanaei, H., Dehghani Qanatqestani, M., Esmailizadeh, A., 2020. Whole-genome resequencing reveals selection signatures associated with milk production traits in African Kenana dairy zebu cattle. Genomics 112, 880–885.

Barceloux, D.G., Barceloux, D., 1999. Copper. Journal of Toxicology: Clinical Toxicology 37, 217–230.

Bonora, M., Bononi, A., Marchi, E. de, Giorgi, C., Lebiedzinska, M., Marchi, S., Patergnani, S., Rimessi, A., Suski, J.M., Wojtala, A., Wieckowski, M.R., Kroemer, G., Galluzzi, L., Pinton, P., 2013. Role of the c subunit of the FO ATP synthase in mitochondrial permeability transition. Cell cycle (Georgetown, Tex.) 12, 674–683.

Bonora, M., Giorgi, C., Pinton, P., 2022. Molecular mechanisms and consequences of mitochondrial permeability transition. Nature reviews. Molecular cell biology 23, 266–285.

Borobia, M., Villanueva-Saz, S., Ruiz de Arcaute, M., Fernández, A., Verde, M.T., González, J.M., Navarro, T., Benito, A.A., Arnal, J.L., Las Heras, M. de, Ortín, A., 2022. Copper Poisoning, a Deadly Hazard for Sheep. Animals 12, 1–16.

Bostwick, J.L., 1982. Copper toxicosis in sheep. Journal of the American Veterinary Medical Association 180, 386–387.

Bremner, I., 1998. Manifestations of copper excess. The American journal of clinical nutrition 67, 1069S-1073S.

Byrne, L., Murphy, R.A., 2022. Relative Bioavailability of Trace Minerals in Production Animal Nutrition: A Review. Animals 12, 1-46.

Campos, B.M., do Carmo, A.S., Da Silva, T.B.R., Verardo, L.L., Simoni Gouveia, J.J. de, Mendes Malhado, C.H., Da Barbosa Silva, M.V.G., Souza Carneiro, P.L., 2017. Identification of artificial selection signatures in Caracu breed lines selected for milk production and meat production. Livestock Science 206, 82–87.

Chen, J., Jiang, Y., Shi, H., Peng, Y., Fan, X., Li, C., 2020. The molecular mechanisms of copper metabolism and its roles in human diseases. Pflugers Archiv : European journal of physiology 472, 1415–1429.

Chen, K.-E., Healy, M.D., Collins, B.M., 2019. Towards a molecular understanding of endosomal trafficking by Retromer and Retriever. Traffic (Copenhagen, Denmark) 20, 465–478.

Chen, L., Min, J., Wang, F., 2022. Copper homeostasis and cuproptosis in health and disease. Signal transduction and targeted therapy 7, 378.

Clarke, N.J., Laurie, S.H., 1980. The copper-molybdenum antagonism in ruminants. I. The formation of thiomolybdates in animal rumen. Journal of Inorganic Biochemistry 12, 37–43.

Clarkson, A.H., Paine, S., Martín-Tereso, J., Kendall, N.R., 2020. Copper physiology in ruminants: trafficking of systemic copper, adaptations to variation in nutritional supply and thiomolybdate challenge. Nutrition research reviews 33, 43–49.

De Bie, P., van de Sluis, B., Klomp, L., Wijmenga, C., 2005. The many faces of the copper metabolism protein MURR1/COMMD1. The Journal of heredity 96, 803–811.

De Sousa, I.K.F., Hamad Minervino, A.H., Sousa, R.D.S., Chaves, D.F., Soares, H.S., Barros, I.d.O., De Araújo, C.A.S.C., Júnior, R.A.B., Ortolani, E.L., 2012. Copper deficiency in sheep with high liver iron accumulation. Veterinary medicine international 2012, 207950.

EFSA Panel on Additives and Products or Substances used in Animal Feed (EFSA FEEDAP Panel), 2016. Scientific opinion on the revision of the currently authorised maximum copper content in complete feed. EFSA Journal 14, 4563.

Fariello, M.I., Boitard, S., Naya, H., SanCristobal, M., Servin, B., 2013. Detecting signatures of selection through haplotype differentiation among hierarchically structured populations. Genetics 193, 929–941.

Ferguson, W.S., Lewis, A.H., Watson, S.J., 1938. Action of Molybdenum in Nutrition of Milking Cattle. Nature 141, 553.

Ferguson, W.S., Lewis, A.H., Watson, S.J., 1943. The teart pastures of Somerset: I. The cause and cure of teartness. The Journal of Agricultural Science 33, 44–51.

Flori, L., Fritz, S., Jaffrézic, F., Boussaha, M., Gut, I., Heath, S., Foulley, J.-L., Gautier, M., 2009. The genome response to artificial selection: a case study in dairy cattle. PloS one 4, 1-13.

Fry, R.S., Spears, J.W., Lloyd, K.E., O'Nan, A.T., Ashwell, M.S., 2013. Effect of dietary copper and breed on gene products involved in copper acquisition, distribution, and use in Angus and Simmental cows and fetuses1,2. Journal of animal science 91, 861–871.

Gaetke, L.M., Chow-Johnson, H.S., Chow, C.K., 2014. Copper: toxicological relevance and mechanisms. Archives of toxicology 88, 1929–1938.

Galyean, M.L., Ralphs, M.H., Reif, M.N., Graham, J.D., Braselton, W. E., Jr., 1996. Effects of previous grazing treatment and consumption of locoweed on liver mineral concentrations in beef steers. Journal of animal science 74, 827–833.

Ghasemi, M., Zamani, P., Vatankhah, M., Abdoli, R., 2019. Genome-wide association study of birth weight in sheep. Animal : an international journal of animal bioscience 13, 1797–1803.

Gooneratne, S.R., Buckley, W.T., Christensen, D.A., 1989. REVIEW OF COPPER DEFICIENCY AND METABOLISM IN RUMINANTS. Canadian Journal of Animal Science 69, 819–845.

Guitart, R., Croubels, S., Caloni, F., Sachana, M., Davanzo, F., Vandenbroucke, V., Berny, P., 2010. Animal poisoning in Europe. Part 1: Farm livestock and poultry. Veterinary journal (London, England : 1997) 183, 249–254.

Haile, A., Hilali, M., Hassen, H., Lobo, R.N.B., Rischkowsky, B., 2019. Estimates of genetic parameters and genetic trends for growth, reproduction, milk production and milk composition traits of Awassi sheep. Animal : an international journal of animal bioscience 13, 240–247.

Haywood, S., Simpson, D.M., Ross, G., Beynon, R.J., 2005. The greater susceptibility of North Ronaldsay sheep compared with Cambridge sheep to copper-induced oxidative stress, mitochondrial damage and hepatic stellate cell activation. Journal of comparative pathology 133, 114–127.

Helmer, C., Hannemann, R., Humann-Ziehank, E., Kleinschmidt, S., Koelln, M., Kamphues, J., Ganter, M., 2021. A Case of Concurrent Molybdenosis, Secondary Copper, Cobalt and Selenium Deficiency in a Small Sheep Herd in Northern Germany. Animals 11,1-14.

Hidiroglou, M., Heaney, D.P., Hartin, K.E., 1984. Copper Poisoning in a Flock of Sheep. Copper Excretion Patterns after Treatment with Molybdenum and Sulfur or Penicillamine. The Canadian Veterinary Journal 25, 377–382.

Hordyjewska, A., Popiołek, Ł., Kocot, J., 2014. The many "faces" of copper in medicine and treatment. Biometals : an international journal on the role of metal ions in biology, biochemistry, and medicine 27, 611–621.

Humann-Ziehank, E., Coenen, M., Ganter, M., Bickhardt, K., 2001. Long-term observation of Subclinical chronic copper poisoning in two sheep breeds. Journal of Veterinary Medicine Series A 48, 429–439.

Huster, D., Lutsenko, S., 2007. Wilson disease: not just a copper disorder. Analysis of a Wilson disease model demonstrates the link between copper and lipid metabolism. Molecular bioSystems 3, 816–824.

Jiang, L., Garrick, M.D., Garrick, L.M., Zhao, L., Collins, J.F., 2013. Divalent metal transporter 1 (Dmt1) mediates copper transport in the duodenum of iron-deficient rats and when overexpressed in iron-deprived HEK-293 cells. The Journal of nutrition 143, 1927–1933.

Jin, X., Meng, L., Qi, Z., Mi, L., 2024. Transcriptomics and metabolomics analysis reveal the dietary copper deficiency and supplementation effects of liver gene expression and metabolite change in grazing sheep. BMC genomics 25, 220.

Johnston, H., Beasley, L., MacPherson, N., 2014. Copper toxicity in a New Zealand dairy herd. Irish Veterinary Journal 67, 20.

Johnston, S.E., McEwan, J.C., Pickering, N.K., Kijas, J.W., Beraldi, D., Pilkington, J.G., Pemberton, J.M., Slate, J., 2011. Genome-wide association mapping identifies the genetic basis of discrete and quantitative variation in sexual weaponry in a wild sheep population. Molecular ecology 20, 2555–2566.

Judson, G.J., Walkley, J. R. W. ., James Peter J., Kleemann David O., Ponzoni R. W., 1994. Genetic variation in trace element status of Merino sheep. Proceedings of the of the Australian Society of Animal Production 20, 438.

Kendall, N.R., Holmes-Pavord, H.R., Bone, P.A., Ander, E.L., Young, S.D., 2015. Liver copper concentrations in cull cattle in the UK: are cattle being copper loaded? The Veterinary record 177, 493.

Kijas, J.W., Hadfield, T., Naval Sanchez, M., Cockett, N., 2016. Genome-wide association reveals the locus responsible for four-horned ruminant. Animal genetics 47, 258–262.

Kijas, J.W., Lenstra, J.A., Hayes, B., Boitard, S., Porto Neto, L.R., San Cristobal, M., Servin, B., McCulloch, R., Whan, V., Gietzen, K., Paiva, S., Barendse, W., Ciani, E., Raadsma, H., McEwan, J., Dalrymple, B., 2012. Genome-wide analysis of the world's

sheep breeds reveals high levels of historic mixture and strong recent selection. PLoS biology 10, e1001258.

Kim, H., Son, H.-Y., Bailey, S.M., Lee, J., 2009. Deletion of hepatic Ctr1 reveals its function in copper acquisition and compensatory mechanisms for copper homeostasis. American journal of physiology. Gastrointestinal and liver physiology 296, G356-64.

Kincaid, R.L., 2000. Assessment of trace mineral status of ruminants: A review. Journal of animal science 77, 1.

Knowles, S.O., Rounce, J.R., Grace, N.D., Lee, J., 1998. 1998 Knowles et al.: Variation in copper metabolism between two flocks of Romney sheep in response to increasing dietary copper. Proceedings of the New Zealand Society of Animal Production 58, 195–198.

Kumaratilake, J.S., 2014. Chronic Copper Poisoning in Sheep: Liver Injury. JTEA.

Li, S.-R., Bu, L.-L., Cai, L., 2022. Cuproptosis: lipoylated TCA cycle proteins-mediated novel cell death pathway. Signal transduction and targeted therapy 7, 158.

Linder, M.C., 2016. Ceruloplasmin and other copper binding components of blood plasma and their functions: an update. Metallomics : integrated biometal science 8, 887–905.

Linder, M.C., 2020. Copper Homeostasis in Mammals, with Emphasis on Secretion and Excretion. A Review. International journal of molecular sciences 21.

Linder, M.C., Wooten, L., Cerveza, P., Cotton, S., Shulze, R., Lomeli, N., 1998. Copper transport. The American journal of clinical nutrition 67, 965S-971S.

López-Alonso, M., Miranda, M., 2020. Copper Supplementation, A Challenge in Cattle. Animals : an open access journal from MDPI 10.

Lutsenko, S., Barnes, N.L., Bartee, M.Y., Dmitriev, O.Y., 2007. Function and regulation of human copper-transporting ATPases. Physiological reviews 87, 1011–1046.

Marshall, A.C., Lopez-Villalobos, N., Loveday, S.M., Weeks, M., McNabb, W., 2024. Estimation of genetic parameters for production, composition and processability of milk from dairy sheep in a New Zealand flock. New Zealand Journal of Agricultural Research, 1–18.

Martin, R., Pook, T., Bennewitz, J., Schmid, M., 2024. Genomic selection strategies for the German Merino sheep breeding programme - A simulation study. Journal of animal breeding and genetics = Zeitschrift fur Tierzuchtung und Zuchtungsbiologie.

McCaughey, W.J., 2007. Inorganic or organic poisons. In: Aitken I. D. (Ed.), Diseases of sheep, 4th ed. Blackwell, Oxford, pp. 424–439.

Muchenditsi, A., Talbot, C.C., Gottlieb, A., Yang, H., Kang, B., Boronina, T., Cole, R., Wang, L., Dev, S., Hamilton, J.P., Lutsenko, S., 2021. Systemic deletion of Atp7b modifies the hepatocytes' response to copper overload in the mouse models of Wilson disease. Scientific reports 11, 5659.

Mullis, L.A., Spears, J.W., McCraw, R.L., 2003. Estimated copper requirements of Angus and Simmental heifers1. Journal of animal science 81, 865–873.

Papachristodoulou, C., Stamoulis, K., Tsakos, P., Vougidou, C., Vozikis, V., Papadopoulou, C., Ioannides, K., 2015. Liver concentrations of copper, zinc, iron and molybdenum in sheep and goats from northern Greece, determined by energy-dispersive X-ray fluorescence spectrometry. Bulletin of environmental contamination and toxicology 94, 460–467.

Polishchuk, E.V., Concilli, M., Iacobacci, S., Chesi, G., Pastore, N., Piccolo, P., Paladino, S., Baldantoni, D., van IJzendoorn, S.C.D., Chan, J., Chang, C.J., Amoresano, A., Pane, F., Pucci, P., Tarallo, A., Parenti, G., Brunetti-Pierri, N., Settembre, C., Ballabio, A., Polishchuk, R.S., 2014. Wilson disease protein ATP7B utilizes lysosomal exocytosis to maintain copper homeostasis. Developmental cell 29, 686–700.

Prohaska, J.R., 2008. Role of copper transporters in copper homeostasis. The American journal of clinical nutrition 88, 826S-829S.

Puls, R., 1994. Mineral Levels in Animal Health: Diagnostic Data. Sherpa International.

Purdie, A.C., Plain, K.M., Begg, D.J., Silva, K. de, Whittington, R.J., 2011. Candidate gene and genome-wide association studies of Mycobacterium avium subsp. paratuberculosis infection in cattle and sheep: a review. Comparative immunology, microbiology and infectious diseases 34, 197–208.

Ranches, J., Alves, R., Vedovatto, M., Palmer, E.A., Moriel, P., Arthington, J.D., 2021. Differences in copper and selenium metabolism between Angus (Bos taurus) and Brahman (Bos indicus) cattle. Journal of animal science 99.

Roberts, E.A., Sarkar, B., 2008. Liver as a key organ in the supply, storage, and excretion of copper. The American journal of clinical nutrition 88, 851S-854S.

Sabeti, P.C., Varilly, P., Fry, B., Lohmueller, J., Hostetter, E., Cotsapas, C., Xie, X., Byrne, E.H., McCarroll, S.A., Gaudet, R., Schaffner, S.F., Lander, E.S., The International HapMap Consortium., 2007. Genome-wide detection and characterization of positive selection in human populations. Nature 449, 913–918.

Sargison, N., 2008. Unexpected Disease or Death. In: Sargison Neil (Ed.), Sheep Flock Health, pp. 228–274.

Shanmughapriya, S., Rajan, S., Hoffman, N.E., Higgins, A.M., Tomar, D., Nemani, N., Hines, K.J., Smith, D.J., Eguchi, A., Vallem, S., Shaikh, F., Cheung, M., Leonard, N.J., Stolakis, R.S., Wolfers, M.P., Ibetti, J., Chuprun, J.K., Jog, N.R., Houser, S.R., Koch, W.J., Elrod, J.W., Madesh, M., 2015. SPG7 Is an Essential and Conserved Component of the Mitochondrial Permeability Transition Pore. Molecular cell 60, 47–62.

Sieuchand, S., 2016. Review on Copper's Functional Roles, Copper X Mineral Interactions Affecting Absorption, Tissue Storage, and Cu Deficiency Swayback of Small Ruminants. ARC Journal of Animal and Veterinary Sciences 2.

Simoni Gouveia, J.J. de, Paiva, S.R., McManus, C.M., Caetano, A.R., Kijas, J.W., Facó, O., Azevedo, H.C., Araujo, A.M. de, Souza, C.J.H. de, Yamagishi, M.E.B., Carneiro, P.L.S., Braga Lôbo, R.N., Oliveira, S.M.P. de, Da Silva, M.V.G., 2017. Genome-wide

search for signatures of selection in three major Brazilian locally adapted sheep breeds. Livestock Science 197, 36–45.

Simpson, D.M., Mobasheri, A., Haywood, S., Beynon, R.J., 2006. A proteomics study of the response of North Ronaldsay sheep to copper challenge. BMC veterinary research 2, 36.

Sivertsen, T., Løvberg, K.E., 2014. Seasonal and individual variation in hepatic copper concentrations in a flock of Norwegian Dala sheep. Small Ruminant Research 116, 57–65.

Song, M.O., Freedman, J.H., 2005. Expression of copper-responsive genes in HepG2 cells. Molecular and cellular biochemistry 279, 141–147.

Spears, J.W., Brandao, V., Heldt, J., 2022. Invited Review: Assessing trace mineral status in ruminants, and factors that affect measurements of trace mineral status. Applied Animal Science 38, 252–267.

Sutera, A.M., Di Gerlando, R., Mastrangelo, S., Sardina, M.T., D'Alessandro, E., Portolano, B., Tolone, M., 2021a. Genome-wide association study for milk production traits in an economically important local dairy sheep breed. Italian Journal of Animal Science 20, 1500–1505.

Sutera, A.M., Tolone, M., Mastrangelo, S., Di Gerlando, R., Sardina, M.T., Portolano, B., Pong-Wong, R., Riggio, V., 2021b. Detection of genomic regions underlying milk production traits in Valle del Belice dairy sheep using regional heritability mapping. Journal of animal breeding and genetics = Zeitschrift fur Tierzuchtung und Zuchtungsbiologie 138, 552–561.

Suttle, N.F., 2010. Mineral nutrition of livestock, 4th ed. CABI, Wallingford, Cambridge, UK, 255-305.

Suttle, N.F., Field, A.C., 1983. Effects of dietary supplements of thiomolybdates on copper and molybdenum metabolism in sheep. Journal of comparative pathology 93, 379–389.

Suttle, N.F., Jones, D.G., 2007. Miconutrient imbalance. In: Aitken I. D. (Ed.), Diseases of sheep, 4th ed. Blackwell, Oxford, pp. 377–394.

Suttle, N.F., Lewis, R.M., Small, J.N.W., 2002. Effects of breed and family on rate of copper accretion in the liver of purebred Charollais, Suffolk and Texel lambs. Anim. Sci. 75, 295–302.

Tao, T.Y., Gitlin, J.D., 2003. Hepatic copper metabolism: insights from genetic disease. Hepatology (Baltimore, Md.) 37, 1241–1247.

van der Berg, R., Levels, F.H., van der Schee, W., 1983. Breed differences in sheep with respect to the accumulation of copper in the liver. The veterinary quarterly 5, 26–31.

Varga, A., Puschner, B., 2012. Retrospective study of cattle poisonings in California: recognition, diagnosis, and treatment. Veterinary medicine (Auckland, N.Z.) 3, 111–127.

Wei, C., Wang, H., Liu, G., Zhao, F., Kijas, J.W., Ma, Y., Lu, J., Zhang, L., Cao, J., Wu, M., Wang, G., Liu, R., Liu, Z., Zhang, S., Liu, C., Du, L., 2016. Genome-wide analysis reveals adaptation to high altitudes in Tibetan sheep. Scientific reports 6, 26770.

Wiener, G., Field, A.C., 1969. Copper concentrations in the liver and blood of sheep of different breeds in relation to swayback history. Journal of comparative pathology 79, 7–14.

Wijmenga, C., Klomp, L.W.J., 2004. Molecular regulation of copper excretion in the liver. Proc. Nutr. Soc. 63, 31–39.

Woodman, P., 2016. ESCRT-III on endosomes: new functions, new activation pathway. The Biochemical journal 473, e5-8.

Woolliams, C., Suttle, N.F., Woolliams, J.A., Jones, D.G., Wiener, G., 1986. Studies on lambs from lines genetically selected for low and high copper status 1. Differences in mortality. Anim. Sci. 43, 293–301.

Woolliams, J.A., Suttle, N.F., Wiener, G., Field A. C., Woolliams, C., 1982. The effect of breed of sire on the accumulation of copper in lambs, with particular reference to copper toxicity. Animal Production 35, 299–307.

Wu, X., Leegwater, P.A.J., Fieten, H., 2016. Canine Models for Copper Homeostasis Disorders. International journal of molecular sciences 17, 196.

Wyant, G.A., Abu-Remaileh, M., Wolfson, R.L., Chen, W.W., Freinkman, E., Danai, L.V., Vander Heiden, M.G., Sabatini, D.M., 2017. mTORC1 Activator SLC38A9 Is Required to Efflux Essential Amino Acids from Lysosomes and Use Protein as a Nutrient. Cell 171, 642-654.e12.

Xiong, C., Ling, H., Hao, Q., Zhou, X., 2023. Cuproptosis: p53-regulated metabolic cell death? Cell death and differentiation 30, 876–884.

ACKNOWLEDGEMENT

The pathway to the completion of a PhD thesis is riddled with exciting challenges that doctoral candidates experience in the search for ground-breaking evidence in their research area. Therefore, it is important to note that my personal commitment alone could not have been sufficient for the successful completion of my PhD dissertation. The success of this project was dependent on the support I received from family, friends and colleagues that are too numerous to be documented. I hereby convey my sincere appreciation to everyone involved in the successful completion of my doctoral thesis.

In particular, I would like to thank God for this success. My sincere appreciation to my supervisor Prof. Dr. Gesine Lühken for the opportunity to conduct this research, the trust in my ability, and the support throughout the duration of this project. In addition, many thanks to Prof. Dr. Klaus Eder for agreeing to co-examine the thesis.

A big thank you to Prof. Dr. Ivica Međugorac, Dr. Ewa Grochowska, Dr. J. A. Lenstra and Dr. S. Mastrangelo for their advice and assistance with many notable sections of this thesis. I deeply appreciate Prof. Dr. Rolf-Alexander Düring for his invaluable contribution to aspects of the dissertation.

I am grateful to all members of the department of animal breeding and genetics, especially those of the Prof. Dr. Gesine Lühken working group including my friend and colleague Rebecca Simon for making the journey worthwhile, Ute Richter for your cheerfulness and encouragement, Carina Crispens and Stephanie Steitz for their assistance and support in the laboratory, and Kirsty Tan for the memorable time as my colleague and “officemate”.

Finally yet importantly, I thank my wife (Omolola) and kids for their physical, moral and emotional support throughout this project, my mum for her consistent encouragement and support, and members of P.I.W.C Gießen for creating an enjoyable fellowship that fueled my will to succeed.

Declaration

I declare that the dissertation here submitted is entirely my own work, written without any illegitimate help by any third party and solely with materials as indicated in the dissertation. I have indicated in the text where I have used texts from already published sources, either word for word or in substance, and where I have made statements based on oral information given to me.

At all times during the investigations carried out by me and described in the dissertation, I have followed the principles of good scientific practice as defined in the “Statutes of the Justus Liebig University Gießen for the Safeguarding of Good Scientific Practice”.

Gießen, 4th November 2024.